KUVEMPU UNIVERSITY

SYNTHESIS AND CHARACTERIZATION OF SMART HYDROGELS IN DRUG DELIVERY SYSTEM

THESIS SUBMITTED TO THE KUVEMPU UNIVERSITY

FOR THE AWARD OF THE DEGREE OF

DOCTOR OF PHILOSOPHY

IN

PHARMACEUTICAL CHEMISTRY

BY

Mr. MADHUSUDANA T. M.Sc.

Research Scholar
Ph.D. Registration No. and Date: 585/02-01-2019
Department of Pharmaceutical Chemistry
Kuvempu University
P.G. Centre, Kadur-577548
India

Guide

Dr. MAMATHA G. P. M.Sc., Ph.D.

Professor
Dept. of Chemistry
Davangere University
Shivagangotri,
Davangere-577007
Karnataka, India

Co-guide

Dr. DEMAPPA T. M.Sc., Ph.D.

Professor
Dept. of Polymer Science
University of Mysore
Sir. M.V.P.G. Centre,
Mandya-571402
Karnataka, India

KUVEMPU UNIVERSITY

Mr. Madhusudana T. M.Sc.

Research Scholar
Department of Pharmaceutical Chemistry
Kuvempu University,
Post Graduate Centre, Kadur - 577 548,
Chikkamagalore (D), Karnataka, INDIA

Phone: +91 9113284599
E-mail: vmskt5@gmail.com

DECLARATION

I hereby declare that the Ph.D., thesis entitled **"Synthesis and characterization of smart hydrogels in drug delivery system"** has been composed by me under the guidance of **Dr. Mamatha G. P.,** Professor, Department of Chemistry, Davangere University, Shivagangotri, Davangere-577007, with co-guidance of **Dr. Demappa T.,** Professor, Department of Polymer Science, University of Mysore, Sir. M.V. P.G. Centre, Mandya-571402, is original in its contents and has not been submitted elsewhere for any other degree/diploma of this or any other university/institution.

Date : 23/11/2022

Mr. Madhusudana T.
(Research Scholar)

DAVANGERE UNIVERSITY

Dr. Mamatha G. P. **M.Sc., Ph.D.**

Professor
Department of Chemistry
Davangere University,
Shivagangotri, Davangere-577007,
Karnataka, INDIA

Phone: + 91 9448422903
E-mail: mamatha_gp2005@rediffmail.com

CERTIFICATE

This is to certify that the thesis entitled **"Synthesis and characterization of smart hydrogels in drug delivery system"** submitted by **Mr. Madhusudana T.** for the award of the degree **Doctor of Philosophy in Pharmaceutical Chemistry** is based on the results of experiments carried out by him under my guidance. The thesis or part of the work has not been previously submitted for any other Degree/diploma of this or any other university/institution.

Date : 28/11/2022

Dr. Mamatha G. P.
(Research Guide)
Dr. Mamatha G.P. M.Sc,PhD
Professor Dept. of Chemistry
Davangere University
Shivagangotri, Davangere-577007

UNIVERSITY OF MYSORE

Dr. Demappa T. **M.Sc., Ph.D.**

Professor
Department of Polymer Science
University of Mysore,
Sir. M.V. P.G. Centre, Mandya-571402,
Karnataka, INDIA

Phone: + 91 9972875448
E-mail: tdemappa2003@yahoo.co.in

CERTIFICATE

This is to certify that the thesis entitled **"Synthesis and characterization of smart hydrogels in drug delivery system"** submitted by **Mr. Madhusudana T.** for the award of the degree **Doctor of Philosophy in Pharmaceutical Chemistry** is based on the results of experiments carried out by him under my co-guidance. The thesis or part of the work has not been previously submitted for any other Degree/diploma of this or any other university/institution.

Date : 28/11/2022

Dr. Demappa T.
(Research Co-guide) Ph.D.
Dr. T. Demappa, M.Sc.,
Professor of Polymer Science
University of Mysore
Sir M. Visvesvaraya Post Graduate Center
Industrial Area, Tubinakere, Mandya-571 402

This thesis is dedicated to my parents

Jayamma and thippeswamy

For their endless love, support and encouragement

ACKNOWLEDGMENTS

It gives me great pleasure to acknowledge the people who came in contact in the way with helping hands, during my research tenure.

With deep gratitude and humility, I express my heartfelt gratitude to **Dr. Mamatha G. P.** Professor, Department of Chemistry, Davangere University, Davangere, Karnataka, for her excellent guidance, constant inspiration, unwavering encouragement, kind cooperation, and excellent support throughout my research work.

I personally express my sincere gratitude to **Dr. Demappa T.** Professor, Department of Polymer Science, University of Mysore, Sir. M.V. P.G. Centre, Mandya, Karnataka, for his valuable co-guidance.

I am highly grateful to **Prof. B. P. Veerabhadrappa,** Vice-Chancellor, Kuvempu University, for giving me an opportunity to pursue my dreams. His encouragement and constant support especially in providing the necessary facilities helped me to make this thesis a better one.

I am immensely thankful to **Dr. N. D. Satyanarayan**, Professor and Chairman, Department of Pharmaceutical Chemistry, Kuvempu University, P.G. Centre, Kadur, who has provided me with the necessary facilities and assistance to complete this research work with ease.

I am grateful to **Dr. Mahadevan K. M.**, Professor, Department of Chemistry, Kuvempu University, P.G. Centre, Kadur, for his valuable assistance in carrying out this research.

I am thankful to **Dr. Shobharani H.**, Associate Professor, Department of Commerce, Kuvempu University, P.G. Centre, Kadur, for her valuable encouragement in carrying out this research.

I am grateful to **Dr. Nagaraju G.**, Assistant Professor, Department of Chemistry, Siddaganga Institute of Technology, Tumkur, for her valuable encouragement and assistance in carrying out this research.

Interaction between academics and industry is essential these days. I also want to thank **Micro Labs Limited,** Bangalore, Karnataka for providing gift samples of Levofloxacin, Moxifloxacin, and Doxycycline for my research work.

I would like to express my gratitude to all of the teaching and non-teaching staff members at Kuvempu University, P.G. Centre, Kadur, Karnataka, who have assisted me in the completion of this research thesis, either directly or indirectly.

I am very thankful to the Faculty members of the Department of Chemistry and Industrial Chemistry, Kuvempu University, Shankaraghatta-577 451, Shimoga,

Karnataka, India. I am also very grateful to Kuvempu University library for providing me with the library facilities during my research work.

I would like to thank my beloved parents, my father **Thippeswamy V.** who always supported me in my career and my mother **Jayamma** who always inspired me to do my best. A special thanks to my dear sister **Kavyashri T.** and brother-in-law **Ramesh Babu** for their support. The love, patience and encouragement they showed throughout my entire life and throughout the period of my research work have brought me a long way in my life. They always believed in me and stood by me and my special thanks to my nephews **Viren** and **Vivan** for their cheerful encouragement.

I would like to express my sincere thanks to all my research colleagues and seniors **Dr. Manjunath K. S., Dr. Harish kumar S., Dr. Deepak M. P., Dr. Santhosh H. M., Dr. Ashok K. S., Dr. Naveen kumar, Dr. Ravindra M. K., Dr. Sudhir ilaigar ramaswamy, Dr. Shivakumar L. R., Dr. Santhosh S., Dr. Ananthacharya, Dr. Chandrashekar, Mr. Nagabhushan, Mr. Prabhakar K. S., Mr. Navaneeth, Mr. Sheshan T. N., Mr. Nippu B. N., Mr. Abdul Rahaman., Mr. Sakshith prasad, Mrs. Pallavi K. M., Mr. Pampapathi., Mr. Vinay kumar, Mis. Vedavi L., Mrs. Ramya B. P., Mr. Pradeep and Mr. Girish H. V.** for the input they provided during numerous formal and informal discussions we had. Thanks a lot for your countless help and support during my Research work in Kuvempu University.

I would like to express my sincere thanks to all my friends **Mr. Pruthviraj T. D., Mr. Gurunandana, Mr. Dimple kallesh kumar, Mr. Narendra, Mr. Anil kumar, Mr. Siddappa desai, Mr. Dinakar patil, Mr. Vikas G., Mr. Akash, Mr. Madhukumar, Mr. Sampath kumar, Mr. Shivakumar, Mis. Shashikala, Mrs. Sindhushri, Mis. Kavya R., Mrs. Komala, Mrs. Pooja, Mrs. Deepika, Mrs. Kavyashri, Mrs. Rekha G. R. and Mr. Kumar B. N.** for their support and encouragement.

I extended my heartfelt gratitude to all of my friends and family members for their unwavering support, encouragement, and timely suggestions throughout the completion of my entire research program.

It is a difficult task to acknowledge all those who have provided valuable assistance, whether directly or indirectly. I express my gratitude to each and every one of them.

Thankful I ever remain**.....** *Madhusudana T.*

List of research publications:

Papers published:

1. **Madhusudana Thippeswamy,** Mamatha Ganjeenahalli Puttagiddappa, Demappa Thippaiah, Nayak Devappa Satyanarayan. **(2021). Synthesis and characterization of poly(acrylamide) hydrogels as pH and salt sensitive material.** ***Asian Journal of Chemistry.*** 33(5), 1019-1024, ISSN: 0970-7077. **https://doi.org/10.14233/ajchem.2021.23124**

2. **Madhusudana T.,** Mamatha G. P., Demappa T., Satyanarayan N. D. **(2021). Controlled drug release of levofloxacin from poly (acrylamide) hydrogel.** ***International Journal of Research in Pharmaceutical Sciences.*** 12(2), 1037-1043. ISSN: 0975-7538. **https://doi.org/10.26452/ijrps.v12i2.4631**

3. **Madhusudana Thippeswamy,** Mamatha Ganjeenahalli Puttagiddappa, Demappa Thippaiah, Nayak Devappa Satyanarayan. **(2021). Poly(acrylamide-co-acrylic acid) synthesized, moxifloxacin drug-loaded hydrogel: Characterization and evaluation studies.** ***Journal of Applied Pharmaceutical Science.*** 11(12), 74-81. ISSN: 2231-3354. **https://doi.org/10.7324/JAPS.2021.1101205**

Papers accepted:

1. **Madhusudana T.,** Mamatha G. P., Demappa T., Shivakumara L. R., N. D. Satyanarayan. **Synthesis and characterization of poly(acrylic acid) hydrogel for doxycycline drug release study.** (***Accepted for Publication in the Thai Journal of Pharmaceutical Sciences,*** ISSN: 0125-4685).

List of Papers Presented in Conferences:

1. Presented paper on **"Synthesis and Characterization of Poly(acrylamide) Hydrogels as pH and Salt Sensitive Material"** in ***'Two-days International Conference on Innovative Trends in Natural and Applied Sciences – 2021 (ICITNAS – 2021)'*** organized by Mahatma Gandhi College Of Science, Gadchandur, Maharashtra, India on 17th -18th August 2021.
2. Presented paper on **"Synthesis, characterization, and moxifloxacin drug release from poly(acrylamide-co-acrylic acid) hydrogel"** in ***'first International Conference on Environment, Economy, Management, Science and Technology (ICEEMST)'*** organized by the Department of Environmental Science, SIES (Nerul) College of Arts, Science and Commerce, Navi Mumbai, Maharashtra, India in collaboration with RSP Conference hub, Coimbatore, India on 24th -25th August 2021.
3. Presented paper on **"Poly(acrylamide) synthesized, levofloxacin drug-loaded hydrogel: Characterization and evaluation studies"** in ***'National Conference on Research & Advanced Innovations in Technology and Sciences (R&AITS-2021)'*** organized by the Department of mechanical engineering annamacharya institute of technology & sciences, Rajampet, Andhra Pradesh, India on 28th August 2021.
4. Presented paper on **"Controlled drug release of doxycycline from poly(acrylic acid) hydrogel"** in ***'Two Day International e-Conference on Drug Discovery & Material Science'*** organized by the JSS College of Arts, Commerce and Science, Mysuru, Karnataka, India on 15th -16th September 2021.

ABBREVIATIONS

PHEMA	:	Poly(2- hydroxyethyl methacrylate)
3D	:	Three-dimensional
PEO	:	Poly(ethylene oxide)
PVA	:	Poly(vinyl alcohol)
PAA	:	Poly(acrylic acid)
PPO	:	Poly(propylene oxide)
HASE	:	Hydrophobically alkali swellable emulsion
HEUR	:	Hydrophobically modified ethoxylated urethane
NIPAm	:	N-Isopropylacrylamide
DN	:	Double network
PEG	:	Poly(ethylene glycol)
PNIPAM	:	Poly(N-isopropyl acrylamide)
EVAc	:	Ethylene-co-vinyl acetate
ECM	:	Extracellular matrix
HA	:	Hyaluronic acid
PLGA	:	Poly(lactic-co-glycolic acid)
PGA	:	Poly(glycolic acid)
PLDLA	:	Polylactic-d-lactic acid

PEU	:	Polyethylene urethane
MSC	:	Maximum safe concentration
MEC	:	Minimum effective concentration
GIT	:	Gastrointestinal tract
FTIR	:	Fourier Transform Infrared
SEM	:	Scanning Electron Microscope
TGA	:	Thermogravimetric Analysis
UV	:	Ultraviolet
SI	:	Swelling Index
HCl	:	Hydrochloric acid
USP	:	United States Pharmacopeia
rpm	:	Revolutions per minute
cm	:	Centimeter
ml	:	Milliliter
l	:	Liter
CH_3COOH	:	Acetic acid
$HClO_4$	:	Perchloric acid
NaOH	:	Sodium hydroxide
NaCl	:	Sodium chloride
$CaCl_2$	:	Calcium chloride

$AlCl_3$	:	Aluminium chloride
KH_2PO_4	:	Potassium dihydrogen orthophosphate
Na_2HPO_4	:	Disodium hydrogen phosphate anhydrous
AAM	:	Acrylamide
AAC	:	Acrylic acid
PPS	:	Potassium persulphate
MBA	:	N, N′-methylene-bis-acrylamide
SMBS	:	Sodium metabisulfite
SDFCL	:	S D Fine-Chem Limited
TG	:	Thermogravimetry
DTG	:	Derivative Thermogravimetry
CR	:	Controlled-release
S. aureus	:	Staphylococcus aureus
E. coli	:	Escherichia coli
LLH	:	Levofloxacin drug-loaded hydrogel
MLH	:	Moxifloxacin drug-loaded hydrogel
DLH	:	Doxycycline drug-loaded hydrogel
SGF	:	Simulated gastric fluid
SIF	:	Simulated intestinal fluid

v/s	:	Versus
M	:	Molar
CBR	:	Cube root
SQRT	:	Square root
AAMH	:	Poly(acrylamide) hydrogel
AACH	:	Poly(acrylic acid) hydrogel
AAMCH	:	Poly(acrylamide-co-acrylic acid) hydrogel

Summary of the thesis

The focus of the work covered in this thesis was to synthesize the various hydrogels using simple and effective methods via free radical polymerization. The synthesized hydrogels were characterized through various analytical techniques such as Fourier transform infrared spectroscopy (FTIR), UV-Visible spectrophotometer, Scanning electron microscope (SEM), Thermogravimetric analyzer (TGA). Further, their swelling properties were analyzed at different temperatures, pH and salt solutions. The synthesized hydrogels show excellent controlled drug release properties. The obtained results prove that the synthesized hydrogels were suitable for drug delivery applications. The present work carried out under the following objectives are described in the corresponding chapters.

Chapter – 1

Introduction

Chapter - 1 is all about the introduction. It provides an overview of Hydrogels and controlled release drug delivery methods as well as a brief history. The importance of classifying polymers according to their sources and applications has been highlighted, as well as the fundamental properties of different polymers and their requirement for chemical modification and drug release methods. This chapter also contains the objectives and scope of the research.

Chapter – 2

Experimental methods

Chapter - 2 informs about the experimentation. It describes the experimental techniques used for material preparation and the tools utilized for material characterization during the investigation. The drug-loaded polymer matrices were characterized using different analytical methods such as UV-Visible spectrophotometer, FTIR Spectrometer, TGA and SEM. Swelling, drug entrapment efficiency, antibacterial activity and an *in-vitro* release study were all tested on the formulations. The release of medicines from drug delivery devices is determined using a variety of mathematical models that have been thoroughly discussed.

Chapter – 3

Synthesis and characterization of poly(acrylamide) hydrogels as pH and salt sensitive material

Chapter - 3 address the synthesis and characterization of poly(acrylamide) hydrogels as pH and salt-sensitive material. Poly(acrylamide) hydrogels were synthesized using acrylamide monomer with methylenebisacrylamide crosslinker and characterized by FT-IR, SEM and TGA. The swelling study was performed at various pH, temperature and salt solutions. In acid and base solutions, the swelling (%) order is HCl < CH_3COOH < $HClO_4$ < NaOH and the swelling (%) order in salt solutions is NaCl > $CaCl_2$ > $AlCl_3$.

Chapter – 4

Controlled drug release of levofloxacin from poly (acrylamide) hydrogel

Chapter - 4 describe the controlled drug release of levofloxacin from poly(acrylamide) hydrogel. Using poly(acrylamide) hydrogel with levofloxacin, an attempt was made to construct a simple and affordable gastrointestinal drug delivery method. FTIR spectrum analysis indicated a conformation of chemical crosslinking by methylenebisacrylamide, while SEM of the hydrogels revealed a shape with a smooth surface. The Thermal stability of the polymer matrix was verified by TGA experiments. The swelling study was conducted by the gravimetric method. *In-vitro* release experiments were done at pH 1.2 and pH 7.4 to replicate genuine gastrointestinal fluid/gastrointestinal tract conditions. The results showed that poly(acrylamide) hydrogel released levofloxacin 17% in an acidic medium and 99% in basic media after 6 hours and it follows the Higuchi model and drug-loaded hydrogel showed good antibacterial activity.

Chapter – 5

Synthesis and characterization of poly(acrylamide-co-acrylic acid) hydrogel for moxifloxacin drug release study

Chapter - 5 deals with the study of synthesis and characterization of poly(acrylamide-co-acrylic acid) hydrogel for moxifloxacin drug release study. The hydrogel is prepared by combining two monomers acrylamide and acrylic acid. Moxifloxacin, an antibiotic was

used as a model drug for encapsulation. FTIR, TGA and SEM were used to characterize the hydrogel. The effect of crosslinking agent concentration on swelling was investigated. Water uptake property increases considerably as the crosslinker content of the matrix decreased and hydrogel with the least crosslinking agent swelled the most. To further understand the release process, the drug release was analyzed using mathematical models. The maximum regression coefficient value R^2 is 0.976 was found in the Higuchi model hence it follows the Higuchi model and drug-loaded hydrogel showed good antibacterial activity.

Chapter – 6

Synthesis and characterization of poly(acrylic acid) hydrogel for doxycycline drug release study

Chapter - 6 is about synthesis, characterization and doxycycline drug release from the poly(acrylic acid) hydrogel. The preparation of poly(acrylic acid) hydrogel crosslinked with methylenebisacrylamide. FTIR spectroscopy was used to characterize the hydrogel. SEM was used to carry out the topographical studies. TGA methods were used to conduct the thermal analysis. The drug was molecularly distributed in hydrogel. This chapter also covered the effects of crosslinker concentration on poly(acrylic acid) hydrogel, water uptake percentage and *in-vitro* drug release. Further, to understand the probable release process, the data was also submitted to kinetic treatment. The kinetic

datas were best fitted to a Higuchi model with a good regression coefficient and drug-loaded hydrogel showed good antibacterial activity.

Chapter – 7

Conclusion

In the present research, we projected to discover a method for the synthesis of the hydrogels by using free-radical initiators. These methodologies are proved to be excellent yields, less time and quick in synthesis. All the materials were evaluated for their swelling property with temperature, pH and salt solutions. In addition, in-depth examination of drug delivery properties and the experimental study reveals that the synthesized materials exhibit promising drug delivery properties in developing biomaterials for drug delivery applications.

TABLE OF CONTENTS

CHAPTER –2

EXPERIMENTAL METHODS

CHAPTER – 3

SYNTHESIS AND CHARACTERIZATION OF POLY(ACRYLAMIDE) HYDROGELS AS pH AND SALT SENSITIVE MATERIAL

CHAPTER – 4

CONTROLLED DRUG RELEASE OF LEVOFLOXACIN FROM POLY(ACRYLAMIDE) HYDROGEL

CHAPTER – 5

SYNTHESIS AND CHARACTERIZATION OF POLY(ACRYLAMIDE-CO-ACRYLIC ACID) HYDROGEL FOR MOXIFLOXACIN DRUG RELEASE STUDY

CHAPTER – 6

SYNTHESIS AND CHARACTERIZATION OF POLY(ACRYLIC ACID) HYDROGEL FOR DOXYCYCLINE DRUG RELEASE STUDY

CHAPTER – 7

CONCLUSION

Chapter – 1

Introduction

Chapter – 1
Introduction

This chapter discusses the recent development of hydrogels as drug delivery carriers for biological and biomedical applications. Various synthetic strategies for the preparation of hydrogels as controlled drug delivery systems have been included in this chapter, namely polymer particles, pH sensitivity and thermo-reactive properties. This chapter also includes several drug loading methods and details of *in-vitro* drug release with a brief review of the literature on this research with including the scope of work.

1.1. Introduction

Polymeric hydrogels have more popular in recent years as a result of their unique physicochemical properties, such as self-healing, water permeability, stimuli responsiveness, biocompatibility and softness [1-9]. As a result, they have a broad range of applications (**Fig. 1.1**), including drug delivery systems [10-11], scaffolds/implants in tissue engineering [12-16], synthetic extracellular matrix [17], robotics [18], enzyme immobilisation [19], actuators [20], sensors [18 21], etc. Hydrogels were first suggested for contact lens use in 1960 by Wichterle and Lim, who used a synthetic hydrogel called Poly (2-hydroxy ethyl methacrylate) (PHEMA) [22]. Hydrogels have also been rigorously applied to a variety of biological, controlled release and medicinal uses [10, 23, 24].

Hydrogels are three-dimensional (3D) hydrophilic polymeric networks (**Fig. 1.2**) that can absorb significant amounts of biological fluids or water and have physical or chemical crosslinks. The volume of water in the completely swollen state

is determined by the combination of elastic retractive force and thermodynamic mixing force of the polymeric network. The retractive power on the other hand is heavily influenced by the network structure's interconnectivity (degree of crosslinking). As a result, there is a lot of scope for developing hydrogels with various swelling capacities by varying the addition of these individual forces.

1.2. Hydrogel classification

Hydrogels are classified according to their source: synthetic or natural; the nature of crosslinking: physically crosslinked or covalently crosslinked; the functional groups: non-ionic and ionic hydrogels; the type of network: interpenetrating networks, co-polymeric networks, homopolymer networks and the influence of microorganisms: non-degradable and degradable.

Hydrogels for tissue engineering and drug delivery applications have been made from a broad range of synthetic and natural materials. Poly(acrylic acid) [PAA], Poly(ethylene oxide) [PEO], copolymers of PEO and PPO [Pluronics], poly(vinyl alcohol) [PVA] and some polypeptides are widely used synthetic polymers. Chitosan, alginates, agarose, collagen, gelatin, hyaluronic acid and fibrin are examples of naturally occurring polymers.

1.3. Hydrogel synthesis

Hydrogels are synthesized by polymerizing hydrophilic monomers with a crosslinker in the presence of an initiator with diluents, such as water or other aqueous solutions. Following that, the formed hydrogel is treated with water to eliminate unreacted crosslinker, initiator, monomers and other unnecessary by-products, resulting in the isolation of pure hydrogel.

The solution, inverse suspension and bulk polymerization techniques are often used to make synthetic hydrogels. The solution and bulk polymerizations are carried out in a homogeneous medium containing water-soluble initiators, crosslinkers and monomers. Hydrogels may be made of any form or size using these processes, depending on the mold in which the polymerization occurs. Furthermore, solution polymerization is favored because the heat of polymerization can be better controlled. Hydrogels in micron sizes (also known as microgels) can be produced using an inverse suspension polymerization method based on the scattered and continuous phases. In certain cases, the monomer dissolves in the scattered form, while the surfactant dissolves in the continuous phase. In the continuous phase, the surfactant allows for homogeneous distribution of the monomer and other reactants. Extremely, acrylamide, salts of acrylic acid and methacrylic acids are better hydrophilic monomers suited to inverse suspension polymerization.

1.4. Chemically and physically cross-linked hydrogels

Two important methods for forming three-dimensional networks in polymer gels are covalent bond formation and reversible non-covalent interactions (physical interactions). As a result, the obtained polymer gels may be classified as physical or chemical gels [12, 13].

External stimuli such as temperature, pH, solvent – nonsolvent and others may trigger volume-phase transitions in chemical gels [27]. In response to external stimuli, physical gels may undergo reversible sol-gel transitions.

Crosslinking through polymer-polymer interactions via functional groups, co-polymerization and polymer precursors (post-crosslinking) are the traditional

methods for creating covalently crosslinked hydrogels. These methods may produce hydrogels with some flaws due to unfavorable side effects. Aqueous polymerization can also produce hydrogels with random crosslink distributions in the network structure if the crosslinking agent is hydrophobic and the monomer is hydrophilic. Hydrogels with a wide range of chemical compositions have been synthesized using a variety of crosslinking agents and monomers. **Table 1.1** lists a few examples of common crosslinking agents and monomers.

Hydrogels that are physically crosslinked, physical interactions such as hydrophobic and van-der Waals interactions, etc are shape the network structure. Due to hydrophobic interactions, water-soluble polymers that have been hydrophobically transformed can self-assemble into hydrogels and undergo reversible sol-gel transformations [28-31]. Hydrophobically modified poly(acrylamides) [32-34], HEUR and HASE are some examples of hydrophobically associating polymers [35-44]. In controlled release technology, reversible sol-gel transition in response to temperature are also becoming increasingly common as smart injectables [45]. In thermo-reversible polymers, the sol-gel transformation is triggered by reversible hydrophobic associations that are triggered by minor temperature changes.

1.5. Drawbacks of conventional hydrogels and new structural attributes

While conventional hydrogels have more applications in tissue engineering and controlled drug delivery, they have a number of disadvantages, including low mechanical strength, non-porous nature and limited self-healing capacity. Designing and creating novel molecular architectures in hydrogels, such as nanocomposite gels

[46-49], slide-ring gels [50-51], double-network hydrogels [52-55], self-healing [8-9] and topological gels [56] is a major focus of study.

Haraguchi and colleagues [46] published novel nanocomposite hydrogels with hectorite as a crosslinking agent, clay as a multifunctional crosslinking agent and NIPAm as a monomer. The hydrogel's mechanical strength was improved by using exfoliated clay in the hydrogel matrix. The double network (DN) hydrogels described by Osada and Gong [52] comprise two separately crosslinked networks, the first is strongly crosslinked, while the second is slightly crosslinked. If the second network's molar ratio to the first network is greater than 10 or more, these hydrogels display outstanding mechanical efficiency. The loosely crosslinked networks are thought to dissipate steam, resulting in improved mechanical properties for these DN hydrogels. This was demonstrated for DN hydrogels made of lightly crosslinked poly(acrylamide) and heavily crosslinked poly(2-acrylamido-2-methyl propanesulfonic acid). Other DN hydrogels based on cellulosic cellulose are being developed now [57]

Okumura and Ito reported a new topological network with a novel sliding ring crosslinking mode [50, 56, 58]. To prevent the cyclodextrins from slipping away, the linear polymers, such as PEGs, were penetrated into them and the ends were covered with bulky groups like adamantine. To make mobile crosslinks, the cyclodextrins were connected in a figure (8) pattern. The "pulley effect" in these sliding ring gels caused the stresses in the network structure to co-operatively equalize, resulting in better mechanical properties.

Mark and co-workers, as well as Peak et al., have published excellent reviews

on novel molecular architectures for hydrogels with enhanced mechanical strengths and toughness [59-60]. Conducting hydrogels has recently gained popularity in neural networks [61], electrochemical biosensors [62] and electro-induced drug release [63]. Incorporating various conducting materials into the hydrogel matrix, such as conducting polymers (e.g., polythiophene, polypyrrole, polyaniline), carbon, metal nanoparticles and so on, will induce electrical conductivity.

1.6. Hydrogels for controlled release applications

Hydrogels are a new type of material that can be used to deliver drugs in a controlled manner. Hydrogels that monitor swelling and respond to stimuli, in particular, are becoming increasingly important in the delivery of controlled drugs. Hydrogels are classified as either matrix or reservoir in drug delivery **(Fig. 1.3)**. Hydrogels can be manufactured in a variety of shapes and sizes, the nature of hydrogel dosage types is determined by the drug's route of administration, which includes: oral – discs, cylindrical, circular; implants – drum shape, disc shape; vaginal – cylindrical; rectal – rods, cylinders; etc.

The simultaneous absorption of water/biofluids and the release of the drug from the hydrogel is accomplished via a swelling-controlled process. Diffusion is by far the most popular method of release. In the matrix system, drug release is equal to the square root of time 't' ($t^{1/2}$), according to Higuchi's model. It is possible that this would not result in consistent release rates. The reservoir system, on the other hand, can deliver near-constant release rates. The degree of crosslinking and mechanical strength of hydrogels for controlled drug delivery applications, network pore size, drug distribution in the hydrogel and drug diffusion are the most significant

parameters.

Hydrogels can swell dramatically in response to a variety of factors, including magnetic field, pH, electric field, temperature, glucose, urea, ultrasonic radiation, etc. These hydrogels are known as "intelligent gels," "stimulus-responsive" or "smart hydrogels". **Table 1.2** lists several examples of hydrogels containing stimuli and drugs for use in controlled drug delivery.

The hydrogel matrix can also be covalently conjugated with drugs, with the degree of enzymatic or chemical cleavage of the drug-polymer bond affecting drug release. Dexamethasone was linked to a photoreactive PEG by a degradable lactide bond are an example [74].

1.7. Hydrogels for Tissue Engineering

Tissue Engineering has grown in importance as a treatment option for patients who have lost or failed an organ as a result of an accident or disease. Tissue or organ transplantation is a common method of replacing damaged tissues or organs in general. However, due to a scarcity of donors, this strategy has been severely limited. In tissue engineering, hydrogels have emerged as the best choice. However, designing and manufacturing a hydrogel scaffold with a highly porous surface, strong mechanical efficiency and the ability to monitor the release kinetics of growth factors during tissue regeneration is a major challenge. The following characteristics are required of hydrogel scaffolds/implants for tissue engineering:

• Non-toxic and biocompatible materials should be used.

• Must resemble the extracellular matrix (ECM).

• It should be mechanically powerful.

• A porous structure with interconnected pores is needed.

• It can promote cell adhesion and proliferation, as well as cell-to-cell interaction and migration.

• Preferably biodegradable and bioadsorbable over a predetermined time span, with growth tissue filling the area previously occupied by the scaffold.

The average pore size of the hydrogel has a significant impact on the growth and penetration of the cells in the hydrogels 3-D structure. Porous structures in polymer scaffolds/implants can be created using a variety of techniques. Particle leaching [75-76], solvent casting [77-78], gas foaming [79], freeze-drying [80-81], electrospinning [82], porogens [83] etc. The best pore sizes for tissue engineering scaffolds have been found to be 20-125 µm for adult mammalian skin regeneration, 100-350 µm for bone regeneration and 5 µm for neovascularization. Aside from these factors, the scaffold's micro-architecture plays an important function in tissue regeneration [84, 85].

Hydrogels for tissue engineering scaffolds/implants have been made from a wide range of natural and synthetic polymers **(Table 1.3)**. Poly anhydrides [86-87], Aliphatic polyesters [88-89], poly orthoesters [90], poly(vinyl alcohol) (PVA) [91-92], poly(ethylene oxide) (PEO) [93-97], polypeptides [98-100], poly(acrylic acid) [101-102] are examples of synthetic polymers. Collagen [103-104], chitosan [105-106], alginates [107-108], agarose [109-110], fibrin [111], hyaluronic acid [112-113] and gelatin [114-115] are examples of naturally derived polymers. Many of these components are often used as sponges, films and foams.

Hydrogels have been used to neural tissue [116], engineer cartilage [117], vocal matrix [118], bone [119], ligaments [120], skeletal muscles [121], heart valves

[122], hair follicles [123], lungs [124] and trachea [125], among other tissues. Scaffolds made of terpolymer have been found to resemble natural cartilage [126].

Scaffolds combining poly-L-lysine, HA and alginate have been developed for a number of tissue engineering applications [127]. Hydrogels have also been used to bone marrow stromal cells [128], culture fibroblasts[129], pre-adipocytes [130], human umbilical vein endothelial cells [131], pancreatic islet cells [132], osteoblasts [133], hepatocytes [134], among other cells. The following are some of the widely available polymers for producing scaffolds.

1.8. Conventional drug delivery

Pharmaceuticals or therapeutic active ingredients in pure form are not administered in the same way; instead, dosage forms of a certain size, shape and texture are manufactured. When it became practicable to produce on an industrial scale, the appropriate dose regimen was developed to achieve an enhanced therapeutic activity to a medication contained in a formulation product [135]. To optimize the therapeutic response, many dosage forms can be devised into which a medication ingredient is contained and administered via all potential delivery channels such as oral, topical and parenteral [136]. Oral delivery of medications through numerous pharmaceutical products such as suspensions, capsules, emulsions, solutions and tablets is the most ancient, convenient and widely utilized process for the systemic administration of medications. These traditional instantaneous-release formulations provide clinically potent therapy while preserving the normal state amount of medication in plasma allowing the patient to get a sufficient quantity of medicine in the body. The few oral therapeutic drugs are those that are low absorbed or have high permeability in the gastrointestinal tract and are

variable in different enzymes [137].

Traditional instant release dosage forms administered in a specific amount and time via the oral route can be used to maintain a steady dose amount in blood plasma **(Fig. 1.4)** [138]. As a result, by repeated administration throughout the day to attain and maintain medication concentrations within the therapeutically effective range required for therapy. This causes a variation in plasma-drug levels which can lead to a variety of dose-related adverse effects as well as a reduction in patient compliance [139].

The half-life or mean residence time of medication, as well as its therapeutic index, determine the frequency with which it is administered. In most circumstances, medicines supplied regularly below their biological half-life have a variety of drawbacks that come with traditional dose regimens.

1.8.1. Conventional drug delivery limitations

1. Patient non-compliance is caused by the frequent administration of medicine with a short biological half-life, which raises the odds of skipping a dosage.
2. When a standard dosage product is given orally in many doses, the drug blood concentration rises fast to a high value (“peak”), then drops abruptly to a more low value (“valley”) because of drug excretion.
3. The dosing period is insufficient for the drug's biological half-life, the drug blood level will have large "peaks" and "valleys". The difficulty arises in maintaining a stable steady-state concentration during the therapy.
4. Unavoidable drug concentration variations may result in under- or over-medication, causing the peak plasma concentration to rise towards the

hazardous range or a range that is beyond the therapeutic range

5. The aforesaid constraints of traditional oral drug administration can be mitigated by creating variously sustained/controlled and targeted drug delivery systems that outperform traditional instant release solutions in terms of pharmacological and clinical efficacy.

1.9. The gastrointestinal tract anatomy and physiological properties

Processes of secretion, digesting and absorption are the fundamental activities of the gastrointestinal tract **(Fig 1.5)**. The gastrointestinal barrier permits most minerals and vitamins to flow quickly into systemic circulation via passive diffusion, but it prevents the entry of greater molecular weight drugs and poisons. These materials must be delivered orally into the GI tract, where they are disseminated to various tissues or organs, then absorbed and removed from the body and should pass through biological membranes/barriers at various sites [140]. The components are maintained in the stomach after oral ingestion, where they mix with gastrointestinal fluid are changed into a liquid mass and then transferred into the upper small intestine [139]. As a result, the gastrointestinal tract serves as a key barrier to medication absorption.

The three basic anatomical parts of the gastrointestinal system are the stomach, small intestine and large intestine. When medicine is administered, it passes through several parts of the gastrointestinal tract and is absorbed in the site of action, depending on the electrolytes, pH, fluidity, enzymes and surface characteristics of the gastrointestinal fluid.

With a smooth mucosa and a small surface area, the stomach is formed like a bag. Its acidic pH of 1-3, which is caused by hydrochloric acid production, improves

acidic drug absorption; if they are soluble in stomach fluids, they stay unionized to a considerable extent at such a pH. Following oral admission, substances are transferred to the stomach, which is responsible for storing, mixing and reducing all components to slurry via gastric secretions and then regulating the emptying of these contents into the upper small intestine.

The small intestine is generally the main source of drug absorption having a metabolism area of between 200 to 600 m^2. Long transit time, slow peristaltic movement and high permeability are all important qualities for medication absorption in the small intestine. The extended travel time in the small intestine, which ranges from 3 to 5 hours is rather consistent and unaltered by meal intake. If the medicine disperses in the stomach contents, the drug solution will travel through the small intestine unhindered allowing for optimum absorption. As a result of the interaction of all of the above elements, the small intestine is the optimal place for drug absorption for the majority of medications [141].

The large intestine, which has a tiny absorptive surface normally plays a little role in drug absorption. The stomach, on the other hand is a secretory instead of an absorptive organ and the colon has a tiny absorptive surface therefore it plays a little role in drug absorption because transit periods through the colon can range from less than an hour to more than 60 hours, it is important to plan ahead, since any residual medicine will be imbedded in semi-solid faeces absorption from the distal region can be deemed insignificant [142].

The drug release/absorption from oral drug delivery devices can be considerably affected by changes in the local environment such as surface area, type of luminal contents, pH, length area, the absorptive capacity of three parts of the

gastrointestinal tract residency and transit periods of a controlled release product in each section. Other parameters that impact drug absorption via the oral route include drug solubility and lipophilicity of the drug, particle size, pKa of the drug, polymorphic character, effective surface area and dissolution rate of the medication [143].

1.10. Novel drug delivery systems

Using innovative ways to customize with long half-lives and big curative indices, the possible issues arising from repeated administration of traditional therapy with short biological half-life medications may be eliminated in order to create a unique medication regimen with long half-lives and big therapeutic indices. Several technological breakthroughs have been created in recent years that can maintain medication release rates and extend the duration of therapeutic efficacy. All of these approaches have been beneficial and give a variety of advantages for developing drug delivery devices employing unique fabrication processes that might enhance medicine and therapeutic methods [144-146].

Traditional pharmacological therapy is often provided in the mode of liquids, suspensions, capsules, injections, pills, emulsions and tablets. These formulations have a high level of therapeutic effectiveness yet they result in inefficient drug release. Furthermore, hazardous effects are precipitated by medicines delivered systemically in high dosages with short half-lives, low water solubility and permeability in membranes [147]. To overcome these obstacles, new dosage forms must be developed and new modalities of administration must be used in order to increase disease bioavailability and pharmacotherapy.

1.10.1. Drug delivery systems with a controlled/sustained release concept.

Sustained release techniques use oral, buccal, nasal and topical channels to deliver a drug over a long duration of time during the course of therapy. Targeting a drug to a specific tissue or organ is referred to as special placement, whilst managing the pace of drug delivery to the target tissue is referred to as temporal delivery. A well-designed prolonged or controlled medication release delivery system might be a significant step in resolving these two issues. The medication is released in a regulated way in sustained/controlled release dose forms, either by temporal or spatial methods or both [148].

Sustained release products allow the medicine to be released gradually over a lengthy period of time. The first therapeutic dosage often achieves steady-state concentration, followed by continuous drug release. As a result, sustained release material maintains a steady plasma drug amount during treatment and reduces the variation produced by zero-order release kinetics.

Controlled release refers to delivery systems that administer a drug for a specific amount of time locally or systemically. The rate of release of active ingredients from controlled release pharmaceutical administration is not only advanced but also constant from one unit to the next. The distribution of medicine from the dosage is the rate-determining process in controlled drug delivery systems [149]. The following are the key benefits of medicine delivery systems with a prolonged or controlled release:

1. Maintaining the optimal therapeutic medication concentration in the blood with the least amount of variability possible.

2. Increased activity duration for medicines with a short half-life.

3. Improve patient compliance by optimizing the treatment.

4. Side effects, frequent dosage and medication waste are all eliminated.

5. Predictable and reproducible release rates for an extended duration.

6. Economical: When compared to quick dose solutions, the expense of therapy over a longer period of time may be lower, as well as a reduction in caring time and hospitalization.

These customized drug delivery systems are extremely suitable for various medications and chronic illness situations such as cancer therapy, arthritis, angina pectoris, fertility control, diabetes, glaucoma and hypertension among others due to the benefits listed above. There are now a variety of medications on the market that are manufactured for nasal, parenteral, pulmonary-through lungs, ocular-through eye, oral and transdermal-through skin, delivery of drugs to the body in order to form them highly effective, simple to give and release them over the length of therapy [150].

1.11. Aim of the present study

In this regard, we have synthesized the various hydrogels using simple and effective methods via free radical polymerization. The synthesized hydrogels were characterized through various analytical techniques such as Fourier transform infrared spectroscopy (FTIR), UV-Visible spectrometry, Scanning electron microscope (SEM) and Thermogravimetric analyzer (TGA). Further, their swelling properties were analyzed at different temperatures, pH and salt solutions. The synthesized hydrogels show excellent controlled drug release properties. The obtained results prove that the synthesized hydrogels were suitable for drug delivery applications. The present work carried out under the following objectives are described in the corresponding chapters.

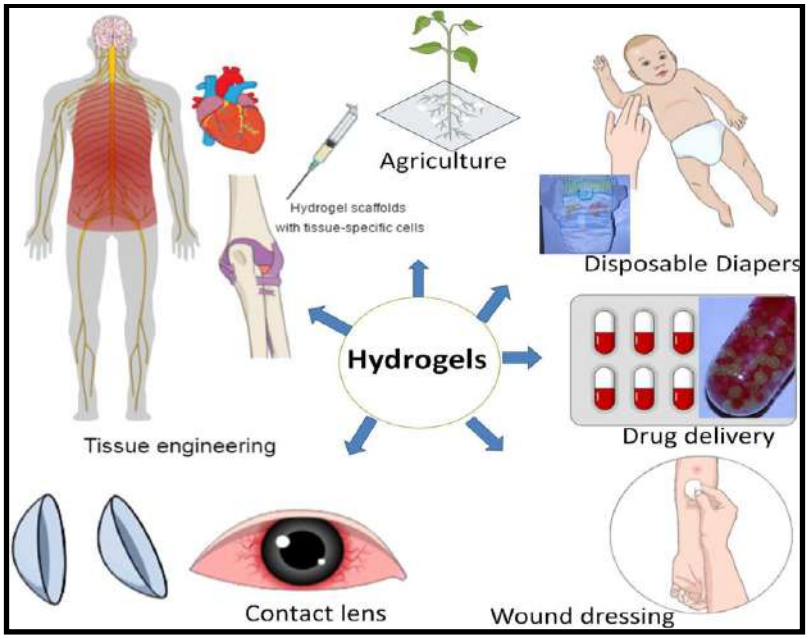

Figure 1.1. Hydrogels and their significance in their various fields of applications [25].

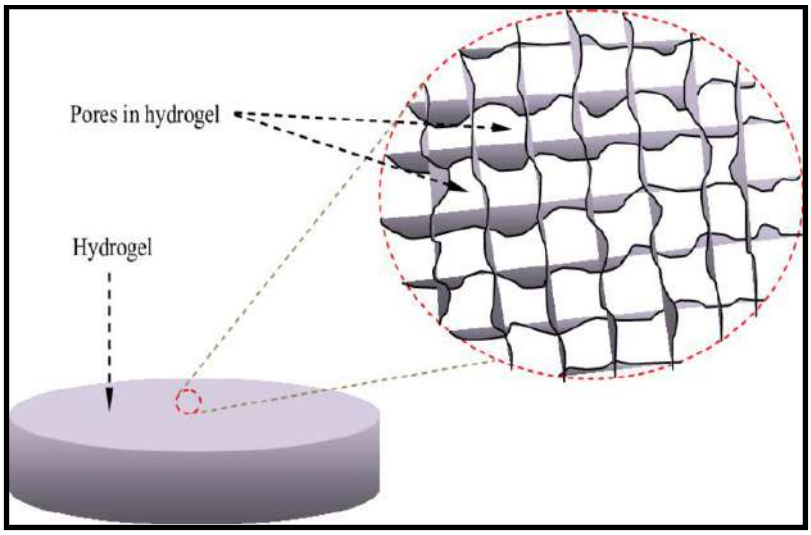

Figure 1.2. Schematic view of 3-dimensionally crosslinked network structure in hydrogel[26].

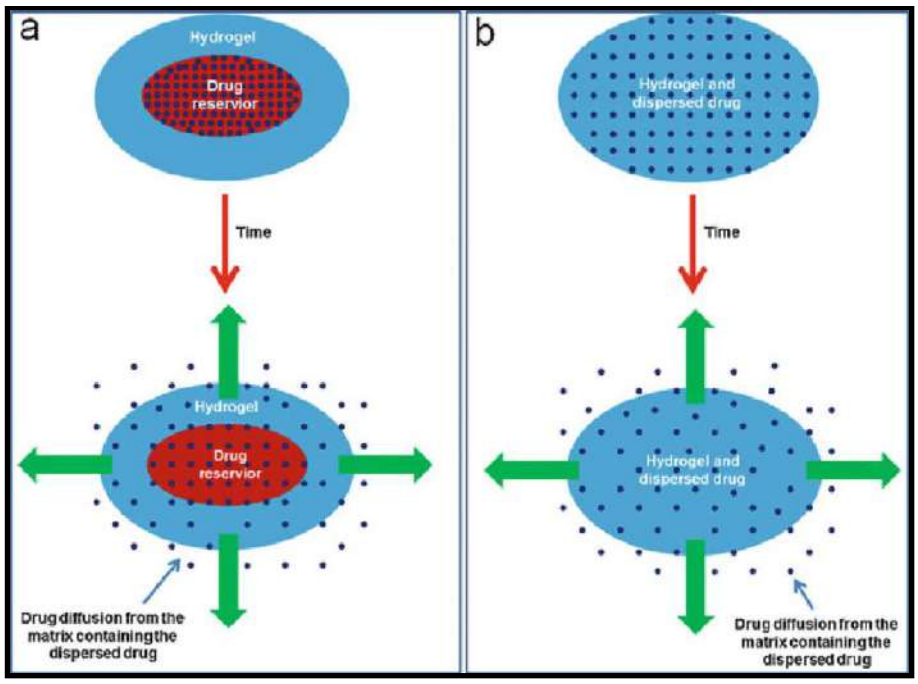

Figure 1.3. Mechanism of drug release through hydrogel membrane in (a) reservoir system and (b) matrix system [64].

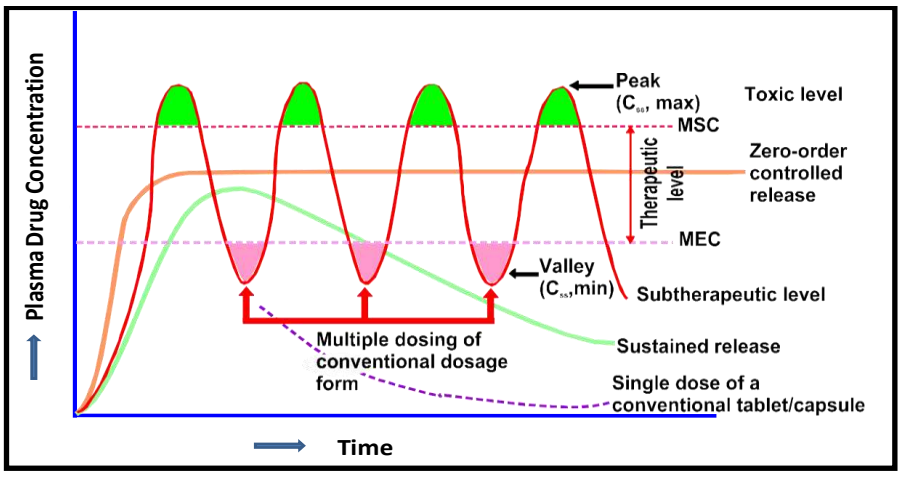

Figure 1.4. The drug level v/s time graph shows the differences between controlled release (zero-order release), immediate release (from a conventional capsule or tablet) and sustained release (delayed first-order) dose forms. (MSC = maximum safe concentration, MEC = minimum effective concentration).

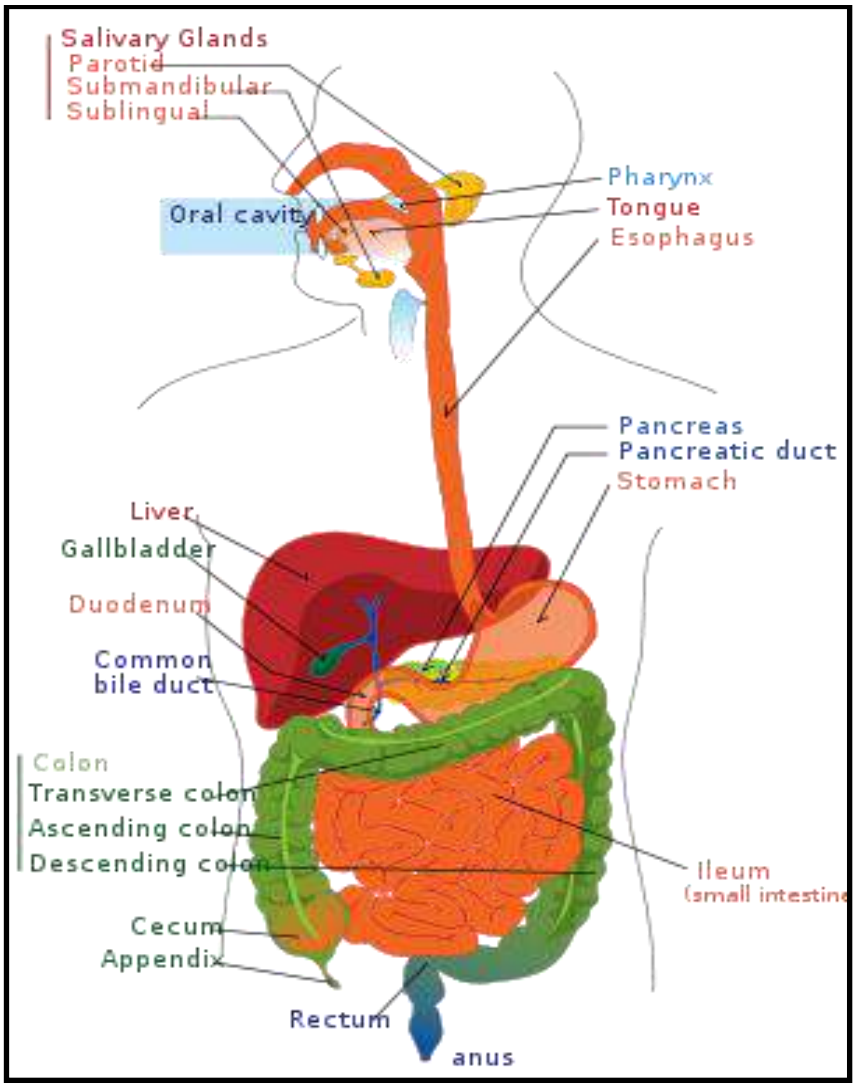

Figure 1.5. The GIT and the many sites of drug absorption are depicted in this diagram.

Table 1.1. Examples of crosslinking agents and monomers used in hydrogel synthesis.

Monomers	
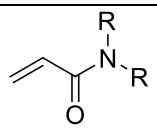	*N*, *N*-dialkylacrylamides
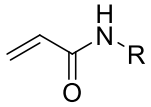	*N*-alkylacrylamides
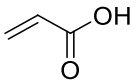	Acrylic acid
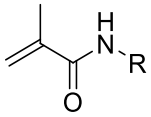	*N*-alkylmethacrylamides
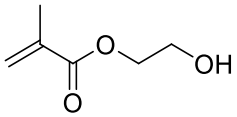	2-Hydroxyethyl methacrylate
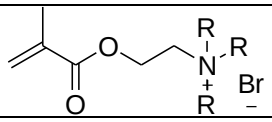	Methacryloyloxy ethyl tri alkylammonium bromide
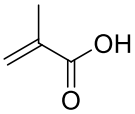	Methacrylic acid
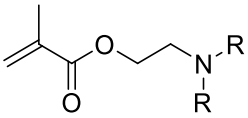	*N*,*N*-dialkylaminoethyl methacrylate
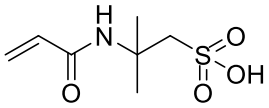	2-Acrylamido-2-methyl propanesulfonic acid
Crosslinking Agents	
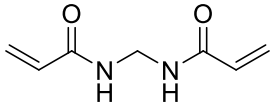	Methylenebisacrylamide
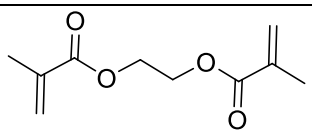	Ethylene dimethacrylate

Table 1.2. Examples of stimuli-responsive hydrogels in drug delivery.

Hydrogels	Stimuli	Drug	References
Ethylene-co-vinyl acetate [EVAc]	Ultrasonic radiation	Insulin	65
Gelatin – PEO	pH	Riboflavin	66
PNIPAM-co-butyl methacrylate-co-AA	pH & Temperature	Calcitonin	67
EVAc	Glucose	Insulin	68
Chitosan – PEO	pH	Amoxicillin, Metronidazole	69
Poly (N-isopropyl acrylamide) [PNIPAM]	Temperature	Heparin	70
EVAc	Magnetic field	Insulin	71
PHEMA [Poly (2, hydroxyl ethyl methacrylate)]	Electric field	Propranolol hydrochloride	72
PHEMA	pH	Salicylic acid	73

Table 1.3. Industrial polymers have been used to make scaffolds for tissue engineering applications.

Polymer	Application	Commercial name
Polyanhydride	Chemo-therapeutic application	Gliadel
PLGA [Poly lactic glycolic acid]	Skin graft	Vicryl Mesh
PGA [Poly glycolic acid]	Biodegradable synthetic suture	Dexor
PLDLA [Poly lactic-d-lactic acid]	Bioresorbable Implant	Resomer
PEU [Polyethylene urethane]	Tissue engineering	Degrapol
HA [Hyaluronic acid]	Bone graft	Ossigel
PLGA-Collagen	Tissue regeneration membrane	Cytoplast Resorb
Collagen	Bioengineered skin equivalent	Transcyte

1.12. References

[1] Yang C. Y., Song B., Ao Y., Nowak A. P., Abelowitz R. B., Korsak R. A., Havton L. A., Deming T. J., Sofroniew M. V.; Biocompatibility of amphiphilic diblock copolypeptide hydrogels in the central nervous system. *Biomaterials*, 2009, 30 (15), 2881-2898.

[2] Darnell M. C., Sun J. Y., Mehta M., Johnson C., Arany P. R., Suo Z., Mooney D. J.; Performance and biocompatibility of extremely tough alginate/polyacrylamide hydrogels. *Biomaterials*, 2013, 34 (33), 8042-8048.

[3] Alexander C.; Stimuli-responsive hydrogels: Drugs take control. *Nature Materials*, 2008, 7 (10), 767-768.

[4] Koetting M. C., Peters J. T., Steichen S. D., Peppas N. A.; Stimulus-responsive hydrogels: Theory modern advances and applications. *Materials Science and Engineering: R: Reports*, 2015, 93, 1-49.

[5] Sood N., Bhardwaj A., Mehta S., Mehta A.; Stimuli-responsive hydrogels in drug delivery and tissue engineering. *Drug Delivery*, 2016, 23 (3), 758-780.

[6] Hoch G., Chauhan A., Radke C. J.; Permeability and diffusivity for water transport through hydrogel membranes. *Journal of Membrane Science*, 2003, 214 (2), 199-209.

[7] Tuncaboylu D. C., Sari M., Oppermann W., Okay O.; Tough and Self-Healing Hydrogels Formed via Hydrophobic Interactions. *Macromolecules* , 2011, 44 (12), 4997-5005.

[8] Gulyuz U., Okay O.; Self-Healing Poly(acrylic acid) Hydrogels with Shape Memory Behavior of High Mechanical Strength. *Macromolecules*, 2014, 47 (19), 6889-6899.

[9] Jacob R. S., Ghosh D., Singh P. K., Basu S. K., Jha N. N., Das S., Sukul P. K., Patil S., Sathaye S., Kumar A., Chowdhury A., Malik S., Sen S., Maji S. K.; Self healing hydrogels composed of amyloid nano fibrils for cell culture and stem cell differentiation. *Biomaterials*, 2015, 54, 97-105.

[10] Hoare T. R., Kohane D. S.; Hydrogels in drug delivery: Progress and challenges. *Polymer*, 2008, 49 (8), 1993-2007.

[11] Zhang H., Patel A., Gaharwar A. K., Mihaila S. M., Iviglia G., Mukundan S., Bae H., Yang H., Khademhosseini A.; Hyperbranched Polyester

Hydrogels with Controlled Drug Release and Cell Adhesion Properties. *Biomacromolecules,* 2013, 14 (5), 1299-1310.

[12] Lee K. Y., Mooney D. J.; Hydrogels for tissue engineering. *Chemical Reviews,* 2001, 101 (7), 1869-1879.

[13] Hoffman A. S.; Hydrogels for biomedical applications. *Advanced Drug Delivery Reviews,* 2002, 54 (1), 3-12.

[14] Zhu J.; Bioactive modification of poly(ethylene glycol) hydrogels for tissue engineering. *Biomaterials,* 2010, 31 (17), 4639-4656.

[15] Van Vlierberghe S., Dubruel P., Schacht E.; Biopolymer-Based Hydrogels As Scaffolds for Tissue Engineering Applications: A Review. *Biomacromolecules,* 2011, 12 (5), 1387-1408.

[16] Hunt J. A., Chen R., van Veen T., Bryan N.; Hydrogels for tissue engineering and regenerative medicine. *Journal of Materials Chemistry B,* 2014, 2 (33), 5319-5338.

[17] Tibbitt M. W., Anseth K. S.; Hydrogels as extracellular matrix mimics for 3Dcell culture. *Biotechnology and Bioengineering,* 2009, 103 (4), 655-663.

[18] Higashi K., Miki N.; A self-swimming microbial robot using microfabricated nanofibrous hydrogel. *Sensors and Actuators B: Chemical,* 2014, 202, 301- 306.

[19] Kim B., Lee Y., Lee K., Koh W. G.; Immobilization of enzymes within hydrogel microparticles to create optical biosensors for the detection of organophosphorus compounds. *Current Applied Physics,* 2009, 9 (4 Supplement), e225-e228.

[20] Ionov L.; Hydrogel-based actuators: possibilities and limitations. *Materials Today,* 2014, 17 (10), 494-503.

[21] Buenger D., Topuz F., Groll J.; Hydrogels in sensing applications. *Progress in Polymer Science,* 2012, 37 (12), 1678-1719.

[22] Wichterle O., Lim D.; Hydrophilic Gels for Biological Use. *Nature,* 1960, 185 (4706), 117-118.

[23] Caló E., Khutoryanskiy V. V.; Biomedical applications of hydrogels: A review of patents and commercial products. *European Polymer Journal,*

2015, 65, 252-267.

[24] Kashyap N., Kumar N., Kumar M. N. V. R.; Hydrogels for Pharmaceutical and Biomedical Applications. *Critical Reviews in therapeutic Drug Carrier Systems,* 2005, 22 (2), 107-150.

[25] Kokkarachedu V., Gownolla M. R., Tippabattini J., Murali M.Y., Rotimi S.; A mini review on hydrogels classification and recent developments in miscellaneous applications. Elsevier. *Materials Science and Engineering C,* 2017, 79, 958-971.

[26] Niladri R. and Nabanita S.; PVP-Based Hydrogels: Synthesis Properties and Applications. 2012, 1-33.

[27] Conley G. M., Nöjd S., Braibanti M., Schurtenberger P., Scheffold F.; Superresolution microscopy of the volume phase transition of pNIPAM microgels. *Colloids and Surfaces A: Physicochemical and Engineering Aspects,* 2016, 499, 18-23.

[28] Philippova O. E., Hourdet D., Audebert R., Khokhlov A. R.; Interaction of Hydrophobically Modified Poly(acrylic acid) Hydrogels with Ionic Surfactants. *Macromolecules,* 1996, 29 (8), 2822-2830.

[29] Karakasyan C., Lack S., Brunel F., Maingault P., Hourdet D.; Synthesis and Rheological Properties of Responsive Thickeners Based on Polysaccharide Architectures. *Biomacromolecules,* 2008, 9 (9), 2419-2429.

[30] Hu J., Ge Z., Zhou Y., Zhang Y., Liu S.; Unique Thermo-Induced Sequential Gel−Sol−Gel Transition of Responsive Multiblock Copolymer Based Hydrogels. *Macromolecules,* 2010, 43 (12), 5184-5187.

[31] Brassinne J., Stevens A. M., Van Ruymbeke E., Gohy J. F., Fustin C. A.; Hydrogels with Dual Relaxation and Two-Step Gel–Sol Transition from Heterotelechelic Polymers. *Macromolecules,* 2013, 46 (22), 9134-9143.

[32] Yang Q., Song C., Chen Q., Zhang P., Wang P.; Synthesis and aqueous solution properties of hydrophobically modified anionic acrylamide copolymers. *Journal of Polymer Science Part B: Polymer Physics,* 2008, 46 (22), 2465-2474.

[33] Shashkina Y. A., Zaroslov Y. D., Smirnov V. A., Philippova O. E.,

Khokhlov A. R., Pryakhina T. A., Churochkina N. A.; Hydrophobic aggregation in aqueous solutions of hydrophobically modified polyacrylamide in the vicinity of overlap concentration. *Polymer*, 2003, 44 (8), 2289-2293.

[34] Al-Sabagh A. M., Kandile N. G., El-Ghazawy R. A., Noor El-Din M. R., El-sharaky E. A.; Synthesis and characterization of high molecular weight hydrophobically modified polyacrylamide nanolatexes using novel nonionic polymerizable surfactants. *Egyptian Journal of Petroleum*, 2013, 22 (4), 531- 538.

[35] Karunasena A., Brown R. G., Glass J. E.; Hydrophobically Modified Ethoxylated Urethane Architecture. *Polymers in Aqueous Media.* American Chemical Society. 1989, 223, 495-525.

[36] Shay G. D.; Alkali-Swellable and Alkali-Soluble Thickener Technology. *Polymers in Aqueous Media.* American Chemical Society. 1989, 223, 457-494.

[37] Shay G. D., Kravitz F. K., Brizgys P. V.; Effects of Process Variables on the Emulsion and Solution Properties of Hydrophobically Modified Alkali-Swellable Emulsion Thickeners. *Polymers as Rheology Modifiers.* American Chemical Society. 1991, 462, 121-141.

[38] Siu H., Duhamel J.; Associations between a Pyrene-Labeled Hydrophobically Modified Alkali Swellable Emulsion Copolymer and Sodium Dodecyl Sulfate Probed by Fluorescence Surface Tension and Viscometry. *Macromolecules*, 1991, 39 (3), 1144-1155.

[39] English R. J., Jenkins R. D., Bassett D. R., Khan S. A.; Rheology of a HASE Associative Polymer and Its Interaction with Non-Ionic Surfactants. *Associative Polymers in Aqueous Media.* American Chemical Society. 2000, 765, 369-380.

[40] English R. J., Laurer J. H., Spontak R. J., Khan S. A.; Hydrophobically Modified Associative Polymer Solutions: Rheology and Microstructure in the Presence of Nonionic Surfactants. *Industrial & Engineering Chemistry Research*, 2000, 41 (25), 6425-6435.

[41] Miller C. M., Olesen K. R., Shay G. D.; Determination of the Thickening

Mechanism of a Hydrophobically Modified Alkali Soluble Emulsion Using Dynamic Viscosity Measurements. *Associative Polymers in Aqueous Media*, American Chemical Society. 2000, 765, 338-350.

[42] Suzuki S., Uneyama T., Watanabe H.; Concentration Dependence of Nonlinear Rheological Properties of Hydrophobically Modified Ethoxylated Urethane Aqueous Solutions. *Macromolecules,* 1989, 46 (9), 3497-3504.

[43] Kaczmarski J. P., Glass J. E.; Synthesis and Characterization of Step Growth Hydrophobically-Modified Ethoxylated Urethane Associative Thickeners. *Langmuir,* 2000, 10 (9), 3035-3042.

[44] Ma Z., Glass J. E.; Complexations of Beta-Cyclodextrin with Surfactants andHydrophobically Modified Ethoxylated Urethanes. *Associative Polymers in Aqueous Media.* American Chemical Society. 2000, 765, 254-270.

[45] Gandhi A., Paul A., Sen S. O., Sen K. K.; Studies on thermoresponsive polymers: Phase behaviour drug delivery and biomedical applications. *Asian Journal of Pharmaceutical Sciences,* 2015, 10 (2), 99-107.

[46] Haraguchi K., Takehisa T.; Nanocomposite hydrogels: A unique organic-inorganic network structure with extraordinary mechanical optical and swelling/de-swelling properties. *Advanced Materials,* 2002, 14 (16), 1120-1124.

[47] Schexnailder P., Schmidt G.; Nanocomposite polymer hydrogels. *Colloid and Polymer Science,* 2009, 287 (1), 1-11.

[48] Wang Q., Mynar J. L., Yoshida M., Lee E., Lee M., Okuro K., Kinbara K., Aida T.; High-water-content mouldable hydrogels by mixing clay and a dendritic molecular binder. *Nature,* 2010, 463 (7279), 339-343.

[49] Gaharwar A. K., Peppas N. A., Khademhosseini A.; Nanocomposite hydrogels for biomedical applications. *Biotechnology and Bioengineering,* 2014, 111 (3), 441-453.

[50] Kato K., Inoue K., Kidowaki M., Ito K.; Organic−Inorganic Hybrid Slide-Ring Gels: Polyrotaxanes Consisting of Poly(dimethylsiloxane) and γ-Cyclodextrin and Subsequent Topological Cross-Linking. *Macromolecules,* 2009, 42 (18), 7129-7136.

[51] Bin Imran A., Esaki K., Gotoh H., Seki T., Ito K., Sakai Y., Takeoka Y.;

Extremely stretchable thermosensitive hydrogels by introducing slide-ring polyrotaxane cross-linkers and ionic groups into the polymer network. *Nature Communications,* 2014, 5.

[52] Gong J. P., Katsuyama Y., Kurokawa T., Osada Y.; Double-network hydrogels with extremely high mechanical strength. *Advanced Materials,* 2003,15 (14), 1155-1158.

[53] Brown H. R.; A Model of the Fracture of Double Network Gels. *Macromolecules,* 2007, 40 (10), 3815-3818.

[54] Webber R. E., Creton C., Brown H. R., Gong J. P.; Large Strain Hysteresis and Mullins Effect of Tough Double-Network Hydrogels. *Macromolecules,* 2007, 40 (8), 2919-2927.

[55] Yu Q. M., Tanaka Y., Furukawa H., Kurokawa T., Gong J. P.; Direct Observation of Damage Zone around Crack Tips in Double-Network Gels. *Macromolecules,* 2009, 42 (12), 3852-3855.

[56] Okumura Y., Ito K.; The Polyrotaxane Gel: A Topological Gel by Figure-of-Eight Cross-links. *Advanced Materials,* 2001, 13 (7), 485-487.

[57] Nakayama A., Kakugo A., Gong J. P., Osada Y., Takai M., Erata T., Kawano S.; High Mechanical Strength Double-Network Hydrogel with Bacterial Cellulose. *Advanced Functional Materials,* 2004, 14 (11), 1124-1128.

[58] Ito K.; Novel Cross-Linking Concept of Polymer Network: Synthesis Structure and Properties of Slide-Ring Gels with Freely Movable Junctions. *Polymer Journal,* 2007, 39 (6), 489-499.

[59] Johnson J. A., Turro N. J., Koberstein J. T., Mark J. E.; Some hydrogels having novel molecular structures. *Progress in Polymer Science,* 2010, 35 (3), 332-337.

[60] Peak C. W., Wilker J. J., Schmidt G.; A review on tough and sticky hydrogels. *Colloid and Polymer Science,* 2013, 291 (9), 2031-2047.

[61] Nyberg T., Inganäs O., Jerregård H.; Polymer Hydrogel Microelectrodes for Neural Communication. *Biomedical Microdevices,* 2002, 4 (1), 43-52.

[62] Brahim S., Narinesingh D., Guiseppi-Elie A.; Polypyrrole-hydrogel

composites for the construction of clinically important biosensors. *Biosensors and Bioelectronics,* 2002, 17 (1–2), 53-59.

[63] Murdan S.; Electro-responsive drug delivery from hydrogels. *Journal of Controlled Release,* 2003, 92 (1–2), 1-17.

[64] Sharma A. K. Priya & Kaith B. S.; Polymer Nanocomposite Matrices: Classification Synthesis Methods and Applications. *Handbook of Polymer and Ceramic Nanotechnology,* 2019, *1–26.*

[65] Lee V. H.; Encyclopedia of Controlled Drug Delivery Volume 1 and 2. *Journal of Controlled Release,* 2001, 71 (3), 353-354.

[66] Amiji M., Tailor R., Ly M. K., Goreham J.; Gelatin-Poly(Ethylene Oxide) Semi-interpenetrating Polymer Network with pH-Sensitive Swelling and Enzyme-Degradable Properties for Oral Drug Delivery. *Drug Development and Industrial Pharmacy,* 1997, 23 (6), 575-582.

[67] Serres A., Baudyš M., Kim S. W.; Temperature and pH-sensitive Polymers for Human Calcitonin Delivery. *Pharmaceutical Research,* 13 (2), 196-201.

[68] Brown L. R., Edelman E. R., Fischel-Ghodsian F., Langer R.; Characterization of glucose-mediated insulin release from implantable polymers. *Journal of Pharmaceutical Sciences,* 1996, 85 (12), 1341-1345.

[69] Patel V. R., Amiji M. M.; Preparation and characterization of freeze-dried chitosan-poly (ethylene oxide) hydrogels for site-specific antibiotic delivery inthe stomach. *Pharmaceutical Research,* 1996, 13 (4), 588-593.

[70] Gutowska A., Bae Y. H., Feijen J., Kim S. W.; Heparin release from thermosensitive hydrogels. *Journal of Controlled Release,* 1992, 22 (2), 95-104.

[71] Creque H. M., Langer R., Folkman J.; One Month of Sustained Release of Insulin from a Polymer Implant. *Diabetes,* 1980, 29 (1), 37-40.

[72] D'Emanuele A., Staniforth J. N.; An electrically modulated drug delivery device: I. *Pharmaceutical Research,* 1991, 8 (7), 913-918.

[73] Ferreira L., Vidal M. M., Gil M. H.; Evaluation of poly(2-hydroxyethyl methacrylate) gels as drug delivery systems at different pH values. *International Journal of Pharmaceutics,* 2000, 194 (2), 169-180.

[74] Nuttelman C. R., Tripodi M. C., Anseth K. S.; Dexamethasone-

functionalized gels induce osteogenic differentiation of encapsulated hMSCs. *Journal of Biomedical Materials Research Part A*, 2006, 76A (1), 183-195.

[75] Suh S. W., Shin J. Y., Kim J. H., Kim J. G., Beak C. H., Kim D. I., Kim S. J., Jeon S. S., Choo I. W.; Effect of different particles on cell proliferation in polymer scaffolds using a solvent-casting and particulate leachingtechnique. *Asaio Journal*, 2002, 48 (5), 460-464.

[76] Zhang J. C., Wu L. B., Jing D. Y., Ding J. D.; A comparative study of porous scaffolds with cubic and spherical macropores. *Polymer*, 2005, 46 (13), 4979-4985.

[77] Sheridan M. H., Shea L. D., Peters M. C., Mooney D. J.; Bioadsorbable polymer scaffolds for tissue engineering capable of sustained growth factor delivery. *Journal of Controlled Release*, 2000, 64 (1-3), 91-102.

[78] Quirk R. A., France R. M., Shakesheff K. M., Howdle S. M.; Supercritical fluid technologies and tissue engineering scaffolds. *Current Opinion in Solid State & Materials Science*, 2004, 8 (3-4), 313-321.

[79] Lips P. A. M., Velthoen I. W., Dijkstra P. J., Wessling M., Feijen J.; Gas foaming of segmented poly(ester amide) films. *Polymer*, 2005, 46 (22), 9396- 9403.

[80] Lin W. C., Yu D. G., Yang M. C.; Blood compatibility of novel poly(γ-glutamic acid)/polyvinyl alcohol hydrogels. *Colloids and Surfaces B: Biointerfaces*, 2006, 47 (1), 43-49.

[81] Lee M., Wu B. M., Dunn J. C. Y.; Effect of scaffold architecture and pore size on smooth muscle cell growth. *Journal of Biomedical Materials Research Part A*, 2008, 87A (4), 1010-1016.

[82] Dhandayuthapani B., Anila M., Ravindran Girija A., Yutaka N., Venugopal K., Yasuhiko Y., Toru M., Sakthikumar D.; Hybrid fluorescent curcumin loaded zein electrospun nanofibrous scaffold for biomedical applications. *Biomedical Materials*, 2012, 7 (4), 045001.

[83] Badiger M. V., McNeill M. E., Graham N. B.; Porogens in the preparation of microporous hydrogels based on poly(ethylene oxides). *Biomaterials*, 1993, 14 (14), 1059-1063.

[84] Annabi N., Nichol J. W., Zhong X., Ji C., Koshy S., Khademhosseini A., Dehghani F.; Controlling the Porosity and Microarchitecture of Hydrogels for Tissue Engineering. *Tissue Engineering. Part B, Reviews,* 2010, 16 (4), 371- 383.

[85] Mata A., Kim E. J., Boehm C. A., Fleischman A. J., Muschler G. F., Roy S.; A three-dimensional scaffold with precise micro-architecture and surface micro-textures. *Biomaterials,* 2009, 30 (27), 4610-4617.

[86] Ashammakhi N., Rokkanen P.; Absorbable polyglycolide devices in trauma and bone surgery. *Biomaterials,* 1997, 18 (1), 3-9.

[87] Burkoth A. K., Anseth K. S.; A review of photocrosslinked polyanhydrides:: in situ forming degradable networks. *Biomaterials,* 2000, 21 (23), 2395-2404.

[88] Thomson R. C., Mikos A. G., Beahm E., Lemon J. C., Satterfield W. C., Aufdemorte T. B., Miller M. J.; Guided tissue fabrication from periosteum using preformed biodegradable polymer scaffolds. *Biomaterials,* 1999, 20 (21), 2007-2018.

[89] Shalaby W. S.; Bioabsorbable Polymers. In *Encyclopedia of Pharmaceutical Technology, Third Edition,* Taylor & Francis: 2013; Vol. 1, pp 155-163.

[90] Andriano K. P., Tabata Y., Ikada Y., Heller J.; In vitro and in vivo comparison of bulk and surface hydrolysis in absorbable polymer scaffolds for tissue engineering. *Journal of Biomedical Materials Research,* 1999, 48 (5), 602-612.

[91] Peppas N. A., Stauffer S. R.; Reinforced uncrosslinked poly (vinyl alcohol) gels produced by cyclic freezing-thawing processes: a short review. *Journal ofControlled Release,* 1991, 16 (3), 305-310.

[92] Burczak K., Gamian E., Kochman A.; Long-term in vivo performance and biocompatibility of poly(vinyl alcohol) hydrogel macrocapsules for hybrid-type artificial pancreas. *Biomaterials,* 1996, 17 (24), 2351-2356.

[93] Zalipsky S.; Synthesis of an end-group functionalized polyethylene glycol-lipid conjugate for preparation of polymer-grafted liposomes. *Bioconjugate Chemistry,* 1993, 4 (4), 296-299.

[94] Zalipsky S.; Functionalized Poly(ethylene glycols) for Preparation of

Biologically Relevant Conjugates. *Bioconjugate Chemistry*, 1995, 6 (2), 150- 165.

[95] Gombotz W. R., Pettit D. K.; Biodegradable Polymers for Protein and Peptide Drug Delivery. *Bioconjugate Chemistry*, 1995, 6 (4), 332-351.

[96] West J. L., Hubbell J. A.; Polymeric Biomaterials with Degradation Sites for Proteases Involved in Cell Migration. *Macromolecules*, 1999, 32 (1), 241-244.

[97] Andreopoulos F. M., Deible C. R., Stauffer M. T., Weber S. G., Wagner W. R., Beckman E. J., Russell A. J.; Photoscissable Hydrogel Synthesis via Rapid Photopolymerization of Novel PEG-Based Polymers in the Absence of Photoinitiators. *Journal of the American Chemical Society*, 1996, 118 (26), 6235-6240.

[98] Deming T. J.; Facile synthesis of block copolypeptides of defined architecture. *Nature*, 1997, 390 (6658), 386-389.

[99] Urry D. W.; Molecular Machines: How Motion and Other Functions of Living Organisms Can Result from Reversible Chemical Changes. *Angewandte Chemie International Edition in English*, 1993, 32 (6), 819-841.

[100] Panitch A., Yamaoka T., Fournier M. J., Mason T. L., Tirrell D. A.; Design and Biosynthesis of Elastin-like Artificial Extracellular Matrix Proteins Containing Periodically Spaced Fibronectin CS5 Domains. *Macromolecules*, 1999, 32 (5), 1701-1703.

[101] Stile R. A., Healy K. E.; Poly (N-isopropylacrylamide)-based semi-interpenetrating polymer networks for tissue engineering applications. 1. Effects of linear poly (acrylic acid) chains on phase behavior. *Biomacromolecules*, 2002, 3 (3), 591-600.

[102] Lu Y., Wang D., Li T., Zhao X., Cao Y., Yang H., Duan Y. Y.; Poly (vinyl alcohol)/poly (acrylic acid) hydrogel coatings for improving electrode neural tissue interface. *Biomaterials*, 2009, 30 (25), 4143-4151.

[103] Rault I., Frei V., Herbage D., Abdul-Malak N., Huc A.; Evaluation of different chemical methods for cros-linking collagen gel, films and sponges. *Journal of Materials Science: Materials in Medicine*, 1996, 7 (4), 215-221.

[104] Srivastava S., Gorham S. D., Courtney J. M.; The attachment and growth of

an established cell line on collagen, chemically modified collagen, and collagen composite surfaces. *Biomaterials,* 1990, 11 (3), 162-168.

[105] Chenite A., Chaput C., Wang D., Combes C., Buschmann M. D., Hoemann C. D., Leroux J. C., Atkinson B. L., Binette F., Selmani A.; Novel injectable neutral solutions of chitosan form biodegradable gels in situ. *Biomaterials,* 2000, 21 (21), 2155-2161.

[106] Muzzarelli R. A. A., Zucchini C., Ilari P., Pugnaloni A., Mattioli Belmonte M., Biagini G., Castaldini C.; Osteoconductive properties of methylpyrrolidinone chitosan in an animal model. *Biomaterials,* 1993, 14 (12),925-929.

[107] Uludag H., De Vos P., Tresco P. A.; Technology of mammalian cell encapsulation. *Advanced Drug Delivery Reviews,* 2000, 42 (1–2), 29-64.

[108] Klöck G., Pfeffermann A., Ryser C., Gröhn P., Kuttler B., Hahn H. J., Zimmermann U.; Biocompatibility of mannuronic acid-rich alginates. *Biomaterials,* 1997, 18 (10), 707-713.

[109] Dillon G. P., Xiaojun Y., Sridharan A., Ranieri J. P., Bellamkonda R. V.; The influence of physical structure and charge on neurite extension in a 3D hydrogel scaffold. *Journal of Biomaterials Science, Polymer Edition,* 1998, 9 (10), 1049-1069.

[110] Borkenhagen M., Clémence J. F., Sigrist H., Aebischer P.; Three-dimensional extracellular matrix engineering in the nervous system. *Journal ofBiomedical Materials Research,* 1998, 40 (3), 392-400.

[111] Schense J. C., Hubbell J. A.; Cross-Linking Exogenous Bifunctional Peptides into Fibrin Gels with Factor XIIIa. *Bioconjugate Chemistry,* 1999, 10 (1), 75- 81.

[112] Vercruysse K. P., Marecak D. M., Marecek J. F., Prestwich G. D.; Synthesis and in Vitro Degradation of New Polyvalent Hydrazide Cross-Linked Hydrogels of Hyaluronic Acid. *Bioconjugate Chemistry,* 1997, 8 (5), 686-694.

[113] Liu L. S., Thompson A. Y., Heidaran M. A., Poser J. W., Spiro R. C., An osteoconductive collagen/hyaluronate matrix for bone regeneration. *Biomaterials,* 1999, 20 (12), 1097-1108.

[114] Kuijpers A. J., Engbers G. H. M., Feijen J., De Smedt S. C., Meyvis T. K. L., Demeester J., Krijgsveld J., Zaat S. A. J., Dankert J.; Characterization of the Network Structure of Carbodiimide Cross-Linked Gelatin Gels. *Macromolecules,* 1999, 32 (10), 3325-3333.

[115] Choi Y. S., Hong S. R., Lee Y. M., Song K. W., Park M. H., Nam Y. S.; Study on gelatin-containing artificial skin: I. Preparation and characteristics of novel gelatin-alginate sponge. *Biomaterials,* 1999, 20 (5), 409-417.

[116] Aurand E. R., Lampe K. J., Bjugstad K. B.; Defining and designing polymers and hydrogels for neural tissue engineering. *Neuroscience Research,* 2012, 72 (3), 199-213.

[117] Kim I. L., Mauck R. L., Burdick J. A.; Hydrogel design for cartilage tissue engineering: A case study with hyaluronic acid. *Biomaterials,* 2011, 32 (34), 8771-8782.

[118] Hammond T. H., Zhou R., Hammond E. H., Pawlak A., Gray S. D.; The intermediate layer: A morphologic study of the elastin and hyaluronic acid constituents of normal human vocal folds. *Journal of Voice,* 1997, 11 (1), 59- 66.

[119] Xavier J. R., Thakur T., Desai P., Jaiswal M. K., Sears N., Cosgriff-Hernandez E., Kaunas R., Gaharwar A. K.; Bioactive Nanoengineered Hydrogels for Bone Tissue Engineering: A Growth-Factor-Free Approach. *AcsNano,* 2015, 9 (3), 3109-3118.

[120] Vavken P.; Tissue Engineering of Ligaments and Tendons. In *Fundamentals of Tissue Engineering and Regenerative Medicine,* Meyer U., Handschel J., Wiesmann P. H., Meyer T.; Eds. Springer Berlin Heidelberg: Berlin, Heidelberg, 2009, pp 317-327.

[121] Caseiro A. R., Pereira T., Bártolo P. J., Santos J. D., Luís A. L., Maurício A. C.; Mesenchymal Stem Cells and Biomaterials Systems – Perspectives for Skeletal Muscle Tissue Repair and Regeneration. *Procedia Engineering,* 2015, 110, 90-97.

[122] Puperi D. S., O'Connell R. W., Punske Z. E., Wu Y., West J. L., Grande-Allen K. J.; Hyaluronan Hydrogels for a Biomimetic Spongiosa Layer of Tissue Engineered Heart Valve Scaffolds. *Biomacromolecules,* 2016.

[123] Yoo B. Y., Shin Y. H., Yoon H. H., Seo Y. K., Park J. K.; Hair follicular cell/organ culture in tissue engineering and regenerative medicine. *Biochemical Engineering Journal*, 2010, 48 (3), 323-331.

[124] Dunphy S. E., Bratt J. A. J., Akram K. M., Forsyth N. R., El Haj A. J.; Hydrogels for lung tissue engineering: Biomechanical properties of thin collagen–elastin constructs. *Journal of the Mechanical Behavior of BiomedicalMaterials*, 2014, 38, 251-259.

[125] He X., Fu W., Zheng J.; Cell sources for trachea tissue engineering: past, present and future. *Regenerative medicine*, 2012, 7 (6), 851-863.

[126] Tan H., Gong Y., Lao L., Mao Z., Gao C.; Gelatin/chitosan/hyaluronan ternary complex scaffold containing basic fibroblast growth factor for cartilage tissue engineering. *Journal of Materials Science: Materials in Medicine*, 2007, 18 (10), 1961-1968.

[127] Mjahed H., Porcel C., Senger B., Chassepot A., Netter P., Gillet P., Decher G., Voegel J. C., Schaaf P., Benkirane-Jessel N., Boulmedais F.; Micro-stratified architectures based on successive stacking of alginate gellayers and poly(l-lysine)-hyaluronic acid multilayer films aimed at tissue engineering. *Soft Matter*, 2008, 4 (7), 1422-1429.

[128] Betz M. W., Modi P. C., Caccamese J. F., Coletti D. P., Sauk J. J., Fisher J. P.; Cyclic acetal hydrogel system for bone marrow stromal cell encapsulation and osteodifferentiation. *Journal of Biomedical Materials Research. Part A*, 2008, 86A (3), 662-670.

[129] Smithmyer M. E., Sawicki L. A., Kloxin A. M., Hydrogel scaffolds as in vitro models to study fibroblast activation in wound healing and disease. *Biomaterials Science*, 2014, 2 (5), 634-650.

[130] Combellack E. J., Jessop Z. M., Naderi N., Griffin M., Dobbs T., Ibrahim A., Evans S., Burnell S., Doak S. H., Whitaker I. S.; Adipose regeneration and implications for breast reconstruction: update and the future. *Gland Surgery*, 2016, 5 (2), 227-241.

[131] Saunders R. L., Hammer D. A.; Assembly of Human Umbilical Vein Endothelial Cells on Compliant Hydrogels. *Cellular and Molecular Bioengineering*, 2010, 3 (1), 60-67.

[132] Su J., Hu B. H., Lowe Jr W. L., Kaufman D. B., Messersmith P. B.; Anti-inflammatory peptide-functionalized hydrogels for insulin-secreting cell encapsulation. *Biomaterials*, 2010, 31 (2), 308-314.

[133] Neufurth M., Wang X., Schröder H. C., Feng Q., Diehl-Seifert B., Ziebart T., Steffen R., Wang S., Müller W. E. G.; Engineering a morphogenetically active hydrogel for bioprinting of bioartificial tissue derived from human osteoblast-like SaOS-2 cells. *Biomaterials*, 2014, 35 (31), 8810-8819.

[134] Motoyama W., Sayo K., Mihara H., Aoki S., Kojima N.; Induction of hepatic tissues in multicellular spheroids composed of murine fetal hepatic cells and embedded hydrogel beads. *Regenerative Therapy*, 2016, 3, 7-10.

[135] Michael E. Aulton; Pharmaceutics; The science of dosage form design, First edition, ELBS Churchill Livigstone, Hong Kong, 1995, 1-5.

[136] Mithal, A text book of pharmaceutical formulation, Second edition, Vallabh Prakashan., New Delhi, 1989, 5-6.

[137] Brahma N Singh, Kwon H Kim, "Drug delivery- Oral route" Encyclopedia of Pharmaceutical technology, 2002, 15, 886-889.

[138] Yie W. Chein, Rate controlling drug delivery systems, *Indian journal of pharmaceutical sciences*, 1998, 3, 63-65.

[139] Brahmankar D.M., Sunil B. Jaiswal; Bio-pharmaceutics and pharmacokinetics A-Treatise, First edition, *Vallabh Prakashan*, New Delhi, 1995, 51-55.

[140] Leon Shargel, Andrew Yu, Susanna, Wu-Pong, Applied bio-pharmaceutics and pharmacokinetics, 5th edition, *Kindle publications*, New York 1996, 138.

[141] Schanker L.S., Mechanism of drug absorption and distribution, *Annual Review of pharmacology*, 1961, 1, 29-45.

[142] Mrsny R.J., Controlled drug delivery: Challenges and strategies, ACS professional reference book, K. Park, *American chemical society*, Washington DC, 1997,107.

[143] Rouge N., Buri P., Doelker E.; Drug absorption sites in the gastrointestinal tractand dosage forms for site-specific delivery, *Int. J. Pharm.* 1996, 136, 117-

139.

[144] Rajan K. Verma and Sanjay Garg, Current status of drug delivery technologies and future directions, *Pharmaceutical technology On-Line*, 2001, 25, 1–14.

[145] Costas K, Sofia, Alexandridou, Katerina Kotti, Sotira Chaitidou, Recent advances in novel drug delivery systems, *Journal of nanotechnology*, 2005, 1-11.

[146] Nandita G. Das and Sudip K. Das, Controlled release of oral dosage forms, *Formulation, Fill & Finish*, 2003, 10-16.

[147] Gilbert S. Banker, Christopher T. Rhodes, Drugs and the pharmaceutical sciences, Third edition, Marcel Dekker, Inc, New York, 1993, 15-17.

[148] Charles S.L, Chiao and Joseph R. Robinson "Sustained release drug delivery systems" Remington's Pharmaceutical Science, 19th edition, Mac Publishing Company, 1999, 1660-1673.

[149] Vyas S. P., Khar R. K.; Proteins and peptides delivery considerations. In: Vyas S. P., Khar R. K., Editor. Controlled drug delivery concepts and advances. First edition, New Delhi: CBS publisher and Distributor. 2002, 549.

[150] Bhalla H. L., Cruz Z. L. D.; Oral sustained drug delivery, *Indian drugs*, 1997, 25, 108-112.

Chapter – 2

Experimental methods

Chapter – 2
Experimental methods

2.1. Introduction

This chapter includes the details of the raw materials, chemicals and experimental procedures used for this research work. The different characterization techniques such as Fourier Transform Infrared Spectroscopy (FTIR), Scanning Electron Microscope (SEM), Thermogravimetric Analysis (TGA) and UV-visible Spectrophotometer have been used to characterize the prepared hydrogels and also kinetic drug release study and antibacterial study was performed for drug-loaded hydrogels for drug delivery applications.

2.2. Materials

Monomers, crosslinker and other chemicals used in the research are listed in **Table 2.1.** The chemicals used were all analytical grade samples and hence, no attempt was made to purify them. Double distilled water was used throughout the research.

2.3. Characterization techniques

Materials are characterized in order to learn more about their structure and characteristics. A number of characterization approaches were used to examine the morphological, physical, mechanical, chemical and drug delivery potentiality of the polymer matrix, which are detailed below.

2.3.1. FTIR Spectroscopy

FTIR (Fourier Transform Infrared Spectroscopy) (**Fig. 2.1 and 2.2**) is a

helpful technique for determining and verifying organic structure. It is frequently used to characterize polymers and polymer composites. This method was utilized to check the structure of the produced hydrogel, drug and drug-loaded hydrogels [1].

The FTIR spectra of samples were qualitatively recorded with the assistance of an FTIR spectrometer in the wide frequency range of 400-4000 cm^{-1} to examine synthesis verifications, interactions and stability. A beam of infrared light was sent through the sample to record the spectrum. Finally, following Fourier processing, the transmitted light indicates how much energy was absorbed in each wavelength and the information appears in the form of a spectrum.

Chemically, FTIR Spectroscopy is a method for identifying chemical compounds and substituent groups. IR radiation is passed through the sample in this approach, with part of it being absorbed and some being transmitted. The resultant spectrum represents the absorption and transmission of the sample and is a molecular fingerprint of the sample. This spectrum is unique to that sample and no two materials have the same infrared spectra. FTIR can identify unknown compounds, assess sample quality and quantify the number of components in a combination. The absorption peaks are caused by various frequencies associated with distinct modes of atom vibration. The amount of material contained in the sample is determined by the size of the peaks. It is a non-destructive procedure because of these features, FTIR is an essential characterization technique for determining the structure and composition of different materials.

2.3.2. Scanning electron microscope (SEM)

Electron diffraction is a material characterization method that involves shining a beam of accelerated electrons onto a sample to produce an interference

pattern (**Fig. 2.3 and 2.4**), which is generally done with a scanning electron microscope (SEM) to examine crystal structure and particular morphology [2]. An SEM photographs a sample by scanning it with an energized electron beam in a raster scan pattern. During each scan, the atoms that make up the chosen sample emit signals that provide information on the sample's surface topography, composition and other characteristics. A field emission cathode is installed in the electron gun of a Field Emission SEM to improve resolution and reduce charge problems.

The SEM (Zeiss) was used to evaluate the phase morphologies of the produced hydrogels. It is a sort of microscope that uses an electron beam to scan the surface of a sample to create pictures. The electrons interact with the atoms in the sample, resulting in a variety of signals that are collected and processed into an image by a computer called a micrograph. The micrograph reveals important details about the surface topography and composition of the material. Double-sided tape was used to adhere the material to the stubs. To avoid the charging effect, the sample was sputtered with a layer of gold film prior to analysis.

2.3.3. Thermogravimetric analysis (TGA)

Thermogravimetric analysis may be used to do thermal analysis on the produced materials (TGA). The TGA thermogram depicts the connection between physical and chemical changes as a function of temperature. Time or mass loss in addition to temperature can be utilized to get information on a material's thermal stability.

In the temperature range up to about 800°C, with a heating rate of 10°C/min under nitrogen stream, a thermogravimetric analyzer (Perkin Elmer STA 600) was

used to quantify thermal weight loss and derivate thermogravimetric analysis (DTA) of hydrogels. We kept track of how much weight we lost at each stage.

Thermogravimetric Analysis (TGA) is a method of determining the weight variations of samples as a result of temperature changes. This technique correctly identifies a sample's weight loss as temperature rises, creating a continuous line to indicate weight loss processes related to the chemical reactions taking place. For various purposes, TGA can be performed in air or noble gases. TGA is frequently used in the case of hydrogel materials as a quantitative technique for estimating the polymer matrix [4, 5]. A typical TGA apparatus from Perkin Elmer STA 600 is shown in **Fig. 2.5 and 2.6.**

2.3.4. Swelling Studies

The swelling study determines the amount of water absorbed. It is commonly used in the production of polymer films. Most mucoadhesive polymers have been found to expand after being hydrated, which is required to begin close contact between the polymer matrix and the mucosal surface [7]. These experiments were carried out in a phosphate buffer with a pH of 7.4 to monitor the swelling index of the polymer matrix. The polymer matrix (surface area: $1cm^2$) was weighed and immersed in 50 ml of phosphate buffer solution in a beaker. The swelled hydrogel was taken from the beaker at the right time intervals and the excess moisture was removed by gently cleaning it with absorbent tissue before it was reweighed. At each time interval, the weight enhancement of the polymer matrix was determined until a consistent weight was found. The degree of the matrix's swelling index was calculated using the following Equation.

$$SI = (W_t - W_0) / W_0 \quad \text{…….. (2.1)}$$

Where, **SI** is Swelling Index, W_t is the weight of the polymer film at the time 't' and W_0 is for the weight of the polymer film at a time '0' [8].

2.3.5. Dissolution Studies

The quantity of drug released by hydrogel was determined through dissolution tests using a dissolution tester (Labindia, India) (**Fig. 2.7**). The drug is dissolved/distributed throughout the hydrogel [9]. Dissolution studies were conducted in simulated gastric fluid (SGF, 0.1 M HCl, pH 1.2) and simulated intestinal fluid (SIF, phosphate buffer, pH 7.4) prepared using 3.6g of KH_2PO_4 and 5.79g of Na_2HPO_4 dissolved in 1 liter water and adjust the pH using dilute NaOH solution according to the procedure outlined in the US Pharmacopeia [10]. At 37°C and a paddle speed of 50 revolutions per minute, dissolution rates were observed. At specified intervals (every 30 minutes), a 1 ml aliquot was removed from the vessel and replaced with an equal volume of matching dissolving media. Before the test, the samples were diluted if required. A UV spectrophotometer was used to examine the samples and the drug concentration was estimated using calibration curves built with reference standards [11].

2.3.6. UV- Visible Spectroscopy

The drug release optical spectra (**Fig. 2.8 and 2.9**) were obtained using a dual beam (Metash UV-Vis Double Beam Scanning Spectrophotometer, Model Name/Number: UV-9000) with a wavelength range of 190 nm to 1100 nm. The samples were placed in two rectangular quartz cells, one for the sample and the other for the reference solvent, each with a capacity of 4 ml and a route length of 1 cm. The incident light beams pass through both cells (sample and reference) at the same

time and the detector compares the intensity of the transmitted beams. A deuterium lamp is utilized to acquire the ultraviolet area, whereas a tungsten/halogen lamp is used to obtain the visible region [12-13]. The device operates on the basis of the Beers-Lambert law, which states that various materials absorb light of different wavelengths. As a result, the absorption spectrum reveals a variety of absorption bands that correlate to material properties or functional groups.

2.4. Evaluation of drug-loaded hydrogel

2.4.1. Yield of Hydrogel

By comparing the functional yield to the theoretical yield, the yield of hydrogel was determined. The following formula was used to measure the yield percentage.

$$\textbf{Hydrogel yield} \quad (\%) = \frac{\textbf{Practical weight}}{\textbf{Theoretical weight}} \textbf{ x 100} \qquad \ldots\ldots\ldots\ldots (\mathbf{2.2})$$

2.4.2. Drug loading and Estimation of drug content

Drug loading is carried out by soaking the dry hydrogel (0.1 g) in the presence of a drug solution (1000 mg/l) in water, the drug would be loaded into the hydrogel. After 48 hours, the loaded hydrogel were removed and weighed, to prevent burst release the loaded hydrogel was washed with ethanol and then placed in the vacuum oven for 24 hours to dry completely. To estimate the amount of drug loaded content, accurately weighed drug-loaded hydrogel was added to 100 ml phosphate buffer of pH 7.4 in a conical flask, which was shaken for 24 hours at room temperature using a mechanical shaker. After dilution, the sample was measured using a UV-Visible spectrophotometer. To determine the precise concentration of the entrapped substance, the obtained absorbance was plotted against the standard curve.

The experiment was performed for three times. The following relationship was used to assess the real drug quantity.

$$\textbf{Content of the drug} = \frac{(\mathbf{S\ x\ A} \pm \mathbf{C})\ \mathbf{x\ BS\ x\ F}}{\mathbf{1000}} \quad \ldots\ldots\ldots\ldots\ldots\ (\mathbf{2.3})$$

Where, **S**= Slope, **A**= Absorbance, **C**= Intercept, **BS**= Bath solution volume, **F**=Dilution factor.

2.4.3. *In-vitro* Drug release studies

The USP paddle dissolution apparatus was used for the drug release trials. The drug release profile from hydrogels was examined in two distinct buffer solutions of pH 1.2 (HCl) and pH 7.4 (Phosphate buffer) respectively which resemble identically the physiological areas of the GI-tract pH. The drug-loaded hydrogels in the vessel was rotated at a constant speed (50 rpm) and were held at a constant temperature of 37^{o}C up to the end of drug release. The sample of 1 ml were taken at every 30 minutes and diluted with the proper medium at the appropriate concentration. Then, using UV-Visible Spectrophotometer, calculate the drug concentration [14]. Based on the sample's absorbance at various intervals of time, the following formulae are used to calculate the amount of drug released, total concentration and percentage of drug release. Following each sampling (30 minutes interval), an equivalent amount of the dissolution media (1 ml) was replaced with a fresh medium of the same volume to maintain constant dissolution media.

$$\textbf{Concentration}\ (\mu\mathbf{g/ml}) = \mathbf{S\ x\ A} \pm \mathbf{I} \quad \ldots\ldots\ldots\ldots\ (\mathbf{2.4})$$

Where, **S** = Slope, **A** = Absorbance, **I** = Intercept.

$$\textbf{Released amount} = \frac{\textbf{C x DV x F}}{\textbf{1000}} \quad \textbf{X 100} \qquad \ldots\ldots\ldots\ldots (\mathbf{2.5})$$

Where, **C**= Concentration (µg/ml), **DV**= Dissolution media volume,

F= Dilution factor.

$$\textbf{Percentage of drug release} = \frac{\textbf{Released amount}}{\textbf{Drug content}} \quad \textbf{X 100} \qquad \ldots\ldots\ldots\ldots (\mathbf{2.6})$$

2.5. Kinetics studies of drug release

Kinetic treatment of the data from the *in-vitro* dissolution investigations was used to identify the release sequence and for the formulation best-fit model. *In-vitro* drug release data for the formulations are analyzed using kinetic equations such as zero-order, Higuchi, first-order, Korsmeyer-Peppas and Hixson-Crowell [15]. The linear curves created by regression analysis are given their coefficients of correlation (R^2) values.

2.5.1. Zero-order:

The following equation was used to calculate the zero-order release.

$$\mathbf{Q_t = Q_0 + k_0 t} \qquad \textbf{……. (2.7)}$$

Where,

Q = The amount of drug that has dissolved in time t,

$\mathbf{Q_0}$ = The amount of drug in the solvent when it was initially generated (Q = 0 in most cases),

$\mathbf{k_0}$ = The release constant of zero order.

The data follows zero-order release kinetics with a slope equal to k_0 when plotted total percent drug release versus time.

2.5.2. First-order:

The first-order release was calculated using the equation below.

$$\mathbf{Log\ C = Log\ C_0 - k_t / 2.303} \qquad \textbf{……. (2.8)}$$

Where,

C = Amount of drug remained at the time (t),

k = Rate constant of the first order (hr^{-1}),

$\mathbf{C_0}$ = Initial amount of drug,

A straight line was obtained when the observed data was plotted as log cumulative % medicine remaining v/s time, suggesting that the drug release followed first-order kinetics.

2.5.3. Higuchi's model:

In this model, the drug release from polymer matrix devices is calculated by using Higuchi's equation.

$$\mathbf{Q = [D\varepsilon/\tau\ (2A - \varepsilon Cs)\ Cs\ t]^{1/2}} \qquad \text{..... (2.9)}$$

Where,

Q = Quantity of drug released at a specific time (t),

D = Diffusion coefficient of a drug in the matrix,

τ = Tortuosity of matrix,

A = Total drug amount per unit volume of a matrix,

Cs = Solubility of drugs in matrices,

ε = matrix porosity,

t = quantity of medicine released over a period of time (hours).

If **D, Cs** and **A** are assumed to be constants, the equation can be simplified. The equation becomes.

$$\mathbf{Q = kt^{1/2}} \qquad \text{..... (2.10)}$$

A straight line occurs when the results are plotted by the average % of drug release v/s square root of time. This means the medicine was released by diffusion.

2.5.4. Korsmeyer-Peppas model:

When the release mechanism is unclear or many kinds of release occur in the same period, this model is widely used to investigate drug release from polymeric dosage forms [16].

$$M_t / M_\infty = kt^n \quad \text{..... (2.11)}$$

$$\text{Log } M_t / M_\infty = \text{Log } k + n \text{ Log } t \quad \text{..... (2.12)}$$

Where,

M_∞ = The amount of drug released at infinite time (t),
M_t = The amount of drug released at a certain point in time (t),
k = The kinetic rate constant.
n = The diffusional exponent.

By plotting the log % of drug release v/s log time, the drug release by the Korsmeyer-Peppas model can be determined.

2.5.5. Hixson-Crowell model:

Hixson-Crowell law discusses the release of particles or tablets from systems with a change in diameter and surface area. As a result, the volume of particles with a regular area is proportional to the cube root of their volume. Hixson-Crowell created a link between drug release and time-based on the aforementioned premise, which may be expressed by the equation as

$$W_0^{1/3} - W_t^{1/3} = k_{HC}t \quad \text{..... (2.13)}$$

Where,

W_0 = Quantity of drug remaining at time 0,
W_t = The amount of drug in the pharmaceutical dosage form at time t,
k_{HC} = Hixson-Crowell constant.

The plot of the cube root of the drug % remaining in the matrix v/s time gives Hixson-Crowell release kinetics.

2.6. Antibacterial study

The synthesized hydrogel and drug-loaded hydrogel were used for the *in-vitro* antibacterial test by using the agar diffusion method against gram-positive *S. aureus* and gram-negative *E. coli*. For this purpose, a part of pure drug, drug-loaded hydrogel and synthesized hydrogel were prepared in distilled water and loaded on nutrient agar plates. After 24 hours of incubation at 37°C the inhibition zones were calculated by averaging the diameters (mm) in three directions of the inoculated plates [17].

Table 2.1. List of monomers, crosslinker, chemicals and drugs with their source of procurement.

Monomers	
Acrylic acid	S.d. fine chemicals, Mumbai, India.
Acrylamide	S.d. fine chemicals, Mumbai, India.
Crosslinker	
N, *N*′-methylene-bis-acrylamide	S.d. fine chemicals, Mumbai, India.
Chemicals	
Potassium persulphate	S.d. fine chemicals, Mumbai, India.
Sodium metabisulfite	Avra Synthesis Pvt Ltd, Hyderabad, India.
Sodium hydroxide	S.d. fine chemicals, Mumbai, India.
Potassium dihydrogen orthophosphate	S.d. fine chemicals, Mumbai, India.
Hydrochloric acid	Merck, Mumbai, India.
Disodium hydrogen phosphate anhydrous	Merck, Mumbai, India.
Aluminum chloride	Merck, Mumbai, India.
Calcium chloride	Merck, Mumbai, India.
Sodium chloride	Merck, Mumbai, India.
Drugs	
Levofloxacin hemihydrate	Micro labs limited, Bangalore, India.
Moxifloxacin hydrochloride	Micro labs limited, Bangalore, India.
Doxycycline hydrochloride	Micro labs limited, Bangalore, India.

Figure 2.1. The FTIR spectrometer (Make: Shimadzu, Country: Japan).

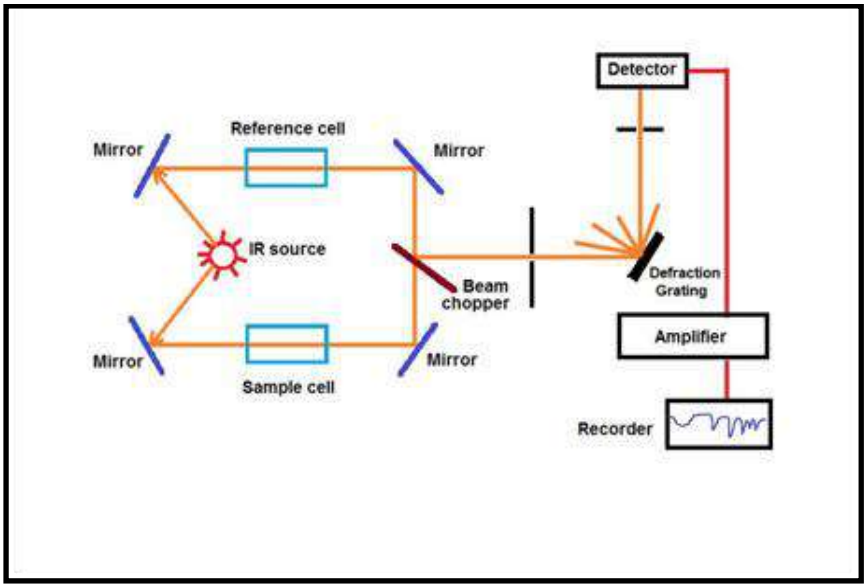

Figure 2.2. The operating principle of an FTIR spectrometer [1].

Figure 2.3. Scanning electron microscope (Make: Zeiss, Country: Germany).

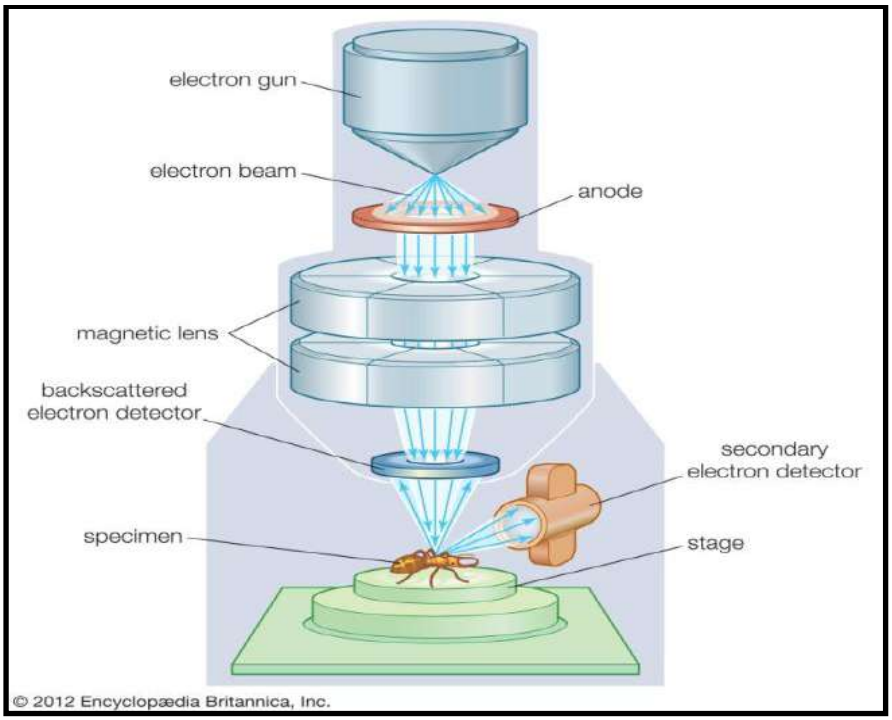

Figure 2.4. Schematic of an SEM instrument [3].

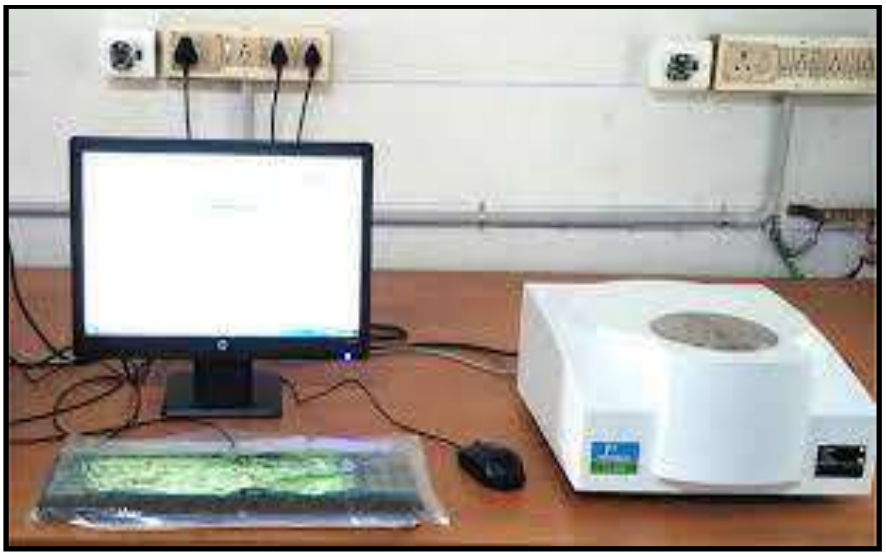

Figure 2.5. TGA/DTA analyzer (Make: Perkin Elmer, Country: America).

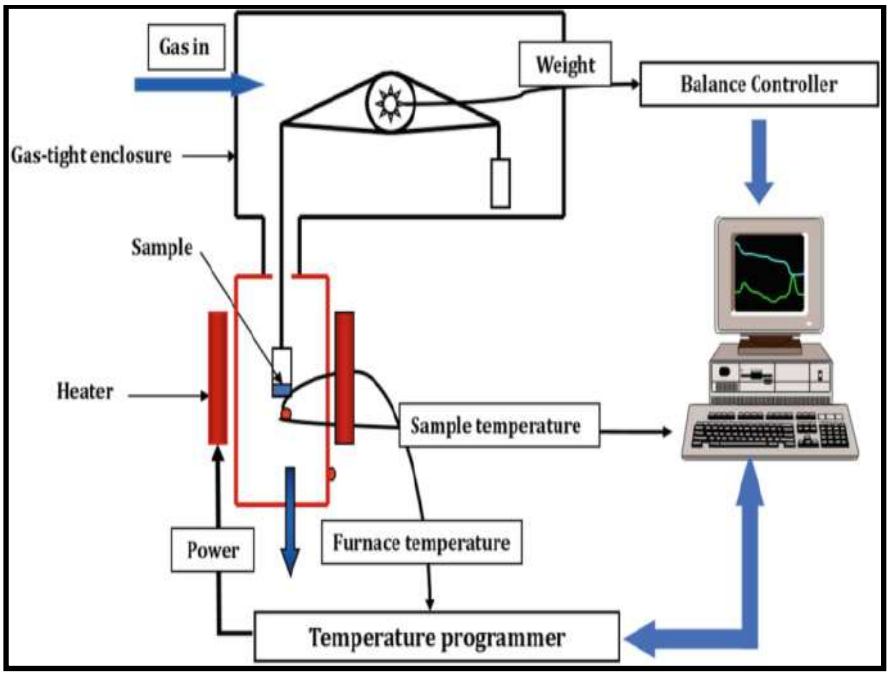

Figure 2.6. The operating principle of the TGA/DTA analyzer [6].

Figure 2.7. Dissolution apparatus (Make: Labindia, Country: India).

Figure 2.8. UV-Visible Spectrophotometer (Make: Metash, Country: China).

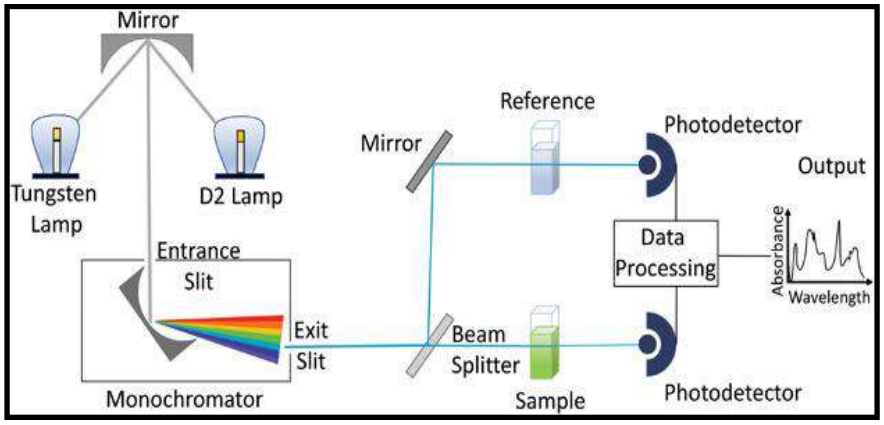

Figure 2.9. The operating principle of UV-Visible Spectrophotometer [13].

2.7. References

[1] Griffiths P. R., Ade Haseth J.; Fourier Transform Infrared Spectroscopy, *ChemicalAnalysis, John Wiley & Sons*, 1986.

[2] Bojeong K., Michael F., Hochella J. R.; "Chapter 4 - Analytical Transmission Electron Microscopy and Scanning Transmission Electron Microscopy Techniques for the Characterization of Nanomaterial Composition, Phase and Crystallinity", *Frontiers of Nanoscience*, 2015, 8, 123-152.

[3] Bradbury S., Ford, Brian J., Joy david C.; Scanning electron microscope. *Encyclopedia Britannica*. https://www.britannica.com/technology/scanning-electron-microscope, 2019.

[4] Aqdas N., Khalid M., Mohammad Z., Shazia T.; "Ameer Fawad Zahoor Biobased polyurethane: An efficient and environment friendly coating systems: A review", *Progress in Organic Coatings*, 2016, 91, 25-32.

[5] Khalid M., Aqdas N., Mohammad Z., Shazia T., Mohammad M.; "Recent developments and future prospects on bio-based polyesters derived from renewable resources: A review", *International Journal of Biological Macromolecules*, 2016, 2, 1028-1040.

[6] Britannica T.; Editors of Encyclopaedia, Differential thermal analysis. *Encyclopedia Britannica*. https://www.britannica.com/science/differential-thermal-analysis, 2016.

[7] Edsman K., Hagerstrom H.; "Pharmaceutical applications of mucoadhesion for the non-oral routes", *Journal of Pharmacy and Pharmacology*, 2005, 57, 3-22.

[8] Peh K. K., Wong C. F., "Polymeric films as vehicles for buccal delivery: Swelling, Mechanical and Bioadhesive properties", *Journal of Pharmacy and Pharmaceutical Sciences*, 1999, 2, 53-61.

[9] Petersen R.V., Endersen C. G., Fang S. M., Gregonis D., Kim S. W., Feijen J., Enderson J. M., Mitra S.; Controlled Release of Bioactive Materials. (Baker R. Ed.), *New York, Academic Press*, 1986, 45.

[10] The United States Pharmacopoeia, XXTV, The United States Pharmacopoeial Convention, Inc. Rockville, MD, 1999.

[11] Shobharani K. N., Goundalkar A. G., Kalyani P.; Preparation and evaluation of microspheres of diclofenac sodium. *Indian Journal of Pharmaceutical Sciences*, 1994, 56(2), 45.

[12] Brett C. M. A., Brett A. M. O.; Electrochemistry Principles, Methods and Applications.*Oxford Science Publications*, 1993.

[13] Rocha F. S., Gomes A. J., Lunardi C. N., Kaliaguine S., Patience G. S.; Experimental Methods in Chemical Engineering: Ultraviolet Visible Spectroscopy. *The Canadian Journal of Chemical Engineering*, 2018.

[14] Gang Cheng et al. Time and pH-dependent colon-specific drug delivery for orally administered diclofenac-sodium and 5-amiosalicylic acid, *World Journal of gastroenterology*, 2004, 10(2), 1769-1774.

[15] Paulo Costa, Jose, Manuel souse lobo, Modeling and comparison of dissolution profiles. *European journal pharmaceutical sciences*, 2001, 13, 123–133.

[16] Korsmeyer R. W., Gurny R., Doelker E., Buri P., Peppas N. A.; Mechanisms of solute release from porous hydrophilic polymers, *International Journal of Pharmaceutics*, 1983, 28, 25–35.

[17] Dil N.N., Sadeghi M.; Free radical synthesis of nanosilver/gelatin-poly (acrylic acid) nanocomposite hydrogels employed for antibacterial activity and removal of cu (II) metal ions. *Journal of Hazardous Materials*, 2018, 351, 38–53.

Chapter – 3

Synthesis and Characterization of Poly(acrylamide) Hydrogels as pH and Salt Sensitive Material

Chapter – 3

Synthesis and Characterization of Poly(acrylamide) Hydrogels as pH and Salt Sensitive Material

This chapter discusses the synthesis of poly(acrylamide) hydrogels and evaluate their pH and salt sensitivity. The investigation is presented in this chapter.

Abstract

This work reports the synthesis of poly(acrylamide) hydrogel and its characterization. Hydrogel will be synthesized by a chemical cross-linking method using sodium metabisulfite and potassium persulphate as initiators with crosslinker methylenebisacrylamide. The synthesized hydrogels were examined by FT-IR, SEM and TGA to determine chemical interactions in the polymer network. Moreover, the swelling study explains that hydrogel swelling capacity and depends on the concentration of the crosslinking agent. The pH, temperature and salt solutions were impacting swelling properties. In acid and base solutions, the swelling (%) order is HCl < CH_3COOH < $HClO_4$ < NaOH and the swelling (%) order in salt solutions is NaCl > $CaCl_2$ > $AlCl_3$.

3.1. Introduction

In current years, there has been significant attention to smart, super absorbent and swellable hydrogels. These hydrogels are 3D polymer networks by physical or chemical crosslinking and it expands in biological fluids or water without dissolving as a consequence of physical or chemical cross-linking [1, 2]. Hydrogels are applied in pharmaceuticals [3], agriculture [4], food additives [5], drug delivery systems, hygienic products, sealing, artificial snow [6, 7], coal dewatering [8], biomedical applications [9, 10], barrier materials to regulate biological adhesions [11], tissue engineering and wound dressing [12], diagnostics [13], regenerative medicines [14, 15], separation of cells or biomolecules [16] and biosensors [17].

Smart or stimuli-sensitive hydrogels are undergo huge changes in the swelling response by changing environmental conditions, such as pH [18,19], temperature [20], light [21], pressure [22], electric field [23, 24], antigens [25, 26] and carbohydrates [27]. Among them, pH-sensitive hydrogels are developed in the evolution of new drug delivery systems, these hydrogels change their properties by responding to the pH of the solution [28]. These gels are good material for drug delivery based on pH conditions [29, 30]. Hydrogels can absorb large amounts of water without being dissolved. This is often thanks to their physical and chemical network of hydrophilic polymeric chains with -OH, -CONH-, -$CONH_2$ and -COOH groups [31-34].

Drug delivery systems in medicine can be developed by utilizing the swelling behavior of hydrogel [32, 33]. Free radical polymerization is a leading process for the polymerization of water-dissolved monomers and for the development of hydrogels [32, 35]. Free radical polymerization is a dynamic and generally used method

and leads to the swift production of the gel even under moderate conditions using lesser molecular weight monomers with the existence of a crosslinker can be used to produce hydrogels for bio-applications [36].

In this work, a hydrogel using acrylamide as a monomer and methylene bisacrylamide as the crosslinker by free radical polymerization is synthesized. The swelling study, FT-IR, SEM and TGA were performed to evaluate the swelling and structural characteristics of the obtained gel. The synthesized gel could also be used as pH and salt-sensitive super absorbent materials and drug delivery applications.

3.2. Materials and Methods

3.2.1. Materials

Acrylamide (AAM), potassium persulphate (PPS), methylenebisacrylamide (MBA), sodium hydroxide, hydrochloric acid, acetic acid and perchloric acid were obtained from SD fine chemical laboratory (SDFCL), Mumbai, India. Sodium metabisulfite (SMBS) was obtained from Avra Synthesis Pvt. Ltd., Hyderabad, India. Aluminum chloride, calcium chloride and sodium chloride were purchased from Merck, Mumbai, India. Distilled water was used throughout the experiment.

3.2.2. Preparation of poly(acrylamide) hydrogels

Poly(acrylamide) hydrogel was synthesized by the free radical mechanism. Primarily free radical initiator pair of potassium persulphate (45 mg) and sodium metabisulfite (32 mg) was taken into a beaker containing water (10 ml). Then add acrylamide (600 mg) and stir for 10 min at room temperature, finally add crosslinker methylenebisacrylamide (06 mg) and the reaction is carried out in a water bath till gel was formed. The prepared hydrogel was washed with water to remove unreacted materials, then cut into suitable sizes and dried at 50ºC in the oven. Similarly,

hydrogel formulations (AAMH1, AAMH2, AAMH3 and AAMH4) were prepared using the same method as given in **Table 3.1.**

3.2.3. FT-IR analysis

FT-IR analysis of acrylamide, methylenebisacrylamide and synthesized hydrogel were administered using an FT-IR spectrometer (Perkin-Elmer FT-IR C94012) in the 400-4000 cm^{-1} range.

3.2.4. Morphology analysis

The surface morphology of the acrylamide, methylenebisacrylamide and synthesized hydrogel samples was observed using scanning electron microscopy (Zeiss, LS15).

3.2.5. Thermal analysis

Thermal stability of hydrogel was performed using Perkin-Elmer STA 600 thermogravimetric analyzer. TGA was performed with a specified amount of sample by increasing the heating rate to 20ºC.

3.2.6. Swelling study

The swelling study was conducted by the gravimetric method using dried hydrogels in water, acids (HCl, CH_3COOH, $HClO_4$), base (NaOH), salts ($AlCl_3$, $CaCl_2$, NaCl) and pH solutions in the range 1 to 12. The dried pre-weighed hydrogel was placed in water, acid, base, salt and pH solutions to investigate swelling (%) at specific intervals. The swelled hydrogel was taken out from the solution and wiped with filter paper for removing excess water, followed by weight measurement, then by using the following equation swelling (%) was calculated.

$$\textbf{Swelling}\ (\%) = \frac{\mathbf{W_b - W_a}}{\mathbf{W_a}}\ \mathbf{x\ 100} \qquad \ldots\ldots\ldots\ldots\ldots\ (\mathbf{3.1})$$

Where, $\mathbf{W_a}$ = Weight of dried hydrogel and $\mathbf{W_b}$ = Weight of swelled hydrogel.

3.3. Results and Discussion

Poly(acrylamide) hydrogel was synthesized successfully from acrylamide monomer using free-radical polymerization method. The free radicals are generated from sodium metabisulfite and potassium persulphate solution. Then hydroxyl free radicals will generate by abstract protons from the water molecules and these radicals further abstract protons from acrylamide and methylenebisacrylamide to initiate polymerization [37, 38]. In this polymerization, methylenebisacrylamide act as a crosslinker inthe system. The mechanism of the reaction is shown in **Scheme I.**

3.3.1. FT-IR studies

FT-IR spectra of acrylamide, methylenebisacrylamide and synthesized hydrogel are shown in **Fig. 3.1.** The spectra of the acrylamide monomer (**Fig. 3.1a**) show the absorption band around 3349 cm^{-1} is due to the NH stretching frequency of the amide group. The peak at 1664 cm^{-1} is attributed due to C=O stretching, while the absorption band around 1134 cm^{-1} is due to the C-N stretching. In the spectra of methylenebisacrylamide (**Fig. 3.1b**), the peak at 3309 cm^{-1} is attributed due to the NH stretching and the absorption band around 1664 cm^{-1} is due to C=O stretching. The C-N stretching gives rise to a band at 1121 cm^{-1} and a band at 2958 cm^{-1} is assigned for C-H stretching vibrations [39, 40]. In the spectra of hydrogel (**Fig. 3.1c**), the absorption peak at 3308 cm^{-1} for the NH stretching is observed. The absorption peaks around 2957 cm^{-1} for C-H stretching, at 1663 cm^{-1} for C=O stretching and at 1119 cm^{-1} for C-N stretching were also observed.

3.3.2. Morphology studies

The surface morphology play important role in swelling and control release behavior. Hence, it is important to explore these properties [41]. SEM images show the morphology of dried hydrogel. The lower mechanical strength hydrogels have a higher swelling rate [42]. According to the SEM images, pure acrylamide and methylenebisacrylamide show a crystal surface (**Fig. 3.2a-b**). However, the addition of methylenebisacrylamide leads to a very smooth and uniform surface structure (**Fig. 3.2c-f**).

3.3.3. Thermal study

The thermal behavior of the synthesized hydrogel was investigated by TGA and the result is shown in **Fig. 3.3.** The initial weight loss was attributed to the evaporation of moisture content present in the hydrogel. Poly(acrylamide) hydrogel was thermally unstable and degradation starts at 159ºC with a mass loss of 5.4% for the elimination of ammonia gas from amide groups of poly(acrylamide) chains, the second degradation at 294ºC with mass loss of 5% and more amount of weight loss occurred at 394ºC with mass loss of 8% due to breakage of the polymer chain and cross-linked network in the hydrogel [43].

3.3.4. Swelling study of poly(acrylamide) hydrogels

The swelling study is the most important to figure out the application of hydrogels. It is investigated using water, acid, base, salt and pH solutions. The dried poly(acrylamide) hydrogel of 1cm in length was soaked in 100 ml of water for 24 hours, the result showed that the size of the hydrogel was increased up to 4.3cm and the corresponding images are showed in **Fig. 3.4.**

3.3.4.1. Swelling study of poly(acrylamide) hydrogels in water

The swelling (%) of the synthesized poly(acrylamide) hydrogels AAMH1, AAMH2, AAMH3 and AAMH4 were studied in water at 37ºC. The results are tabulated in the **Table 3.2.** The maximum swelling % was found to be 3449.43 for AAMH1. The corresponding plot of swelling (%) v/s time is shown in the **Fig. 3.5.** The result showed that the swelling (%) of these hydrogels decreased as the amount of crosslinker increased. Since the maximum swelling was obsorved for AAMH1, for further swelling studies AAMH1 is taken as standard. The less amount of crosslinking agent usage leads to a maximum swelling (%) due to less crosslinking points and availability of free space between crosslinking points, which helps the gels to hold more amount of solvent molecules. Similarly, large amount of crosslinking agent usage will lead to minimum swelling (%) due to more crosslinking points and less space [44]. Hence, more amount of crosslinker promotes tight-packed polymer networks, which avoid flexibility and decreases the space in a polymer network and the swelling rate decreases.

3.3.4.2. Swelling study of AAMH1 hydrogel in acid and base solutions

The swelling study of AAMH1 hydrogel was investigated in HCl, CH_3COOH, $HClO_4$ and NaOH solutions at room temperature. The results are tabulated in **Tables 3.3 to 3.6.** The corresponding plot of swelling (%) of AAMH1 hydrogel v/s time is shown in the **Fig. 3.6 to Fig. 3.9.** Hydrogels swelling ability will explain the interaction between functional groups and osmotic pressure [45]. In acid solutions like HCl, CH_3COOH and $HClO_4$, the amide group of acrylamide hydrogel mainly controlled the swelling capacity. It will get protonated (NH_3^+) and electrostatic repulsion occurs with osmotic pressure resulting shows swelling. However, in an

acidic solution like HCl the screening effect of chloride (Cl^-) counter-ion guard the ammonium cation charges and avoid a dynamic repulsion in HCl solution. Hence, the swelling was decreased in the HCl solution compared to CH_3COOH and $HClO_4$ solution. Under basic condition like NaOH solution, the -$CONH_2$ and -CONH- groups are deprotonated and electrostatic repulsion occurs. The existence of sodium ions (Na^+) will lead to high osmotic swelling pressure and help to increase swelling even in a very low concentration of NaOH solution. The swelling percentage in acid and base solution is in the order: HCl < CH_3COOH < $HClO_4$ < NaOH shown in **Fig 3.10** [46, 47].

3.3.4.3. Swelling study of AAMH1 hydrogel in different pH solutions

Swelling studies of AAMH1 hydrogel is carried out in the solutions of HCl and NaOH in the pH range from 1 to 12 at temperature 37ºC. The result is reported in **Table 3.7.** The maximum swelling % was found to be 4904.28 in pH 12. The swelling (%) depends on the pH of the solution [37]. The corresponding plot of swelling (%) of AAMH1 hydrogel v/s pH is shown in the **Fig. 3.11.** The stock solutions of 0.1 M HCl (pH 1.0) and 1.0 M NaOH (pH 12.0) were diluted with deionized water to prepare solutions of different pH and no additional ions were added to the medium for setting the pH of the solutions because the hydrogel is more influenced by ionic strength. The swelling (%) increased with increase of pH from 1 to 12 and when the temperature increased swelling also increases, it was evident from the data given [45]. However, up to pH 4.0 swelling is very less due to the screening effect of (Cl^-) counter-ion. From pH 5 to 12, the swelling increases due to deprotonation of amide groups and the presence of osmotic pressure of Na^+ ions. The result shows when pH increases the swelling (%) also increases [46].

3.3.4.4. Swelling study of AAMH1 hydrogel in salt solutions

Swelling studies of AAMH1 hydrogel is carried out in the salt solutions of 0.15M NaCl, $CaCl_2$ and $AlCl_3$. The result is tabulated in **Table 3.8.** The corresponding plot of swelling (%) of AAMH1 hydrogel v/s time is shown in the **Fig. 3.12.** On comparing the swelling studies of AAMH1 hydrogel in water with salt solutions. The maximum swelling 3449.43 % was observed for water **(Fig. 3.5)**, where as for NaCl solution it was found to be 401.90 % **(Fig. 3.12)** is observed due to the presence of additional ions and leads to the osmotic pressure between the hydrogel network and external solution with a screening effect. The swelling percentage decrease with increase in the charge of the metal cation ($Na^+ > Ca^{2+} > Al^{3+}$) [37, 45]. In crosslinked hydrogel, the screening effect of Chloride counterion and complex formation between ionic groups leads to an increase in the crosslinking density and decreasing swelling capacity.

3.4. Conclusion

In this investigation, the poly(acrylamide) hydrogels were synthesized by using both potassium persulphate and sodium metabisulfite as a free radical generator for polymerization. Different hydrogels were synthesized by increasing the amount of crosslinker. The increasing amount of crosslinker will affect the characterization and swelling study. Further, the changes in swelling (%) is based on the composition of the hydrogel, ionic strength, temperature and pH. Synthesized hydrogels exhibit good swelling nature in water, acid, base and salt solutions. The composition of hydrogel and the surrounding environment will affect the swelling capacity. The swelling response of the hydrogel can be considered it as a good material for the study of controlled release of fertilizers in agriculture applications and biomedical drug delivery systems.

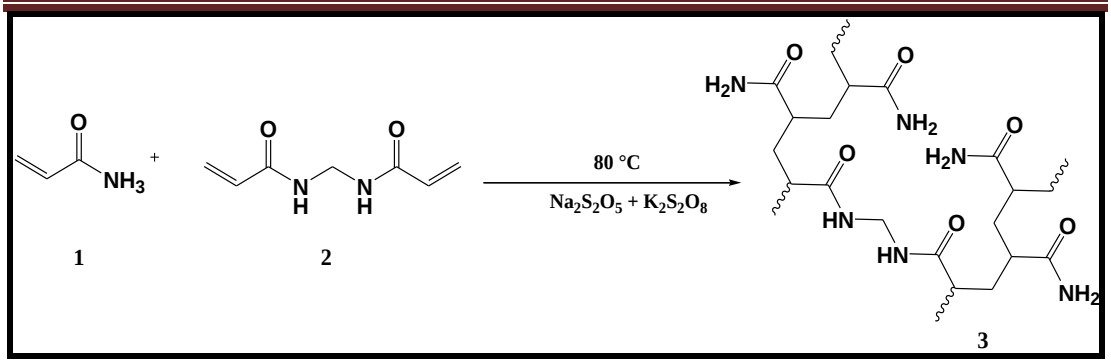

Scheme I. Synthesis of poly(acrylamide) hydrogel, (1) acrylamide, (2) methylenebisacrylamide and (3) poly(acrylamide) hydrogel.

Table 3.1. Synthesis schemes of poly(acrylamide) hydrogel.

Formulation code	Water (ml)	Acrylamide (mg)	Initiator		MBA (mg)
			SMBS (mg)	PPS (mg)	
AAMH1	10	600	32	45	06
AAMH2	10	600	32	45	11
AAMH3	10	600	32	45	16
AAMH4	10	600	32	45	21

Table 3.2. Statistical data of the poly(acrylamide) hydrogel swelling (%) changes in water over time.

Time (hours)	AAMH1 Swelling (%)	AAMH2 Swelling (%)	AAMH3 Swelling (%)	AAMH4 Swelling (%)
0	0.00	0.00	0.00	0.00
6	1062.92	911.22	821.78	726.80
12	1364.04	1081.63	982.17	830.92
18	1669.66	1431.63	1201.98	1025.77
24	1875.28	1626.53	1302.97	1158.76
30	2261.79	1974.48	1733.66	1548.45
36	2474.15	2261.22	1965.34	1758.76
42	2728.08	2463.26	2273.26	2024.74
48	2906.74	2715.30	2551.48	2285.56
54	3252.80	2952.04	2655.44	2386.59
60	3430.33	3254.08	3026.73	2689.69
66	3446.06	3283.67	3037.62	2703.09
72	**3449.43**	3286.73	3040.59	2705.15

Table 3.3. Statistical data of the poly(acrylamide) hydrogel swelling (%) in HCl of different concentrations.

Time (hours)	1 M HCl Swelling (%)	2 M HCl Swelling (%)	4 M HCl Swelling (%)	6 M HCl Swelling (%)
0	0.00	0.00	0.00	0.00
6	157.81	197.14	301.25	498.21
12	162.50	232.85	347.50	578.57
18	165.62	254.28	391.25	641.07
24	175.00	242.85	408.75	641.07
30	160.93	241.42	417.50	589.28
36	131.25	202.85	371.25	528.57
42	151.56	191.42	341.25	417.85
48	121.87	167.14	332.50	403.57

Table 3.4. Statistical data of the poly(acrylamide) hydrogel swelling (%) in CH_3COOH of different concentrations.

Time (hours)	1 M CH_3COOH Swelling (%)	2 M CH_3COOH Swelling (%)	4 M CH_3COOH Swelling (%)	6 M CH_3COOH Swelling (%)
0	0.00	0.00	0.00	0.00
6	197.77	234.32	344.87	442.62
12	208.88	247.76	412.82	521.31
18	215.55	267.16	462.82	591.80
24	221.11	283.58	491.02	655.73
30	228.88	301.49	532.05	718.03
36	237.77	316.41	564.10	739.34
42	245.55	323.88	576.92	822.95
48	254.44	331.34	601.28	847.54

Table 3.5. Statistical data of the poly(acrylamide) hydrogel swelling (%) in $HClO_4$ of different concentrations.

Time (hours)	1 M $HClO_4$ Swelling (%)	2 M $HClO_4$ Swelling (%)	4 M $HClO_4$ Swelling (%)	6 M $HClO_4$ Swelling (%)
0	0.00	0.00	0.00	0.00
6	347.69	406.89	582.25	697.05
12	450.76	518.96	729.03	876.47
18	503.07	598.27	924.19	1048.52
24	558.46	646.55	1054.83	1123.52
30	570.76	658.62	1132.25	1258.82
36	595.38	698.27	1219.35	1405.88
42	610.76	741.37	1275.80	1452.94
48	621.53	777.58	1283.87	1480.88

Table 3.6. Statistical data of the poly(acrylamide) hydrogel swelling (%) in NaOH of different concentrations.

Time (hours)	0.001 M NaOH Swelling (%)	0.002 M NaOH Swelling (%)	0.004 M NaOH Swelling (%)	0.006 M NaOH Swelling (%)
0	0.00	0.00	0.00	0.00
6	229.76	283.54	307.52	494.17
12	265.47	348.10	527.95	1237.86
18	295.23	372.15	752.68	1779.61
24	326.19	435.44	1024.73	2111.65
30	342.85	492.40	1111.82	2242.71
36	373.80	529.11	1200.00	2329.12
42	405.95	613.92	1263.44	2422.33
48	413.09	631.64	1270.96	2450.48

Table 3.7. Statistical data of the poly(acrylamide) hydrogel swelling (%) in the pH range 1 to 12.

pH	**1**	**2**	**3**	**4**	**5**	**6**
Swelling (%)	115.09	267.30	321.27	336.95	1863.49	1969.01
pH	**7**	**8**	**9**	**10**	**11**	**12**
Swelling (%)	2611.70	3162.12	3482.96	4593.75	4687.82	**4904.28**

Table 3.8. Statistical data of the poly(acrylamide) hydrogel swelling (%) in the different salt solutions.

Time (hours)	0.15 M NaCl Swelling (%)	0.15 M $CaCl_2$ Swelling (%)	0.15 M $AlCl_3$ Swelling (%)
6	239.31	201.87	159.07
12	293.51	242.48	179.35
18	335.87	262.40	186.12
24	353.05	283.08	197.86
30	369.08	288.72	219.21
36	398.47	312.78	244.48
42	400.76	328.94	245.55
48	**401.90**	329.69	246.26

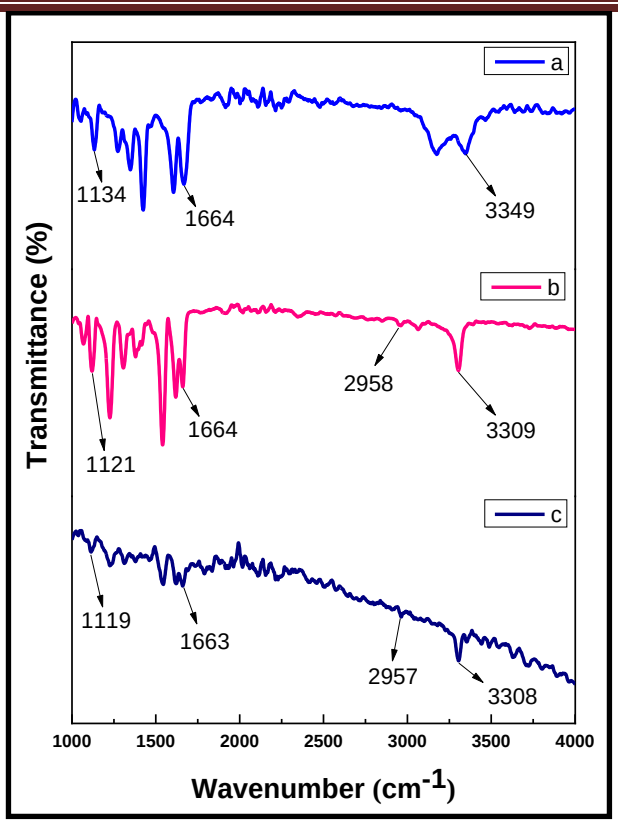

Figure 3.1. FT-IR spectra of (a) acrylamide, (b) methylenebisacrylamide and (c) poly(acrylamide) hydrogel.

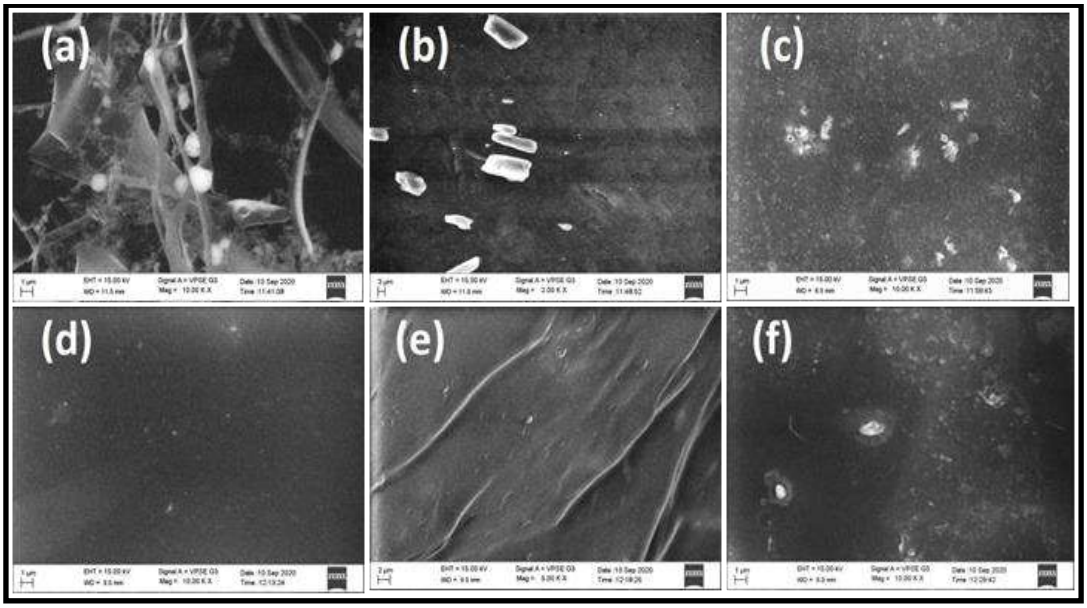

Figure 3.2. SEM images of (a) acrylamide, (b) methylenebisacrylamide, (c) AAMH1, (d) AAMH2, (e) AAMH3 and (f) AAMH4.

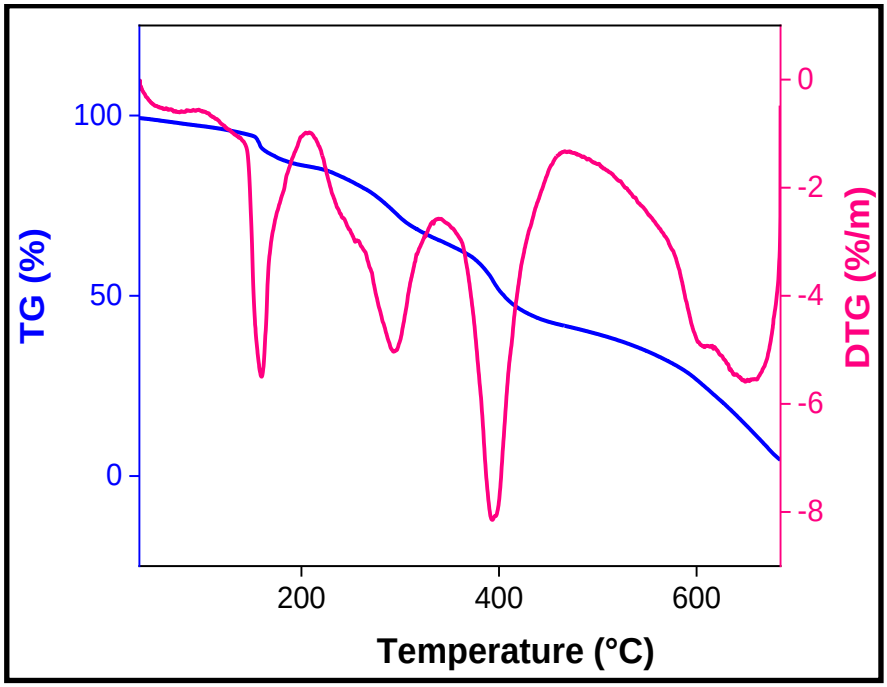

Figure 3.3. Thermogravimetric graph of poly(acrylamide) hydrogel.

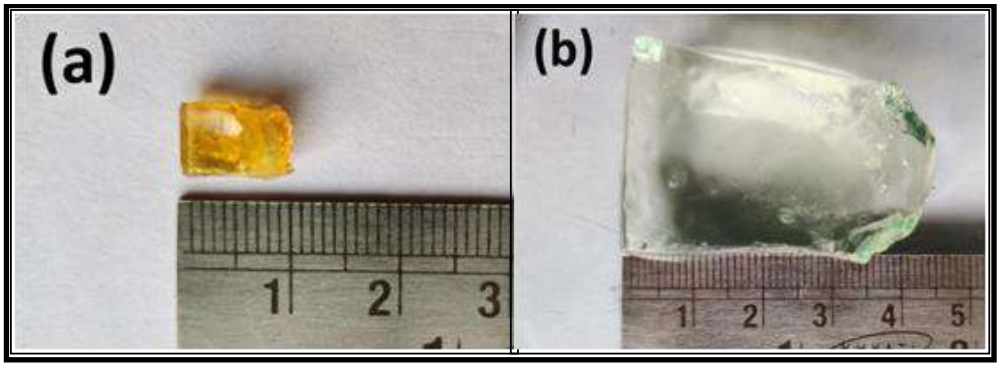

Figure 3.4. Digital camera photographs of (a) dried and (b) swollen poly(acrylamide) hydrogel in water.

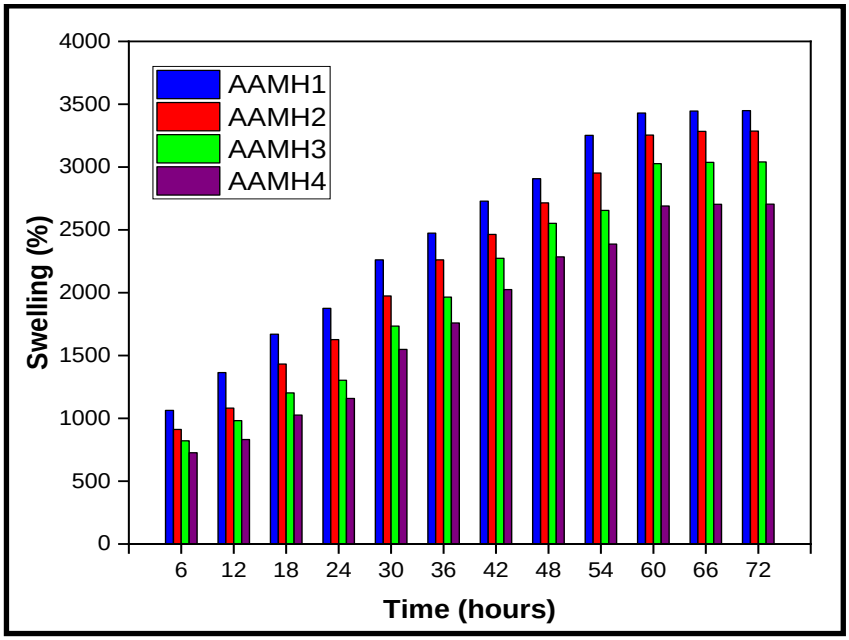

Figure 3.5. Swelling (%) of poly(acrylamide) hydrogel in water.

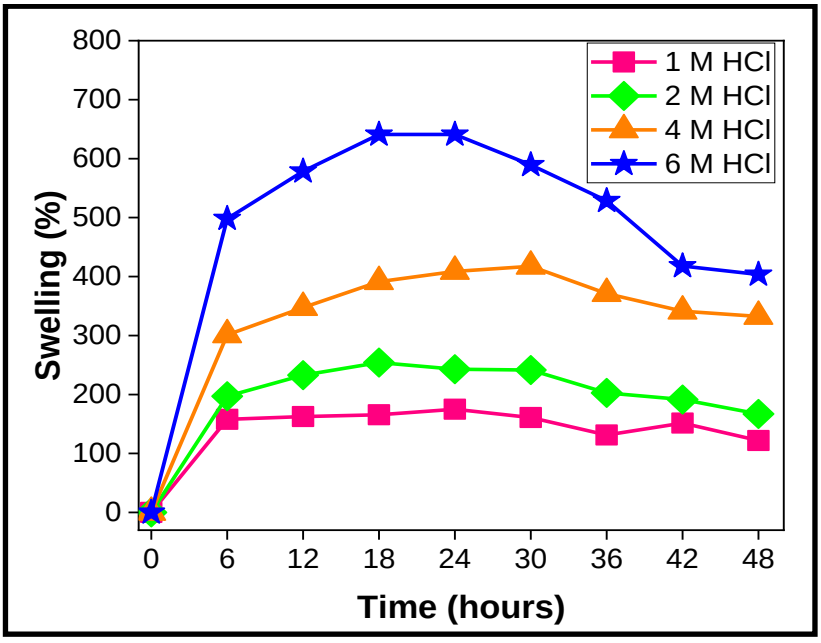

Figure 3.6. Swelling (%) of poly(acrylamide) hydrogel in HCl of concentration range 1 M to 6 M.

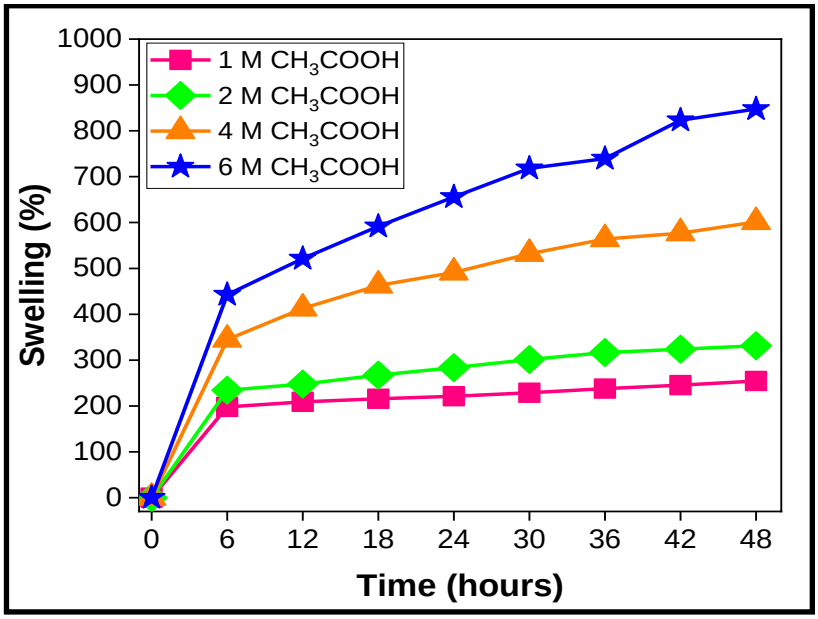

Figure 3.7. Swelling (%) of poly(acrylamide) hydrogel in CH_3COOH of concentration range 1 M to 6 M.

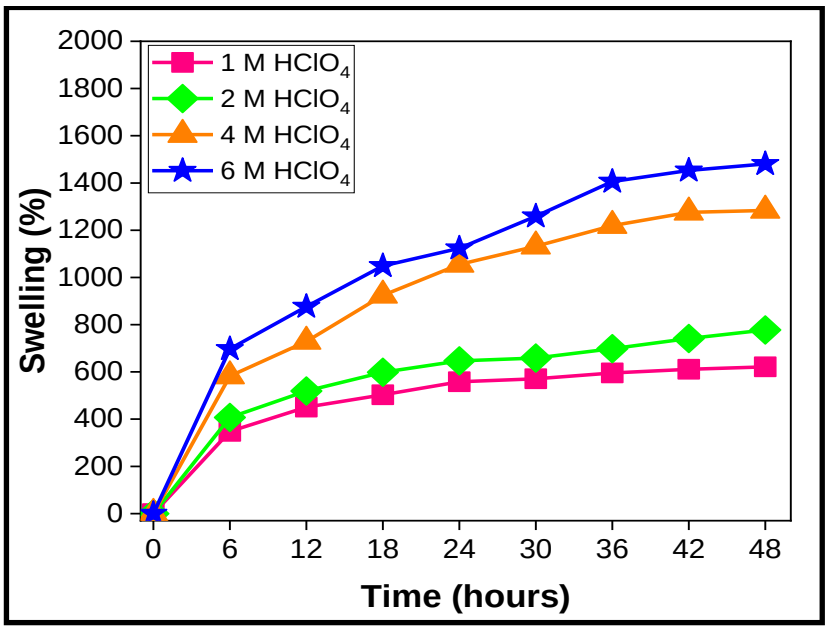

Figure 3.8. Swelling (%) of poly(acrylamide) hydrogel in $HClO_4$ of concentration range 1 M to 6 M.

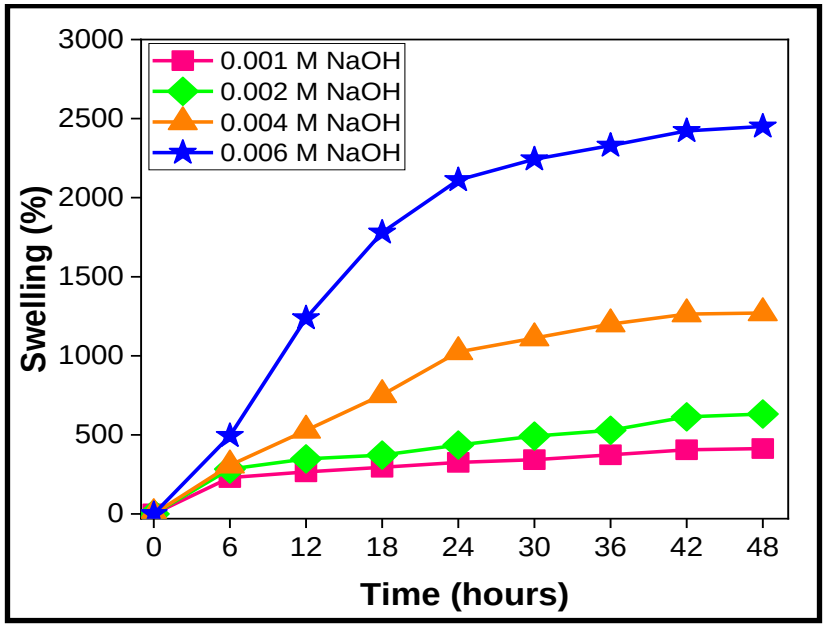

Figure 3.9. Swelling (%) of poly(acrylamide) hydrogel in NaOH of concentration range 0.001 M to 0.006 M.

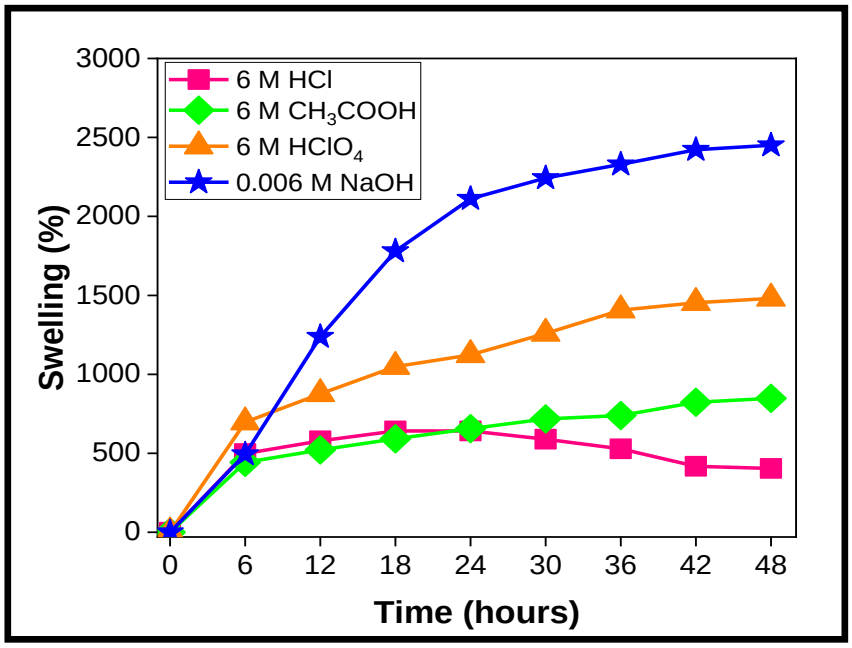

Figure 3.10. Comparison Swelling (%) of poly(acrylamide) hydrogel in acid and base media.

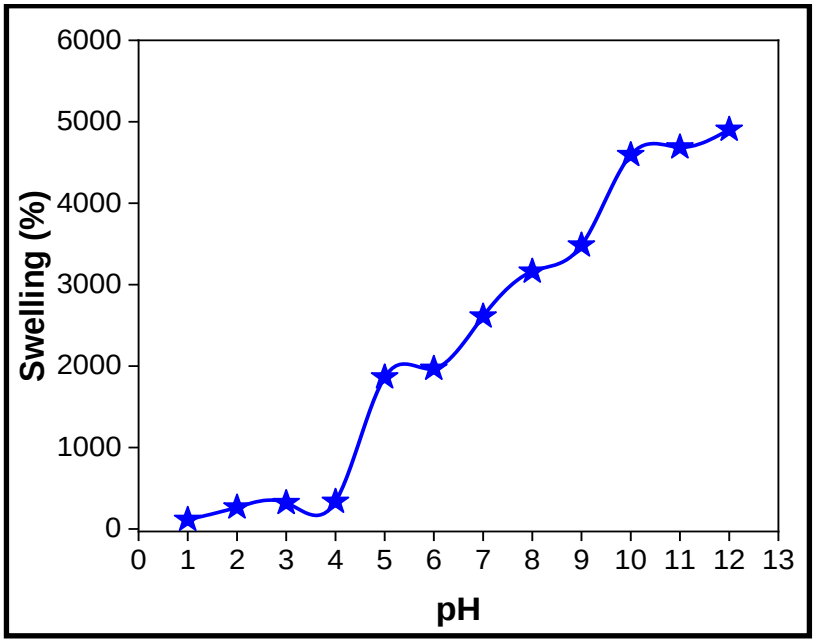

Figure 3.11. Swelling (%) of poly(acrylamide) hydrogel in pH 1 to 12 at 37°C.

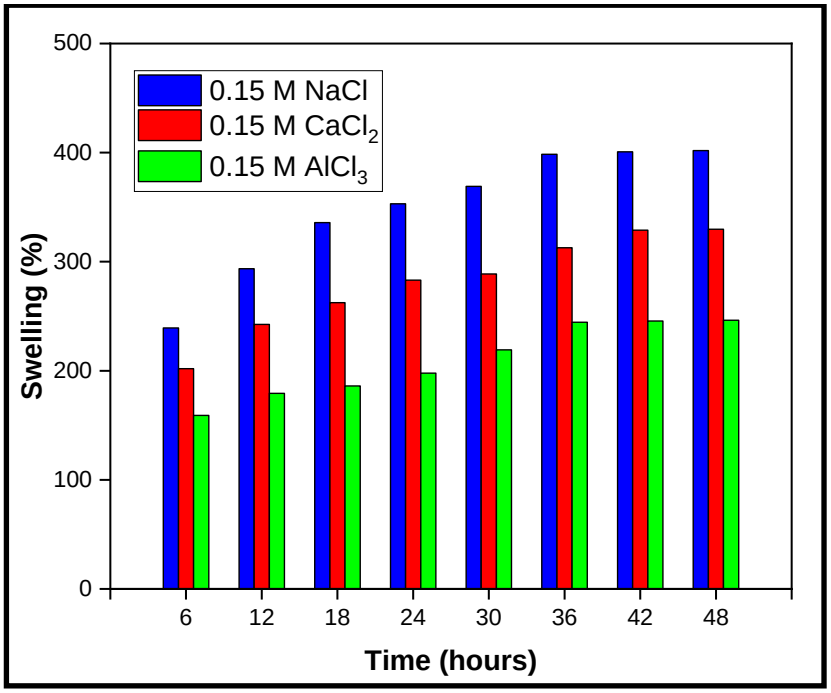

Figure 3.12. Swelling (%) of poly(acrylamide) hydrogel in salt solutions.

3.5. References

[1] Peppas N. A., Khare A. R.; Preparation, structure and diffusional behavior of hydrogels in controlled release. *Advanced Drug Delivery Reviews,* 1993, 11, 1–35.

[2] Niladri R., Nabanita S.; PVP-Based Hydrogels: Synthesis, Properties and Peppas Applications. 2012, 1-33.

[3] Kashyap N., Kumar N., Kumar M.; Hydrogels for pharmaceutical and biomedical applications. *Critical Reviews in Therapeutic Drug Carrier Systems,* 2005, 22, 107–149.

[4] Karada E., Saraydin D., Caldiran Y., Guven O.; Swelling studies of copolymeric acrylamide/crotonic acid hydrogels as carriers for agricultural uses. *Polymers for Advanced Technologies,* 2000, 11(2), 59–68.

[5] Chen X., Martin B. D., Neubauer T. K., Linhardt R. J., Dordick J. S., Rethwisch D. G. Enzymatic and chemoenzymatic approaches to synthesis of sugar based polymer and hydrogels. *Carbohydrate Polymers,* 1995, 28, 15–21.

[6] Singh A., Sharma P. K., Garg V. K., Garg G.; Hydrogels: a review. *International Journal of Pharmaceutical Sciences Review and Research,* 2010, 4(2), 97-105.

[7] Hamidi M., Azadi A., Rafiei P.; Hydrogel nanoparticles in drug delivery. *Advanced Drug Delivery Reviews,* 2009, 60(15), 1638–1649.

[8] Dzinomwa G. P. T., Wood C. J., Hill D. J. T.; Fine Coal Dewatering Using pH- and Temperature-Sensitive Superabsorbent Polymers. *Polymers for Advanced Technologies,* 1997, 8, 767– 772

[9] Kaihara S., Matsumura S., Fisher J. P.; Synthesis and characterization of cyclic acetal based degradable hydrogels. *European Journal of Pharmaceutics and Biopharmaceutics,* 2008, 68(1), 67–73.

[10] Stamatialis D. F., Papenburg B. J., Girones M., Saiful S., Bettahalli S. N. M., Schmitmeier S., Wessling M.; Medical applications of membranes: drug delivery, artificial organs and tissue engineering. *Journal of Membrane Science*, 2008, 308(1–2), 1–34.

[11] Roy D., Cambre J. N., Brent S.; Sumerlin future perspectives and recent advances in stimuli-responsive materials. *Progress in Polymer Science,* 2010,

35(12), 278–301.

[12] Sikareepaisan P., Ruktanonchai U., Supaphol P.; Preparation and characterization of asiaticoside-loaded alginate films and their potential for use as effectual wound dressings. *Carbohydrate Polymers,* 2011, 83(4), 1457–1469.

[13] Van der Linden H. J., Herber S., Olthuis W., Bergveld P.; Patterned dual pH responsive core shell hydrogels with controllable swelling kinetics and volume. *Analyst*, 2003, 128, 325–331.

[14] Zhang L., Li K., Xiao W., Zheng L., Xiao Y., Fan H., Zhang X. Preparation of collagen–chondroitin sulfate–hyaluronic acid hybrid hydrogel scaffolds and cell compatibility in vitro. *Carbohydrate Polymers,* 2011, 84(1), 118–125.

[15] Saul J. M., Williams D. F.; Hydrogels in regenerative medicine, principles of regenerative medicine, 2011, 2, 637–661.

[16] Wang F., Li Z., Khan M., Tamama K., Kuppusamy P., Wagner W. R., Sen C. K., Guan J. Injectable, rapid gelling and highly flexible hydrogel composites as growth factor and cell carriers. *Acta Biomaterialia,* 2010, 6(6), 1978–1991.

[17] Krsko P., McCann T. E., Thach T. T., Laabs T. L., Geller H. M., Libera M. R. Length-scale mediated adhesion and directed growth of neural cells by surface-patterned poly(ethylene glycol) hydrogels. *Biomaterials,* 2009, 30(5), 721–729.

[18] Chu Y., Varanasi P. P., McGlade M. J., Varanasi S.; pH-induced swelling kinetics of polyelectrolyte hydrogels. *Journal of Applied Polymer Science,* 1995, 58, 2161-2176.

[19] Firestone B. A., Siegel R. A.; pH, salt and buffer dependent swelling in ionizable copolymer gels: Tests of the ideal Donnan equilibrium theory. *Journal of Biomaterials Science, Polymer Edition*. 1994, 5, 433-450.

[20] Yoshida R., Uchida K., Kaneko Y., Sakai K., Kikuchi A., Sakurai Y., Okano T.; Comb-type grafted hydrogels with rapid deswelling response to temperature changes. *Nature*. 1995, 374, 240-242.

[21] Mamada A., Tanaka T., Kungwatchakun D., Irie M.; Photoinduced phase transition of gels. *Macromolecules*. 1990, 23, 1517-1519.

[22] Zhong X., Wang Y. X., Wang S. C.; Pressure dependence of the volume phase-transition of temperature-sensitive gels. *Chemical Engineering Science*. 1996,

51, 3235-3239.

[23] Shiga T., Hirose Y., Okada A., Kurauchi T.; Electric field-associated deformation of polyelectrolyte gel near a phase transition point. *Journal of Applied Polymer Science*. 1992, 46, 635-640.

[24] Osada Y., Okuzaki H., Hori H.; A polymer gel with electrically driven motility. *Nature*. 1992, 355, 242-244.

[25] Miyata T., Asami N., Uragami T.; A reversibly antigen-responsive hydrogel. *Nature*. 1999, 399, 766-769.

[26] Dabbagh M. A., Moghimipour E., Ameri A., Sayfoddin A.; Physicochemical characterization and antimicrobial activity of nanosilver containing hydrogels. *Iranian Journal of Pharmaceutical Research*. 2008, 7, 21-28.

[27] Obaidat A. A., Park K.; Characterization of protein release through glucose-sensitive hydrogel membranes. *Biomaterials*, 1997, 18, 801-806.

[28] Peppas N. A., Buresa P., Leobandunga W., Ichikawa H.; Hydrogels in pharmaceutical formulations. *European Journal of Pharmaceutics and Biopharmaceutics*, 2000, 50, 27-46.

[29] Kost J., Langer R.; Responsive polymeric delivery systems. *Advanced Drug Delivery Reviews*, 2001, 46, 125-148.

[30] Qui Y., Park K.; Environment-sensitive hydrogels for drug delivery. *Advanced Drug Delivery Reviews*, 2001, 53, 321-339.

[31] Tasdelen B., Apohan N. K., Guven O., Baysal B. M.; pH-Thermoreversible hydrogels. I. Synthesis and characterization of poly(N-isopropylacrylamide/maleic acid) copolymeric hydrogels. *Radiation Physics and Chemistry*, 2004, 69, 303-310.

[32] Tang S. Y., Shridharan P., Sivakumar M.; Impact of process parameters in the generation of novel aspirin nanoemulsions – Comparative studies between ultrasound cavitation and microfluidizer. *Ultrasonics Sonochemistry*, 2013, 20, 485-497.

[33] Jokanovic V., Colovic B., Dutour Sikiric M., Trajkovic V.; A new approach to the drug release kinetics of a discrete system: SiO2 system obtained by ultrasonic dry spraying. *Ultrasonics Sonochemistry*, 2013, 20, 535-545.

[34] Shelly, Setia H., Takur A., Wanchoo R. K.; Structural parameters and swelling

behaviour of pH sensitive poly (vinyl alcohol)/Poly (ethylene oxide) and poly (vinyl alcohol)/xanthan gum hydrogels. *Journal of Polymer Materials,* 2012, 29, 401–409.

[35] Cass P., Knower W., Pereeia E., Holmes N., Hughes T.; Preparation of hydrogels via ultrasonic polymerization. *Ultrasonics Sonochemistry*, 2010, 17, 326.

[36] Varaprasad K., Raghavendra G. M., Jayaramudu T., Yallapu M. M., Sadiku R.; A mini review on hydrogels classification and recent developments in miscellaneous applications. *Materials Science and Engineering: C,* 2017, 79, 958-971.

[37] Mahdavinia G., Pourjavadi A., Hosseinzadeh H., Zohuriaan M.; Modified chitosan 4. Superabsorbent hydrogels from poly (acrylic acid-co-acrylamide) grafted chitosan with salt-and pH-responsiveness properties. *European Polymer Journal,* 2004, 40, 1399-1407.

[38] Ebdon J. R., Huckerby T. N., Hunter T. C.; Free-radical aqueous slurry polymerizations of acrylonitrile: 1. End-groups and other minor structures in polyacrylonitriles initiated by ammonium persulfate/sodium metabisulfite. *Polymer*, 1994, 35, 250-256.

[39] Reddy B. V., Rao R. B.; Vibrational spectra and modified valence force field for N, NC-methylenebisacrylamide. *Indian Journal of Pure and Applied Physics*, 2008, 46, 611–616.

[40] Avsar A., Gokbulut Y., Ay B., Serin S.; A novel catalyst system for the synthesis of N,N′-Methylenebisacrylamide from acrylamide. *Designed Monomers and Polymers*. 2017, 20(1), 434-440.

[41] Chen J., Liu M., Liu H., Ma L.; Synthesis, swelling and drug release behavior of poly (N, N-diethylacrylamide-co-N-hydroxymethyl acrylamide) hydrogel. *Materials Science and Engineering: C,* 2009, 29, 2116-2123.

[42] Aouada F. A., Chiou B. S., Orts W. J., Mattoso L. H.; Physicochemical and morphological properties of poly (acrylamide) and methylcellulose hydrogels: effects of monomer, crosslinker and polysaccharide compositions. *Polymer Engineering* & *Science,* 2009, 49, 2467-2474

[43] Ebrahimi R., Salavaty M.; Controlled drug delivery of ciprofloxacin

from ultrasonic hydrogel. *e-Polymers*, 2018, 18(2), 187–195.

[44] Wu J., Lin J., Li G., Wei C.; Influence of the COOH and COONa groups and crosslink density of poly (acrylic acid)/montmorillonite superabsorbent composite on water absorbency, *Polymer International*, 2001, 50, 1050-1053.

[45] Nesrinne S., Djamel A.; Synthesis, characterization and rheological behavior of pH sensitive poly (acrylamide-co-acrylic acid) hydrogels, *Arabian Journal of Chemistry*, 2017, 10(4), 539-547.

[46] Pourjavadi A., Mahdavinia G. R.; Superabsorbency, pH-Sensitivity and Swelling Kinetics of Partially Hydrolyzed Chitosan-g-poly(Acrylamide) Hydrogels. *Turkish Journal of Chemistry*, 2006, 30, 595-608.

[47] Shivakumara L. R., Demappa T.; Synthesis and Swelling Behavior of Sodium Alginate / Poly(vinyl alcohol) Hydrogels. *Turkish Journal of Pharmaceutical Sciences*, 2019, 16(1), 252-260.

Chapter – 4

Controlled drug release of levofloxacin from poly(acrylamide) hydrogel

Chapter – 4

Controlled drug release of levofloxacin from poly(acrylamide) hydrogel

This chapter discusses the development of poly(acrylamide) hydrogels for the controlled release of levofloxacin.

Abstract

Hydrogels are 3D polymer networks capable to absorb and release water or biological fluids. They are stimuli-responsive materials, which can show rapid volume changes with response to small changes in environmental parameters such as ionic strength, pH and temperature. In this work, we performed a synthesis of Poly(acrylamide) hydrogel and tested for controlled release of levofloxacin hemihydrate as a model drug. We used sodium metabisulfite and potassium persulphate as free radical initiators to prepare hydrogel with methylenebisacrylamide as a crosslinker. Characterization of hydrogel was performed by TGA, SEM and FT-IR. Swelling study and drug release were performed at pH 1.2 and 7.4, identical to the gastrointestinal fluid at 37°C (human body temperature) to examine possible site-specific drug delivery. UV-Visible spectrophotometer was used to measure the concentration of drug release. Results exhibited the pH and temperature-dependent drug release. After 6 hours the amount of drug release was found to be 17% and 99% in acidic and alkaline pH of 1.2 and 7.4 respectively and drug-loaded hydrogel shows good antibacterial activity.

4.1. Introduction

The polymers are continuous repeating monomer units. The general biomedical uses of polymers are in drug delivery systems, pharmaceutical adhesives, coating material and emulsifying agents for dosage forms in site-specific and controlled drug delivery systems. Polymer molecules are linear or branched or may be crosslinked. The chemical response of polymers depends on the monomer unit present in the polymer chain. The homopolymers are having identical monomeric units and copolymers are formed from more than one monomer [1-3].

The first polymer gel was prepared in 1949 by Katchalsky. This gel responds to the surrounding environment solution by swelling or gathering from a network of water-soluble polyelectrolytes [4]. In 1950 medical applications and the importance of hydrogels were revealed and using 2-hydroxyethyl methacrylate gel, soft contact lenses are manufactured. The smart hydrogel, like temperature-sensitive hydrogels, is focused till the mid-1980 [5]. In the drug delivery systems, pH-sensitive hydrogels are the best materials for drug release to the target site of the body [6-7].

Poly(acrylamide) hydrogel polymer backbone containing functional group like amine is sensitive to charge either by releasing or accepting protons in the aqueous media. The electrostatic repulsion in the polymer backbone network promotes swelling and then water diffusion. These hydrogels are more sensitive to slight changes in environmental factors. These are called smart hydrogels [8, 9, 4].

Levofloxacin, molecular formula $C_{18}H_{20}FN_3O_4$, and **Fig. 4.1** show its molecular structure. Levofloxacin is a fluoroquinolone antibacterial drug with an active L-isomer of ofloxacin [10, 11]. Levofloxacin is used to cure the disease of gram-negative and gram-positive bacteria like keratitis, bacterial conjunctivitis and

other eye infections by inhibiting topoisomerase IV and DNA gyrase enzymes. These enzymes are important to DNA replication, recombination, transcription and repair [12, 13].

In the present work, we evaluate the drug release from poly(acrylamide) hydrogel using different temperature and pH solutions. Crosslinker methylenebisacrylamide was used to control the network characteristic and model drug levofloxacinhemihydrate was used for drug release studies.

4.2. Materials and Methods

4.2.1. Materials

Sodium metabisulfite was received from Avra Synthesis Pvt. Ltd, Hyderabad, India. Potassium persulphate, methylenebisacrylamide, acrylamide, Potassium dihydrogen orthophosphate and sodium hydroxide were obtained from SDFCL, Mumbai, India. Hydrochloric acid, disodium hydrogen phosphate anhydrous were from Merck, Mumbai, India. Levofloxacin hemihydrate was gifted from Microlabs limited, Bangalore, India.

4.2.2. Poly(acrylamide) hydrogel synthesis

Poly(acrylamide) hydrogel was synthesized by a free radical mechanism. Primarily, redox initiators of potassium persulphate (45 mg) and sodium metabisulfite (32 mg) were shifted into a glass vial containing 10 ml of deionized water. Then, add acrylamide (600 mg), allowed to stir for 10 minutes at room temperature after this crosslinker methylenebisacrylamide (06 mg) was added. Then, this composite was kept in a water bath until the gel was formed. The

synthesized gel was washed with water to remove unreacted components. Then, the hydrogel was dried at 50^{o}C in the oven for 24 hours.

4.2.3. FT-IR analysis

Levofloxacin, poly(acrylamide) hydrogel and levofloxacin-loaded hydrogel spectra were recorded using an FT-IR spectrometer (Shimadzu ATR) in the range of 400 to 4000 cm^{-1} to determine their intermolecular interactions and structure.

4.2.4. TGA analysis

To determine the thermal stability of poly(acrylamide) hydrogel was performed using a thermogravimetric analyzer (Perkin Elmer STA 600) by increasing the heating rate to 20^{o}C.

4.2.5. Morphological examination

The morphology of poly(acrylamide) hydrogel structures was determined using SEM (scanning electron microscope). Hydrogel composites were cut to expose their structure and imaged in an (SEM Zeiss, LS15) scanning electron microscope.

4.2.6. Swelling study of poly(acrylamide) hydrogel

The swelling study of synthesized poly(acrylamide) hydrogel was determined using dry samples in acidic buffer pH 1.2 and phosphate buffer pH 7.4. The pre-weighed hydrogel samples were immersed in solutions at 37^{o}C for swelling. At periodic intervals, the swollen samples were taken out from the solution and excess droplets on the surface of the hydrogel were withdrawn by wiping with filter paper and then weighed. The swelling (%) of hydrogel was determined from the following equation. Similarly, the swelling (%) was observed

at 27^{o}C in pH 7.4 with time intervals.

$$\textbf{Swelling}\ (\%) = \frac{\mathbf{W_b - W_a}}{\mathbf{W_a}}\ \mathbf{x\ 100} \qquad \ldots\ldots\ldots\ldots\ (\mathbf{4.1})$$

Where, $\mathbf{W_a}$ and $\mathbf{W_b}$ are the weight of dry and swollen gel.

4.2.7. Construction of Levofloxacin calibration curve

The stock solution of 1000 mg/l of Levofloxacin drug solution was prepared using distilled water as a solvent, then 2, 4, 6, 8 and 10 mg/l solutions were prepared by dilution of the stock solution. Using a UV-9000A spectrophotometer (Shanghai Metash), scan the solutions between 200 to 400 nm and the absorption maximum was recorded to construct the calibration curve.

4.2.8. Drug loading and drug release studies

Levofloxacin hemihydrate was selected as a model drug. The loading of the drug was conducted in a 1000 mg/l solution using water as a solvent. Place 0.1 g of dry hydrogel in 100 ml levofloxacin solution. The loaded hydrogel was dried and note down the loaded hydrogel weight. The *in-vitro* release study was conducted by placing drug-loaded hydrogel in acidic buffer pH 1.2 and phosphate buffer pH 7.4 at 37^{o}C and 27^{o}C respectively using the paddle method in the dissolution test apparatus (LabIndia, DS-8000, India). Next withdraw dissolution medium sample at regular time intervals (30 minutes) with stirring and replace fresh solution to maintain constant dissolution media. Using a UV-Visible spectrophotometer, scan the solutions between 200 to 400 nm with suitable dilution and note down the λ_{max} absorbance. The percentage of released levofloxacin was calculated and its corresponding drug release graph was plotted. Similarly, effects of temperature on

drug release has been studied at 27^{o}C and 37^{o}C respectively in pH 7.4.

4.2.9. Kinetics model drug release

The kinetics models of drug release will determine using Zero-order, first-order, Hixson-Crowell, Higuchi and Korsmeyer-Peppas models [14, 15].

4.2.10. Antibacterial study

The synthesized hydrogel and levofloxacin drug-loaded hydrogel were used for the *in-vitro* antibacterial test by using the agar diffusion method. For this purpose, 5 μg/ml of levofloxacin drug, levofloxacin drug-loaded hydrogel and synthesized hydrogel were prepared in distilled water and each 0.1 ml loaded on nutrient agar plates. After 24 hours of incubation at 37°C the inhibition zones were calculated.

4.3. Results and Discussion

Poly(acrylamide) hydrogel was synthesized by a radical polymerization method and its swelling study was performed. Moreover, drug loading and drug release were also performed using levofloxacin as a model drug and the effect of pH, temperature and time of the drug release will also be studied.

4.3.1. Hydrogel preparation

The various steps involved in the preparation of Poly(acrylamide) hydrogel are shown in **Fig. 4.2.** After the gel preparation, the swelling study was performed [16 - 18].

4.3.2. FT-IR analysis

The FT-IR spectra of levofloxacin, poly(acrylamide) hydrogel and levofloxacin loaded poly(acrylamide) hydrogel were recorded are shown in **Fig. 4.3.**

The characteristic peaks of levofloxacin (**Fig. 4.3a**) were found at 3243 $cm^{-1}$and 1439 cm^{-1}(stretching and bending vibrations of the carboxylic acid -OH group), 2849 cm^{-1} and 1618 cm^{-1} (C-H stretching of -CH_3 and aromatic rings respectively), 1712 cm^{-1} (C=O stretching of the cyclohexanone), 1289 cm^{-1} (C-F stretching peak). The poly(acrylamide) hydrogel spectra (**Fig. 4.3b**) show the peaks at 3348 cm^{-1} (-NH stretching of hydrogel), 1648 cm^{-1} (C=O stretching). The levofloxacin-loaded poly(acrylamide) hydrogel spectra (**Fig. 4.3c**) show the peaks at 3348 cm^{-1} (-NH stretching of hydrogel), 3196 cm^{-1} (carboxylic acid -OH stretching of levofloxacin), 1667 cm^{-1} (C=O stretching), 1616 cm^{-1} (C=C stretching), 1296 cm^{-1} (C-F stretching), 1209 cm^{-1} (C-N stretching). The presence of amide, fluoro and carbonyl groups in loadedhydrogel confirms the drug loading in acrylamide hydrogel [19, 20].

4.3.3. TGA analysis

The thermogram of poly(acrylamide) hydrogel was shown in **Fig. 4.4.** The first stage of weight loss, consider as loss of moisture present in the hydrogel was observed at 169ºC with a mass loss of 3.4% then degradation occurred at 179ºC with weight loss of 9.6% for the elimination of ammonia gas from amide groups of poly(acrylamide) chains and maximum weight loss occurred at 381ºC with mass loss of 24.4% due to cleavage of the polymer chain and cross-linked network in hydrogel [21].

4.3.4. Morphological examination

The surface morphology of synthesized hydrogel was studied by SEM. The micrographs **Fig. 4.5(a)** and **Fig. 4.5(b)** reveal that the surface is uniform and smooth in nature [22, 23].

4.3.5. Swelling study of poly(acrylamide) hydrogel in pH solutions

The swelling study of the synthesized poly(acrylamide) hydrogel was performed in pH 1.2 and 7.4. The swelling study results of pH 7.4 are tabulated in the **Table 4.3** and their corresponding graphical representation is showed in **Fig. 4.6**. The comparison of poly(acrylamide) hydrogel swelling (%) in pH 1.2 and 7.4 at 37^{o}C is showed in **Fig. 4.7** and their corresponding statistical data was given in **Table 4.1.** From these results, a higher swelling rate was observed at pH 7.4 when compared to the pH 1.2. In an acidic medium of pH 1.2, the ammonium groups (NH_3^+) are formed by protonation but due to the presence of chloride (Cl^-) counterions the swelling decreased drastically [24, 25]. However, at pH 7.4 the (-$CONH_2$) and (-CONH-) groups are deprotonated and the presence of sodium (Na^+) ions in the solution will produce high osmotic swelling pressure hence showing maximum swelling. Similarly, for temperature sensitivity the swelling study was conducted at temperatures of 27^{o}C and 37^{o}C respectively. The results are tabulated in the **Table 4.2** and their corresponding graphical representation is showed in **Fig. 4.8**. The results showed that when the temperature increases swelling (%) also increases.

4.3.6. Construction of Levofloxacin calibration curve

Drug selection for the drug loading and drug release is most important because it should not react with hydrogel and solvents. This helps to avoid the λ_{max} shift. Levofloxacin drug is better material because no change was observed in the λ_{max} over time. Using a UV-Visible spectrophotometer, the solutions were scanned between 200 nm to 400 nm. The absorption maximum were recorded at λ_{max} 286 nm. The results are tabulated in the **Table 4.4** and their corresponding graphical

representation is showed in **Fig. 4.9 and 4.10.** From the calibration curve, the slope and intercept are found to be 0.144 and 0.017 respectively and the correlation coefficient (R^2) is 0.999.

4.3.7. Levofloxacin drug release study from poly(acrylamide) hydrogel

4.3.7.1. Levofloxacin drug release study in pH 1.2 and 7.4

The swelling studies of the synthesized hydrogel are carried out in the solution of pH 1.2 (acidic buffer) and pH 7.4 (phosphate buffer). The result showed that the maximum swelling % 3590.25 in pH 7.4 and the minimum swelling % 117.50 in pH 1.2. The results are tabulated in the **Table 4.1** and their corresponding graphical representation is showed in **Fig. 4.7**. The drug-loaded hydrogels were placed in the solutions of pH 1.2 and pH 7.4. About 99.92 % of levofloxacin drug was released in the solution of pH 7.4, where as only 16.82% of drug was released in the solution of pH 1.2. The results are tabulated in the **Table 4.5** and their corresponding graphical representation is showed in **Fig. 4.11**. Hence, we conclude that drug release depends on the pH of the solution because the swelling (%) is more in pH 7.4 than in the pH 1.2. The drug release from hydrogel into solution depends on swelling and the controlled release of levofloxacin was observed for up to 6 hours.

4.3.7.2. Levofloxacin drug release study at different temperature

The effect of temperature on Levofloxacin drug release was studied at temperatures of 27ºC and 37ºC respectively. The results are tabulated in the **Table 4.6** and their corresponding graphical representation is showed in **Fig. 4.12**. About 71.69% of drug has released at 27ºC and at 37ºC 99.92% of drug has been released. This indicates that as the temperature increases, the drug release also

increased. When the temperature increases, the hydrogel network flexibility also increases, as a result more amount of buffer solution enters into hydrogel which releases more amount of drug.

4.3.8. Kinetic model for drug release

The kinetic model of drug release has been studied by using various mathematical models like Zero-order, first-order, Hixson-Crowell, Higuchi and Korsmeyer-Peppas models. The obtained results are given in **Table 4.7** and their corresponding graphical representation is showed in **Fig. 4.13.** The observed maximum correlation coefficient (R^2) is 0.967 for the Higuchi model; hence the synthesized poly(acrylamide) hydrogel follows the Higuchi model.

4.3.9. Antibacterial activities

The levofloxacin drug-loaded hydrogel was investigated for *in-vitro* antibacterial effect. **Fig. 4.14** illustrated that Levofloxacin (L) pure drug and levofloxacin drug-loaded hydrogel (LLH) had an antibacterial effect on *S. aureus* and *E. coli* bacteria and no effect at unloaded hydrogel (H) after 24 hours incubation at 37°C. After measuring the inhibition zone the levofloxacin pure drug exhibited 11mm and 10mm for the levofloxacin drug-loaded hydrogels against *S. aureus* **(Fig 4.14a)** and 12mm and 10mm against *E. coli*, respectively **(Fig. 4.14b)**. As the result showed, levofloxacin pure drug and levofloxacin drug-loaded hydrogel shows antibacterial activity because of the bioactivity of the drug but the unloaded hydrogel will not show a zone of inhibition compared to pure drug and drug-loaded hydrogel. This effect could be due to the presence of levofloxacin in drug-loaded hydrogel [26].

4.4. Conclusion

Poly(acrylamide) hydrogel cross-linked with methylenebisacrylamide was synthesized and studied their swelling and drug release properties. The swelling study of synthesized hydrogel was examined at pH 1.2 and pH 7.4 at 37^{o}C and levofloxacin drug release studies were carried out under the same conditions. The drug released amount from the hydrogel was more at alkaline pH 7.4 than in the acidic pH 1.2. Because of its hydrophilic nature and the capability of hydrogen bonding of acrylamide molecules with water, it will produce high osmotic swelling pressure hence it will swell more and the amount of drug release is more. The temperature and pH effects on drug release were also studied, the hydrogel follows a Higuchi model and drug-loaded hydrogel shows good antibacterial activity; hence these hydrogels can be used in controlled drug release and biomedical applications due to good swelling properties.

Table 4.1. Statistical data of the poly(acrylamide) hydrogel swelling (%) in pH 1.2 and 7.4

Time (min)	pH 1.2 Swelling (%)	pH 7.4 Swelling (%)
0	0.00	0.00
360	113.33	637.01
720	121.66	1367.53
1080	125.83	1760.38
1440	129.16	2272.72
1800	127.50	2673.37
2160	120.83	3331.16
2520	118.33	3588.96
2880	**117.50**	**3590.25**

Table 4.2. Statistical data of the poly(acrylamide) hydrogel swelling (%) in a pH 7.4 at 27°C and 37°C.

Time (min)	27°C Swelling (%)	37°C Swelling (%)
0	0.00	0.00
360	547.02	637.01
720	1036.75	1367.53
1080	1353.51	1760.38
1440	1547.02	2272.72
1800	1821.08	2673.37
2160	2006.48	3331.16
2520	2058.91	3588.96
2880	**2104.32**	**3590.25**

Table 4.3. Statistical data of the poly(acrylamide) hydrogel swelling (%) changes in pH 7.4 over time

Time (hours)	pH 7.4 Swelling (%)
0	0.00
6	637.01
12	1367.53
18	1760.38
24	2272.72
30	2673.37
36	3331.16
42	3588.96
48	3590.25

Table 4.4. Statistical data of the calibration curve for levofloxacin (Absorbance v/s Concentration).

Concentration (mg/l)	Absorbance
0	0.00000
2	0.16078
4	0.30437
6	0.45747
8	0.60067
10	0.73669

Table 4.5. Statistical data of the levofloxacin drug release (%) over time in pH 1.2 and 7.4 from poly(acrylamide) hydrogel.

Time (min)	pH 1.2 Drug release (%)	pH 7.4 Drug release (%)
0	0.00	0.00
30	6.07	14.45
60	8.72	26.69
90	9.93	36.14
120	11.86	46.59
150	12.46	56.38
180	13.47	67.82
210	13.90	76.94
240	14.81	85.84
270	15.31	92.72
300	15.39	94.99
330	15.98	99.73
360	**16.82**	**99.92**

Table 4.6. Statistical data of the levofloxacin drug release (%) over time at 27°C and 37°C in pH 7.4 from poly(acrylamide) hydrogel.

Time (min)	27°C Drug release (%)	37°C Drug release (%)
0	0.00	0.00
30	8.78	14.45
60	14.43	26.69
90	21.27	36.14
120	28.41	46.59
150	35.46	56.38
180	41.03	67.82
210	48.55	76.94
240	57.04	85.84
270	61.92	92.72
300	64.60	94.99
330	67.97	99.73
360	**71.69**	**99.92**

Table 4.7. Levofloxacin drug release results in different kinetic models for up to 6 hours.

Name of the kinetic model	R^2	Slope	Intercept
Zero order	0.963	17.16	10.08
First order	0.773	-0.444	2.470
Higuchi	**0.967**	0.02	0.323
Korsmeyer-Peppas	0.541	1.207	1.159
Hixson-Crowell	0.958	0.698	-0.346

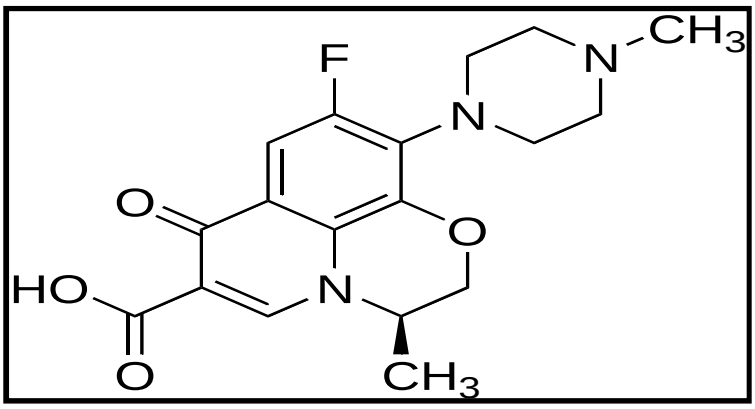

Figure 4.1. Molecular structure of levofloxacin.

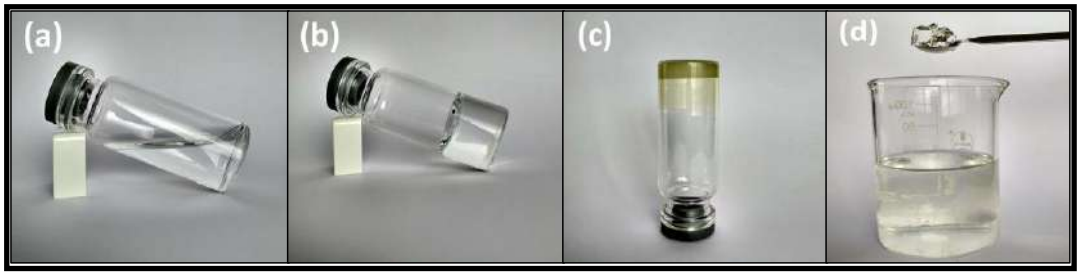

Figure 4.2. Poly(acrylamide) hydrogel preparation steps (a) initial solution, (b) after gel formation, (c) drying and (d) swelling.

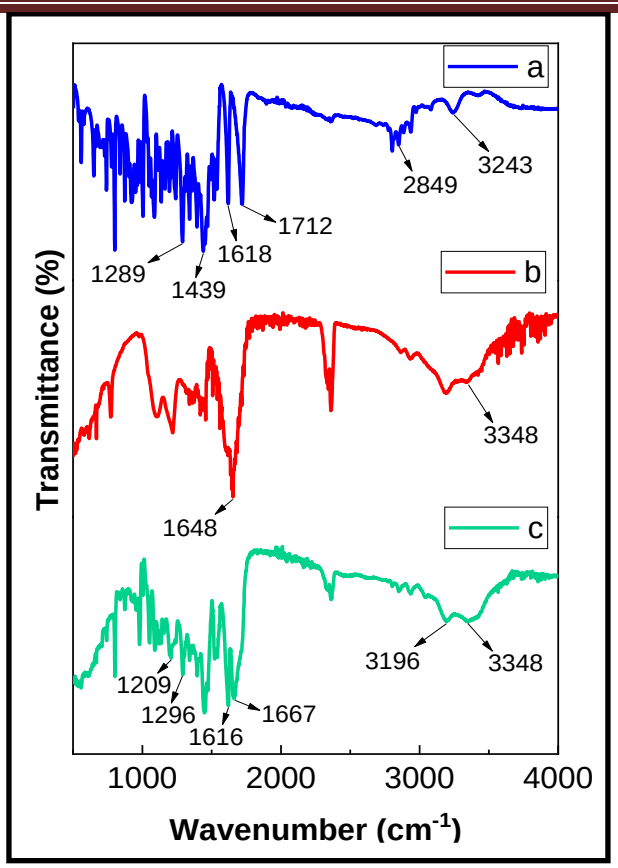

Figure 4.3. FTIR spectra of (a) levofloxacin, (b) poly(acrylamide) hydrogel and (c) levofloxacin loaded poly(acrylamide) hydrogel.

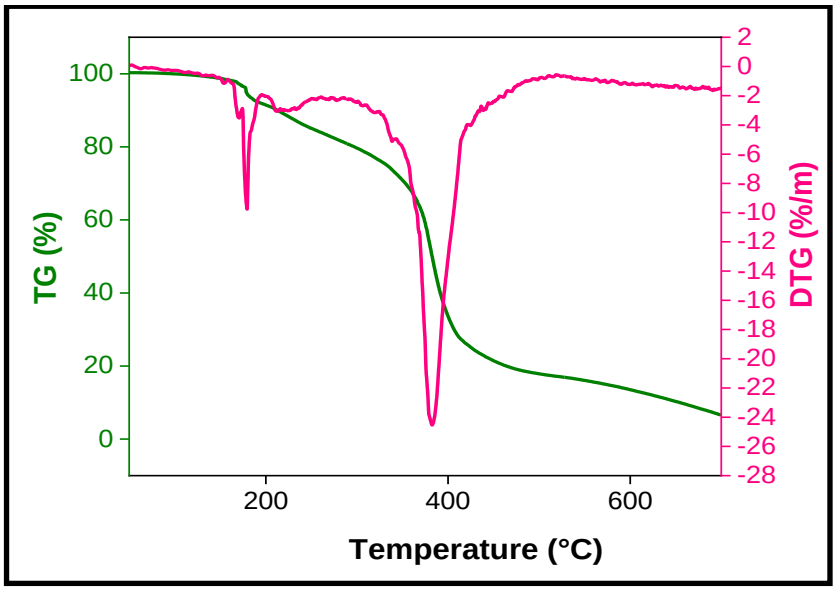

Figure 4.4. TGA graph of poly(acrylamide)hydrogel.

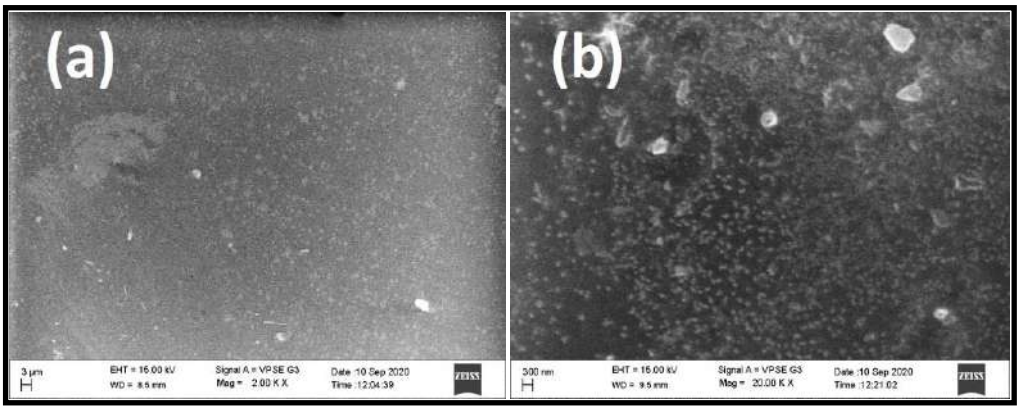

Figure 4.5. SEM images of poly(acrylamide)hydrogel.

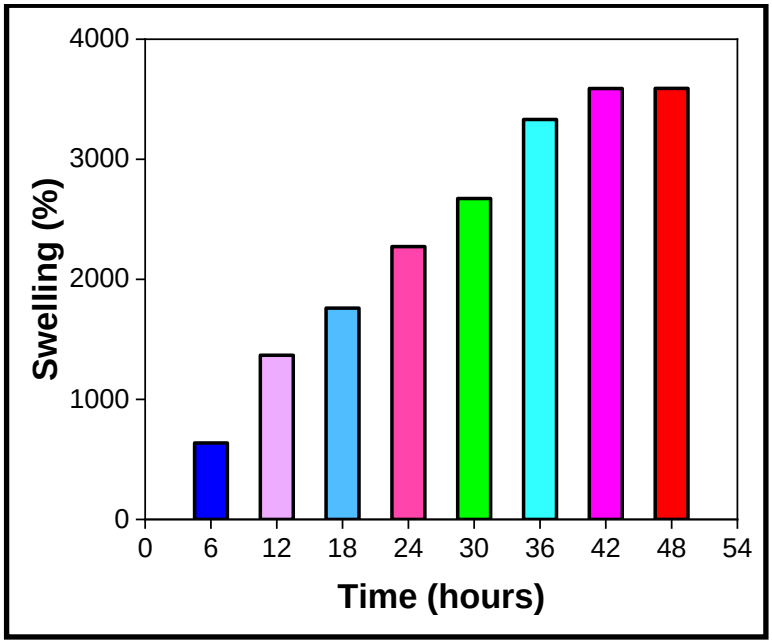

Figure 4.6. Poly(acrylamide) hydrogel swelling (%) changes over time in pH 7.4.

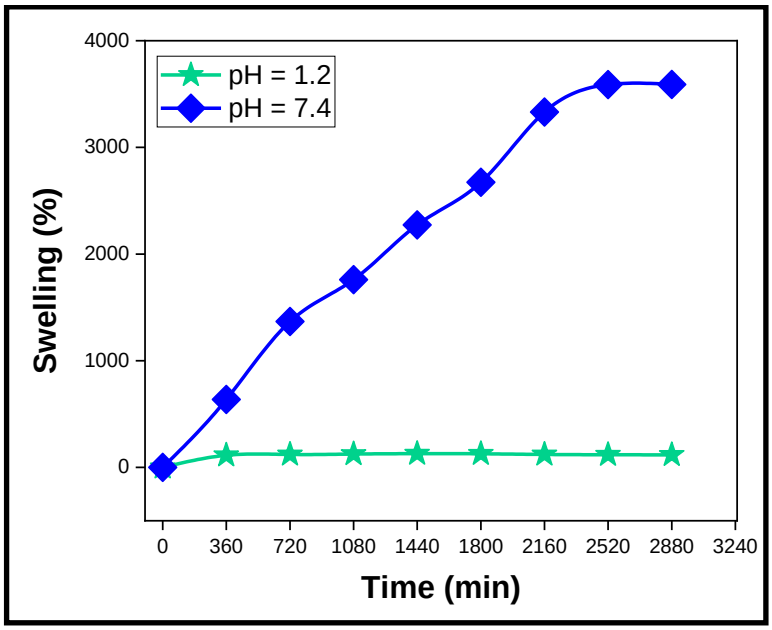

Figure 4.7. Swelling (%) of the poly(acrylamide) hydrogel in pH 1.2 and pH 7.4.

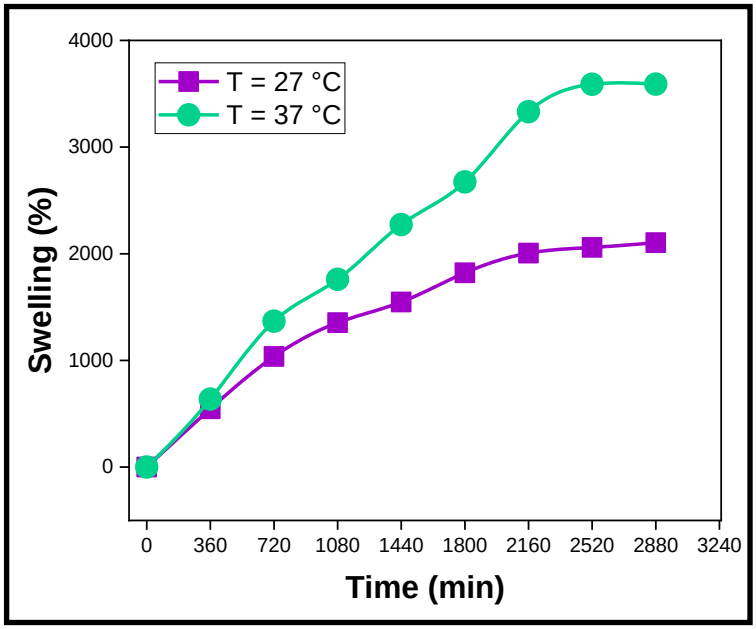

Figure 4.8. Swelling (%) of the poly(acrylamide) hydrogel at 27^{o}C and 37^{o}C temperatures in pH 7.4.

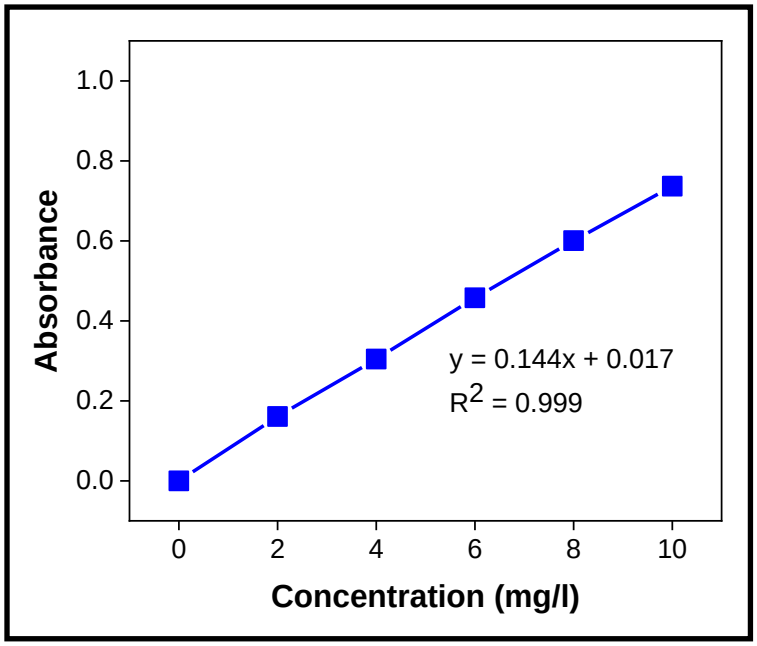

Figure 4.9. Calibration curve of levofloxacin (Absorbance v/s Concentration).

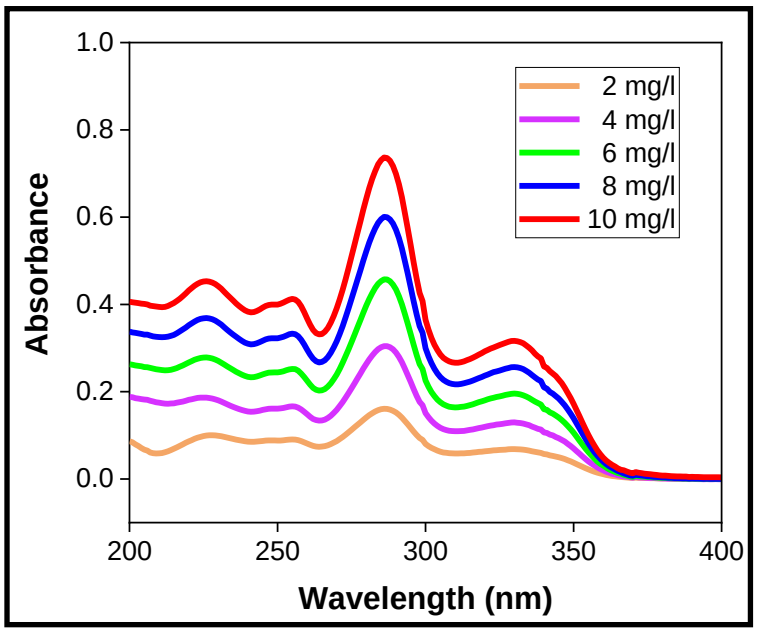

Figure 4.10. Spectral graph of the levofloxacin calibration curve.

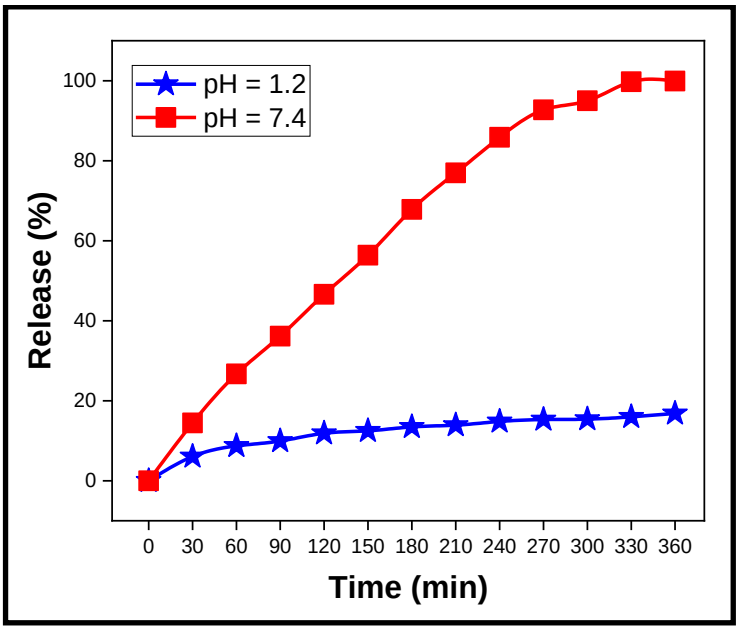

Figure 4.11. Levofloxacin drug release in pH 1.2 and pH 7.4 from poly(acrylamide) hydrogel with time.

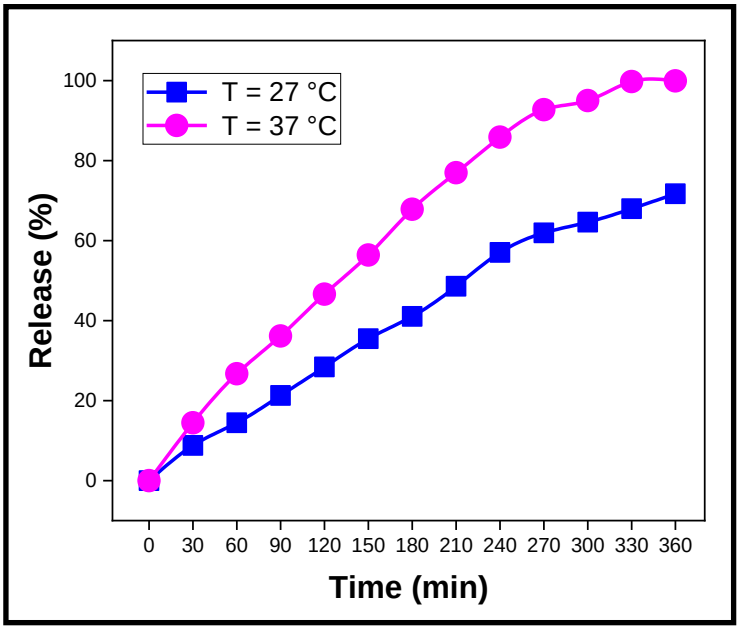

Figure 4.12. Levofloxacin drug release from poly(acrylamide) hydrogel with time at 27°C and 37°C temperature.

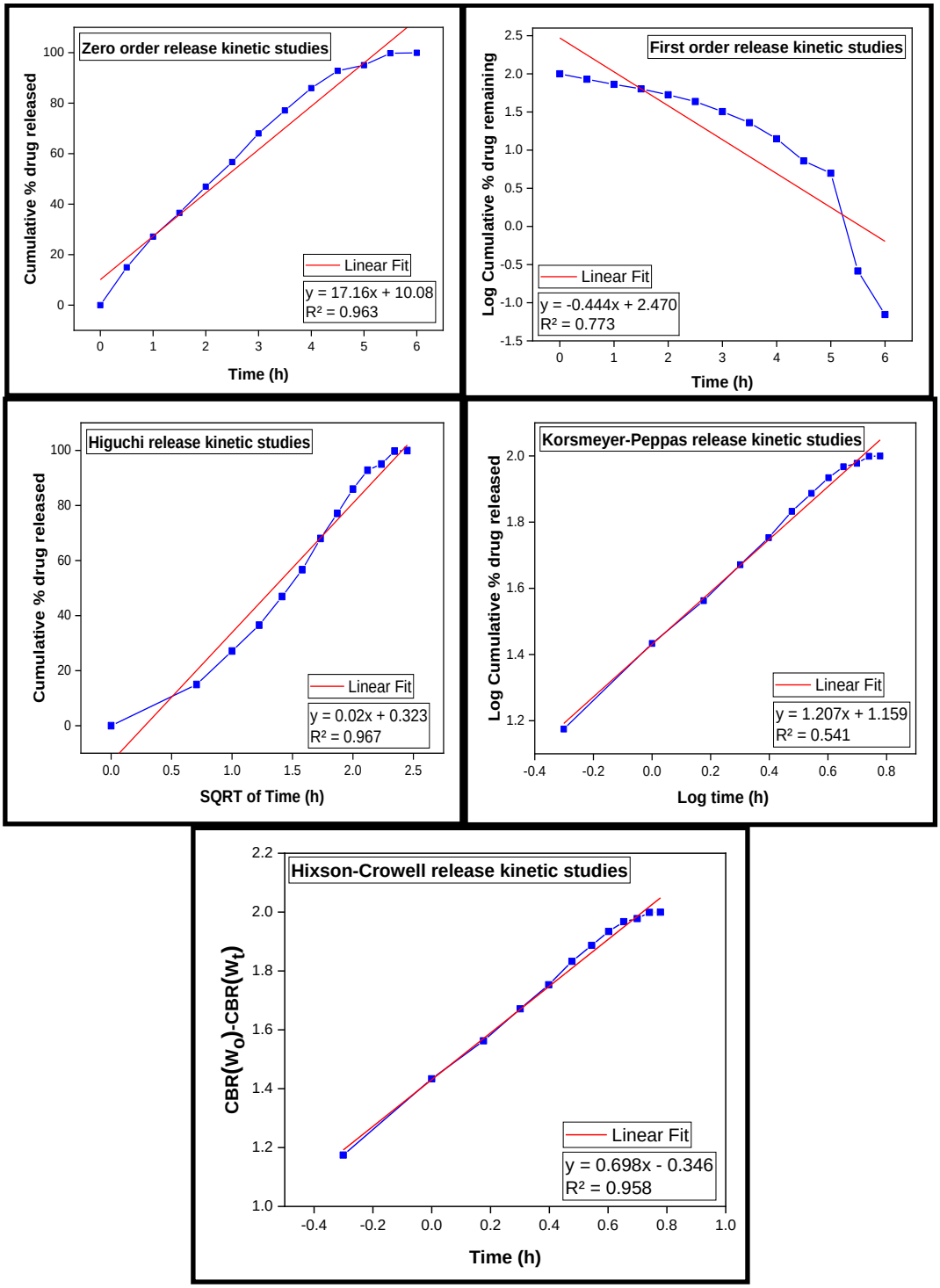

Figure 4.13. Graphical representation of kinetic model drug release from poly(acrylamide) hydrogel.

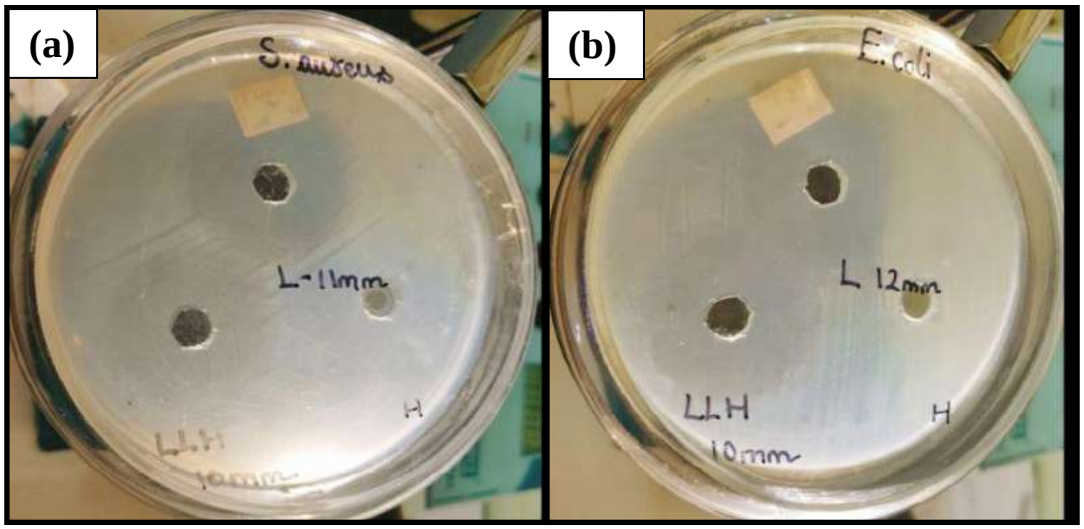

Figure 4.14. Antibacterial activity of levofloxacin drug-loaded hydrogel on **(a)** *S.aureus* (Gram-positive bacteria) and **(b)** *E.Coli* (Gram-negative bacteria).

4.5. References

[1] Kamboj V. K., Verma P. K.; Poloxamers based nanocarriers for drug delivery system. *Der Pharmacia Lettre*, 2015, 7(2), 264–269.

[2] Florence A. T., Attwood D.; Physicochemical Principles of Pharmacy, sixth edition. London.*Macmillan Press.* 1998, ISBN 9780857111746.

[3] Moghimi S. M., Hunter A. C.; Poloxamers and poloxamines in nanoparticle engineering and experimental medicine. *Trends in Biotechnology*, 2000, 18(10), 412–420.

[4] Katchalsky A., Gillis J.; Theory of the potentiometric titration of polymeric acids. *Recueil des Travaux Chimiques des Pays-Bas*, 1949, 68(9), 879–897.

[5] Kim J. K., Basavaraja C., Yamaguchi T., Huh D. S.; Preparation and characterization of smart hydrogel nanocomposites sensitive to oxidation-reduction. *Polymer Bulletin*, 2013, 70(1), 207–220.

[6] Hamidi M., Azadi A., Rafiei P.; Hydrogel nanoparticles in drug delivery. *Advanced Drug Delivery Reviews*, 2008, 60(15), 1638–1649.

[7] Huynh C. T., Nguyen M. K., Lee D. S.; Biodegradable pH/temperature sensitive oligo (*β*- amino ester urethane) hydrogels for controlled release of doxorubicin. *Acta Biomaterialia*, 2011, 7(8), 3123– 3130.

[8] Wan T., Xiong J., Zhao Q.; Crosslinker effects on swelling and gel properties of pH- and temperature-responsive poly (NIPAM/IA/AM) hydrogels. *Polymer Bulletin*, 2016, 73, 1447–1458.

[9] Wu C., Wang D., Wu H., Dan Y.; Synthesis and characterization of macroporous sodium alginate-g-poly(AA-co-DMAPMA) hydrogel. *Polymer Bulletin*, 2016, 73, 3255–3269.

[10] Hurst M., Lamb H. M., Scott L. J., Figgitt D. P.; Levofloxacin: an updated review of its use in the treatment of bacterial infections. *Drugs*, 2002, 62(14), 2127–2167.

[11] Chen T., Embree H. D., Brown E. M., Taylor M. M., Payne G. F.; Enzyme-catalyzed gel formation of gelatin and chitosan: potential for in situ applications. *Biomaterials*, 2003, 24(17), 2831–2841.

[12] Noel G. J.; A Review of Levofloxacin for the Treatment of Bacterial Infections. *Clinical Medicine Insights*, 2009, 1, 433–458.

[13] Hooper D. C.; Mode of Action of Fluoroquinolones. *Drugs*, 1999, 58(Supplement 2), 6–10.

[14] Baishya H.; Application of Mathematical Models in Drug Release Kinetics of Carbidopa and Levodopa ER Tablets. *Journal of Developing Drugs*, 2017, 6(2), 1–8.

[15] Kadam S., Dattatray A., Landge D.; Formulation and evaluation of colon targeted matrix tablet of azathioprine. *Indo American Journal of Pharmaceutical Research*, 2019, 9(7), 3157–3168.

[16] Anbarasan R., Jayaseharan J., Sudha M., Gopalan A.; Sonochemical polymerization of acrylic acid and acrylamide in the presence of a new redox system. A comparative study. *Journal of Applied Polymer Science*, 2003, 89(13), 3685–3692.

[17] Isık B., Kıs M.; Preparation and determination of swelling behavior of poly(acrylamide-co- acrylic acid) hydrogels in water. *Journal of Applied Polymer Science*, 2004, 94(4), 1526–1531.

[18] Teo B. M., Prescott S. W., Ashokkumar M., Grieser F.; Ultrasound initiated miniemulsion polymerization of methacrylate monomers. *Ultrasonics Sonochemistry*, 2008, 15(1), 89–94.

[19] Mouzam M. I., Dehghan M. H. G., Asif S., Sahuji T., Chudiwal P.; Preparation of a novel floating ring capsule type dosage form for stomach specific delivery. *Saudi Pharmaceutical Journal*, 2011, 19(2), 85–93.

[20] Sagdinc S., Bayari S.; Theoretical study of ofloxacin: geometrical parameters and vibrational wavenumbers. *Journal of Molecular Structure: Theochem*, 2004, 668(2-3) 93–99.

[21] Ebrahimi R., Salavaty M.; Controlled drug delivery of ciprofloxacin from ultrasonic hydrogel. *e-Polymers*, 2018, 18(2), 187–195.

[22] Chen J., Liu M., Liu H., Ma L.; Synthesis, swelling and drug release behavior of poly (N, N-diethylacrylamide-co-N-hydroxymethyl acrylamide)

hydrogel. *Materials Science and Engineering: C*, 2009, 29(7), 2116– 2123.

[23] Aouada F. A., Chiou B. S., Orts W. J., Mattoso L. H.; Physicochemical and morphological properties of poly(acrylamide) and methylcellulose hydrogels: Effects of monomer, crosslinker and polysaccharide compositions. *Polymer Engineering & Science*, 2009, 49(12), 2467–2474.

[24] Wu J., Lin J., Li G., Wei C.; Influence of the COOH and COONa groups and crosslink density of poly(acrylic acid)/montmorillonite superabsorbent composite on water absorbency. *Polymer International*, 2001, 50(9), 1050–1053.

[25] Pourjavadi A., Mahdavinia G. R.; Super absorbency, pH-Sensitivity and Swelling Kinetics of Partially Hydrolyzed Chitosan-g-poly(Acrylamide) Hydrogels. *Turkish Journal of Chemistry*, 2006, 30(5), 595–608.

[26] Croom K. F., Goa K. L.; Levofloxacin. *Drugs*, 2003, 63(24), 2769–2802.

Chapter – 5

Synthesis and characterization of poly(acrylamide-co-acrylic acid) hydrogel for moxifloxacin drug release study

Chapter – 5

Synthesis and characterization of poly(acrylamide-co-acrylic acid) hydrogel for moxifloxacin drug release study

This chapter discusses the synthesis and characterization of poly(acrylamide-co-acrylic acid) hydrogels for the controlled release of moxifloxacin.

Abstract

Sustained and controlled drug release has become the most attractive research work for obtaining a better drug delivery system with reliability, performance and safe drug release in the modern pharmaceutical drug delivery design. In this view, different polymers in controlled drug delivery applications are very useful. Therefore, using copolymerization by free-radical crosslinking and methylenebisacrylamide as the crosslinker with potassium persulfate and sodium metabisulfite as initiators, we synthesized poly(acrylamide-co-acrylic acid) hydrogels. The synthesized hydrogels were characterized by FTIR, TGA, SEM, swelling and *in-vitro* drug release studies. The hydrogel swelling analysis was analyzed using buffer solutions at varying pH and temperature levels. Drug release was investigated using moxifloxacin hydrochloride as a model drug. The drug release data indicate that after 5 hours, the drug release was found to be 18% at acidic pH 1.2 and 99% at alkaline pH 7.4 and it followed the Higuchi model and drug-loaded hydrogel shows good antibacterial activity.

5.1. Introduction

Hydrogels are polymer networks capable of carrying more water or biological fluid that are hydrophilic in nature. Due to the existence of physical or chemical crosslinks, polymer networks are formed by homopolymers or copolymers of an insoluble nature. These hydrogels have a thermodynamic affinity for water, which allows them to expand in an aqueous solution [1]. These hydrogels have a broader range of applications, especially in the medical and pharmaceutical fields [2-4]. The presence of extra water content and softness in the hydrogel is similar to the natural living tissue than any other synthetic biomaterial [3]. Also, because of the presence of extra water content, hydrogels have a biocompatibility quality. Hydrogels can also be used as biosensor membranes, drug delivery systems, artificial skin fabrics, linings for artificial hearts and contact lenses [5, 6].

In response to slight changes in environmental parameters such as ionic pressure, pH and temperature, hydrogels can show rapid volume changes known as stimuli-responsive materials. In smart hydrogels, stimulus-responsive polymers play a major role and these hydrogels are used in separation processes for industrial applications as potential economic alternatives to conventional separation processes [7]. Regulated permeability variations of sensitive gels may accomplish the charge or size-selective separations. The magnetic or electric field reveals powerful improvements in their swelling behavior, in addition to the temperature and pH sensitivity of the swelling behavior.

The copolymer, which consists of acrylic acid (AAC) and acrylamide (AAM) units is poly(AAM-co-AAC). A charge hydrogen-bonding capacity and adequate polarity for hydration are provided by the hydrophilic carboxylic acid and

amide moieties in the polymer backbone. The copolymer is very sensitive to pH and temperature, so in response to changes in pH and temperature this hydrogel shows a shift in swelling behavior [8].

Moxifloxacin is classified as a Biopharmaceutical Classification System (BCS) class I drug due to its high solubility and high permeability. If a drug substance has an absorption rate of 85% in humans, it is characterized as "highly permeable". We chosemoxifloxacin as a model drug because it has a rapid and nearly complete absorption in humans with an absolute bioavailability of around 90% [9].

A class of fourth-generation fluoroquinolone antibiotic drugs is moxifloxacin hydrochloride (**Fig. 5.1**). A bulk side chain in the C-7 position and a methoxy group in the C-8 position is present in the structure [10-12]. This antibiotic property is effective against both Gram-positive and Gram-negative bacteria. The mechanism of action of moxifloxacin is involvedin the inhibition of topoisomerase IV and DNA gyrase enzymes essential for the replication, repair and transcription of bacterial DNA [13-15].

The current study targeted the synthesis of poly(AAM-co-AAC) hydrogels by using AAM and AAC as monomers for varying crosslinkers with sodium metabisulfite (SMBS) and potassium persulfate as initiators. AAC allows water to swell further and AAM increases the hydrogel mechanical strength, so these hydrogels have strong mechanical and swelling potential. The presence of amide and acidic groups causes pH sensitivity in the polymer chain. As a model drug, the drug release analysis was carried out using moxifloxacin hydrochloride. In this study, the synthesized hydrogelis used to controlled release of the moxifloxacin drug.

5.2. Materials and Methods

5.2.1. Materials

AAC, MBA, potassium persulfate (PPS), AAM, sodium hydroxide and potassium dihydrogen orthophosphate were received from Sd Fine Chem Limited (SDFCL), Mumbai, India. Hydrochloric acid and disodium hydrogen phosphate anhydrous were from Merck, Mumbai, India. SMBS was obtained from Avra Synthesis Pvt Ltd, Hyderabad, India. Moxifloxacin hydrochloride was received as a gift sample from Micro Labs Limited, Bangalore, India.

5.2.2. Poly(AAM-co-AAC) hydrogel synthesis

The poly(AAM-co-AAC) hydrogel was synthesized in a glass vial using free-radical initiators of SMBS and PPS by dissolving in distilled water to generate free radicals. Then, AAC and AAM monomers were added and allowed to blend for 10 minutes at an ambient temperature, then crosslinker MBA was added with uniform stirring. Then, this blend was placed in a water bath (80°C) for 1 hour until gel formation. After gel formation, it was washed with distilled water for 24 hours to eliminate unreacted constituents and eventually dried for 24 hours in the hot air oven at 50°C and stored in a closed container to avoid moisture absorbance.

5.2.3. FT-IR analysis

To determine the molecular interactions and structure, moxifloxacin hydrochloride, synthesized hydrogel and moxifloxacin-loaded hydrogel samples were analyzed using the Fourier Transform Infrared Spectroscopy (FTIR) instrument (Shimadzu, IRAffinity 1S FTIR, Japan).

5.2.4. TGA analysis

In a thermogravimetric analyzer (Perkin Elmer, STA6000, USA), Thermogravimetric analysis (TGA) of the synthesized hydrogel was carried out. TGA was carried out by increasing the heat flow rate under the nitrogen atmosphere to 20°C/minute.

5.2.5. SEM Study

To study the surface morphology of dried hydrogels, a scanning electron microscope was used. Using a Scanning electron microscope (SEM) (Zeiss, LS15, Germany) instrument, the hydrogel composites were exposed and imaged.

5.2.6. Swelling study

The swelling study of synthesized poly(AAM-co-AAC) hydrogels were determined using dry samples in the pH range pH 1 to 10. The pre-weighed 0.1g poly(AAM-co-AAC) hydrogel samples were immersed in 100 ml solutions for swelling. The swollen samples were removed at particular time intervals and the surface water was absorbed with filter paper to eliminate excess outer surface droplets and then swollen poly(AAM-co-AAC) hydrogel were weighed and swelling (%) measured by following Equation.

$$\textbf{Swelling}\ (\%) = \frac{\mathbf{W_2 - W_1}}{\mathbf{W_1}}\ \mathbf{x\ 100} \qquad \ldots\ldots\ldots\ldots\ldots\ (\mathbf{5.1})$$

Where, $\mathbf{W_1}$ and $\mathbf{W_2}$ are the initial and final weights of the hydrogel.

5.2.7. Construction of Moxifloxacin calibration curve

The stock solution of 1000 mg/l of Moxifloxacin drug solution was prepared using phosphate buffer pH 7.4 as a solvent, then 2, 4, 6, 8 and 10 mg/l solutions were prepared by dilution of the stock solution. Using a UV-9000A spectrophotometer (Shanghai Metash), scan the solutions between 200 to 400 nm and the absorption maximum was recorded to construct the calibration curve.

5.2.8. Moxifloxacin drug loading and drug release studies

By soaking the dry hydrogel in the presence of a drug-containing solution, the drug would be loaded into the hydrogel. Moxifloxacin hydrochloride was selected as a model drug for the study of drug release. To 100 ml of moxifloxacin solution (1 mg/ml) in water, 0.1 g of dry hydrogel was added for drug loading. After 48 hours, the loaded hydrogels were weighed and washed with ethanol to prevent burst release, then placed in the vacuum oven for 24 hours to dry completely. The dried hydrogels were then weighed and the drug load was determined by using Equation (5.2). The *in-vitro* release efficiency of drug-loaded hydrogel in an acid buffer solution of pH 1.2 and phosphate buffer solution of pH 7.4 was evaluated at 37°C and 27°C using the paddle method in the dissolution test apparatus (LabIndia, DS-8000, India) respectively. The release solution was withdrawn at regular time intervals (30 minutes) with a sufficient dilution and then scanned the solutions between 200 nm to 400 nm using a UV-Visible spectrophotometer. The maximum absorption λ_{max} was found to be at 288 nm. The release percentage was determined and the zero-order, first-order, Higuchi, Korsmeyer-Peppas and Hixson-Crowell models were used to measure the statistical kinetic model of drug release [16, 17].

$$\textbf{Drug Loading}\ (\%) = \frac{\mathbf{W_D - W_0}}{\mathbf{W_0}}\ \mathbf{x\ 100} \qquad \ldots\ldots\ldots\ldots\ (\mathbf{5.2})$$

Where, $\mathbf{W_0}$ is the initial weight of the hydrogel and $\mathbf{W_D}$ is the weight of the drug-loaded hydrogel.

5.2.9. Antibacterial study

The synthesized hydrogel and moxifloxacin drug-loaded hydrogel was used for the *in-vitro* antibacterial test by using the agar diffusion method. For this purpose

5 µg/ml of moxifloxacin drug, moxifloxacin drug-loaded hydrogel and synthesized hydrogel were prepared in distilled water and each 0.1 ml loaded on nutrient agar plates. After 24 hours of incubation at 37°C the inhibition zones were calculated.

5.3. Results and Discussion

5.3.1. Poly(AAM-co-AAC) hydrogel preparation

Using AAM and AAC as monomers with MBA as a crosslinker, hydrogels were prepared. As free radical generators, potassium persulfate and SMBS are used [18, 19]. **Fig. 5.2** shows the hydrogel preparation steps. The swelling analysis was conducted after gel preparation [20-22]. The mechanism of the reaction is shown in **Scheme II** and the hydrogel formulations AAMCH1, AAMCH2, AAMCH3 and AAMCH4 are given in **Table 5.1.**

5.3.2. FT-IR analysis

Moxifloxacin hydrochloride FTIR spectra (**Fig. 5.3a**) showed aromatic C=C stretching at 1619 cm^{-1} and also demonstrated carboxylic acid C=O stretching at 1703 cm^{-1}, C-N stretching at 1315 cm^{-1} and monofluorobenzene stretching at 1044 cm^{-1}. The poly(AAM-co-AAC) hydrogel spectra (**Fig. 5.3b**) showed carboxylic acid stretching at 3213 cm^{-1} corresponding to the –OH. CH groups provided absorption at 1450 cm^{-1} on the chain. The 2925 cm^{-1} absorbance is the acrylate unit C-H stretching. The absorption can be attributed to the C=O group at 1681 cm^{-1}. The drug-loaded hydrogel peaks (**Fig. 5.3c**) observed were 3203 cm^{-1} corresponding to the carboxylic acid -OH stretching. The 2934 cm^{-1} absorbance is the C-H stretching and C=O group at 1666 cm^{-1}. Aromatic C=C stretching was at 1615 cm^{-1} and monofluorobenzene stretching was at 1044 cm^{-1} [23, 24].

5.3.3. TGA analysis of poly(AAM-co-AAC) hydrogel

TGA has analyzed the thermal stability of the prepared hydrogel and the results are shown in **Fig. 5.4.** Owing to the presence of moisture content in the hydrogel, the primary weight loss was observed. The poly(AAM-co-AAC) hydrogel was thermally unstable and degradation started at 178°C with a weight loss of 1.9% for the elimination of ammonia gas from amide groups, at 240°C with a weight loss of 3.2% for the dehydration of adjacent carboxylic groups to form anhydrides and a maximum mass loss was observed at 384°C with a weight loss of 22.0% due to breaking of crosslinking chain. This reduction has continued up to 700°C with a lesser amount [25].

5.3.4. SEM Study poly(AAM-co-AAC) hydrogel

The synthesized hydrogel micrographs (**Fig. 5.5**) were analyzed by SEM. The SEM Figures indicate that the surface is hard and it has been found to be slightly porous [26, 27].

5.3.5. Swelling study of poly(AAM-co-AAC) hydrogel in water and pH solutions

The swelling study of poly(AAM-co-AAC) hydrogel was performed in water. The dried hydrogel of 1cm in length was soaked in 100 ml of water for 24 hours, the result showed that the size of the hydrogel was increased to 4.5cm and their corresponding images are showed in **Fig. 5.6.** The swelling efficiency of the prepared hydrogels AAMCH1, AAMCH2, AAMCH3 and AAMCH4 were studied in the pH range 1 to 10. The maximum swelling of 7211.69% was observed for AAMCH1 compare to the swelling % of other hydrogels hence for further swelling and drug release studies AAMCH1 is taken as standard. The swelling (%) was decreased as the amount of crosslinker increased. The results are tabulated in the

Table 5.2 and their corresponding graphical representation is showed in **Fig. 5.7**. The swelling (%) of the hydrogel in pH 1.2 and 7.4 buffer solutions similar to gastrointestinal fluids is shown in **Fig. 5.9.** and their corresponding statistical data given in **Table 5.4.** The results showed a high swelling rate (7258.60%) observed at pH 7.4 compared to the pH 1.2 (115.06%). The results of the swelling (%) in pH 7.4 are tabulated in the **Table 5.6** and their corresponding graphical representation is showed in **Fig. 4.11**. The $–CONH_2$ groups are protonated at a lower pH (HCl solutions) and create $NH_3^+–NH_3^+$ electrostatic repulsion for swelling, but its swelling will be decreased due to the presence of Chloride ions. Carboxylic acid – COOH groups are deprotonated ($–COO^–$) at higher pH and create electrostatic swelling repulsions, but the presence of more sodium ions (Na^+) in pH 9 and 10 will decrease the swelling (%) compared to pH 8 by forming -COONa group [28, 29]. The results are tabulated in the **Table 5.3** and their corresponding graphical representation is showed in **Fig. 5.8.**

5.3.6. Construction of calibration curve

The selection of the drug for the release of the drug is critical because to avoid λ_{max} change, the drug should not react with solvents and hydrogels. Moxifloxacin drug has excellent content since no difference in λ_{max} has been observed as time shifts. In order to assess maximal absorption at λ_{max} 288 nm, solutions were scanned between 200 nm to 400 nm from the UV- Visible spectrophotometer. The results are tabulated in the **Table 5.7** and their corresponding graphical representation is showed in **Fig. 5.12 and 5.13.** The calibration curve shows that R^2 is 0.999 (coefficient of correlation).

5.3.7. Moxifloxacin drug release study from poly(AAM-co-AAC) hydrogel

5.3.7.1. Moxifloxacin drug release study in pH 1.2 and 7.4

The outcome of the swelling analysis helps to assess the study of drug release. In acid and alkaline pH, the swelling (%) in pH 1.2 and 7.4 suggests maximum swelling occurs at alkaline pH 7.4 (7258.60%) compared to pH 1.2 (115.06%) similar to gastrointestinal fluid-like solutions The results are tabulated in the **Table 5.4** and their corresponding graphical representation is showed in **Fig. 5.9.** The drug release percentage of moxifloxacin is maximum (99.89%) at pH 7.4 than at pH 1.2 (18.59%) due to the swelling (%) maximum at pH 7.4. The hydrogel induces pH-sensitive drug release at maximum pH of 7.4 than a pH of 1.2. The results are tabulated in the **Table 5.8** and their corresponding graphical representation is showed in **Fig. 5.14.**

5.3.7.2. Moxifloxacin drug release study at different temperature

The effect of temperature on swelling of poly(AAM-co-AAC) hydrogel was studied at 27°C and 37°C. The result showed that the maximum swelling % 7258.60 in 37°C and the minimum swelling % 5085.29 in 27°C. The results are tabulated in the **Table 5.5** and their corresponding graphical representation is showed in **Fig. 5.10**. The temperature sensitivity of the hydrogel in drug release is studied at the temperature 27°C and 37°C respectively at pH 7.4 over time. The outcome indicates that drug release has increased with temperature increase. The minimum amount (71.56%) of drug release was observed at 27°C and the maximum amount (99.89%) of drug release was observed at 37°C. The results are tabulated in the **Table 5.9** and their corresponding graphical representation is showed in **Fig. 5.15**. The swelling (%) increases as the temperature increases due to the versatile nature produced in the polymer network, hence water quickly enters the hydrogel network and swells.

Similarly, the buffer solution enters the hydrogel polymer network and contributes to the increase in swelling and drug release.

5.3.8. Kinetic model drug release

The *in-vitro* release of the drug was estimated using different mathematical models and the effects of the correlation coefficient (R^2) shown in **Table 5.10** and their corresponding graphical representation is showed in **Fig. 5.16**. The maximum degree of the coefficient of correlation contributes to finding a suitable mathematical model that fits to the kinetic of release. The result shows that the highest correlation coefficient (R^2) is 0.976, hence the hydrogel fits the Higuchi model drug release.

5.3.9. Antibacterial activities

The moxifloxacin drug-loaded hydrogel was investigated for *in-vitro* antibacterial effect. **Fig. 5.17** illustrated that Moxifloxacin (M) pure drug and moxifloxacin drug-loaded hydrogel (MLH) had an antibacterial effect on *S. aureus* and *E. coli* bacteria and no effect on unloaded hydrogel (H) after 24 hours incubation at 37°C. After measuring the inhibition zone the moxifloxacin pure drug exhibited 13mm and 9mm for the moxifloxacin drug-loaded hydrogels against *S. aureus* **(Fig. 5.17a)** and 13mm and 8mm against *E. coli*, respectively **(Fig. 5.17b)**. As the result showed, moxifloxacin pure drug and moxifloxacin drug-loaded hydrogel shows antibacterial activity because of the bioactivity of the drug but the unloaded hydrogel will not show a zone of inhibition compared to pure drug and drug-loaded hydrogel. This effect could be due to the presence of moxifloxacin in drug-loaded hydrogel [30].

5.4. Conclusion

By crosslinking with MBA as a crosslinker, poly(AAM-co-AAC) hydrogels were synthesized using SMBS and potassium persulfate as initiators. At different temperatures and pH levels, the swelling and drug release experiments were carried out. The outcome of the swelling analysis indicates maximum swelling occur at alkaline pH than acidic pH and the swelling (%) also increases as the temperature increases. Drug release experiments using moxifloxacin as a model drug have been conducted and the findings indicate maximum drug released at pH 7.4 compared to pH 1.2. Since the acid groups are deprotonated at pH 7.4 and amide groups are protonated to generate electrostatic repulsion, this electrostatic repulsion allows the hydrogel to swell further, hence more dissolution media entering the hydrogel enables further drug release. This hydrogel follows the kinetic release of the Higuchi model and drug-loaded hydrogel shows good antibacterial activity and hence can be used in biomedical applications, particularly for controlled drug delivery systems.

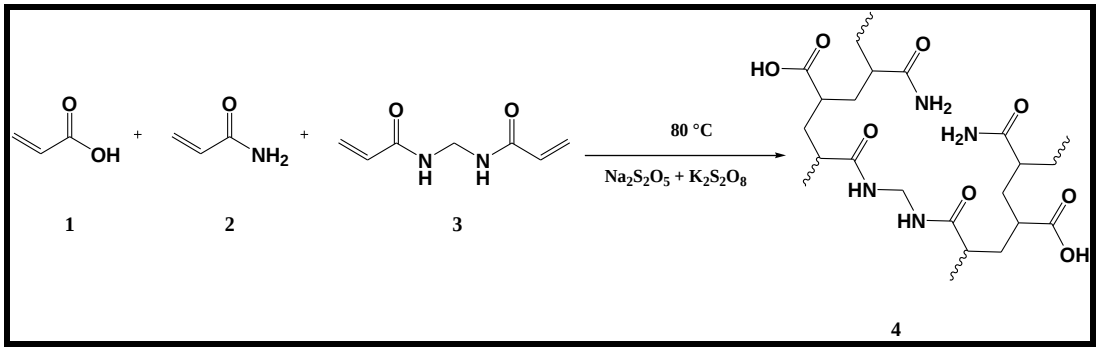

Scheme II. Poly(AAM-co-AAC) hydrogel synthesis, (1) acrylic acid, (2) acrylamide, (3) methylenebisacrylamide and (4) poly(acrylamide-co-acrylic acid) hydrogel.

Table 5.1. Schemes for the synthesis of poly(AAM-co-AAC) hydrogels.

Formulation code	Water (ml)	Acrylamide (mg)	Acrylic acid (ml)	Initiator		MBA (mg)
				SMBS (mg)	PPS (mg)	
AAMCH1	10	300	0.3	32	45	06
AAMCH2	10	300	0.3	32	45	11
AAMCH3	10	300	0.3	32	45	16
AAMCH4	10	300	0.3	32	45	21

Table 5.2. Statistical data of Swelling (%) of poly(AAM-co-AAC) hydrogel formulations.

pH	AAMCH1 Swelling (%)	AAMCH2 Swelling (%)	AAMCH3 Swelling (%)	AAMCH4 Swelling (%)
2	126.21	106.30	104.71	91.66
4	1079.43	424.77	193.10	170.70
6	1940.87	1376.52	1091.66	911.40
7	6360.13	4024.81	2480.16	1752.17
8	**7211.69**	5414.50	3711.64	3201.29
10	4189.85	3277.56	2295.79	1601.11

Table 5.3. Statistical data of Swelling (%) of poly(AAM-co-AAC) hydrogel at pH 1 to 10.

pH	**1**	**2**	**3**	**4**	**5**
Swelling (%)	114.28	126.21	765.75	1079.43	1534.88
pH	**6**	**7**	**8**	**9**	**10**
Swelling (%)	3309.75	6360.13	**7211.69**	5140.70	4189.85

Table 5.4. Statistical data of the swelling (%) of the poly(AAM-co-AAC) hydrogel at pH 1.2 and 7.4

Time (min)	**pH 1.2 Swelling (%)**	**pH 7.4 Swelling (%)**
0	0.00	0.00
360	82.19	1283.87
720	97.26	3058.06
1080	101.36	4118.27
1440	109.58	5391.93
1800	112.32	6812.90
2160	113.69	7197.31
2520	115.06	7258.06
2880	**115.06**	**7258.60**

Table 5.5. Statistical data of the poly(AAM-co-AAC) hydrogel swelling (%) in a pH 7.4 at 27°C and 37°C.

Time (min)	**27°C Swelling (%)**	**37°C Swelling (%)**
0	0.00	0.00
360	1191.17	1283.87
720	1880.14	3058.06
1080	2576.47	4118.27
1440	3455.88	5391.93
1800	4030.88	6812.90
2160	4605.88	7197.31
2520	4947.79	7258.06
2880	**5085.29**	**7258.60**

Table 5.6. Statistical data of the poly(AAM-co-AAC) hydrogel swelling (%) changes in pH 7.4 over time.

Time (hours)	**pH 7.4 Swelling (%)**
0	0.00
6	1283.87
12	3058.06
18	4118.27
24	5391.93
30	6812.90
36	7197.31
42	7258.06
48	7258.60

Table 5.7. Statistical data of the calibration curve for moxifloxacin (Absorbance v/s Concentration).

Concentration (mg/l)	**Absorbance**
0	0.00000
2	0.18235
4	0.36927
6	0.55509
8	0.74747
10	0.92631

Table 5.8. Statistical data of the moxifloxacin drug release (%) over time in pH 1.2 and 7.4 from poly(AAM-co-AAC) hydrogel.

Time (min)	pH 1.2 Drug release (%)	pH 7.4 Drug release (%)
0	0.00	0.00
30	3.08	16.74
60	6.12	31.80
90	8.68	45.03
120	10.90	56.40
150	12.60	66.64
180	14.43	73.67
210	15.66	83.77
240	16.67	90.13
270	18.01	96.64
300	**18.59**	**99.89**

Table 5.9. Statistical data of the moxifloxacin drug release (%) over time at 27°C and 37°C in pH 7.4 from poly(AAM-co-AAC) hydrogel.

Time (min)	27°C Drug release (%)	37°C Drug release (%)
0	0.00	0.00
30	10.10	16.74
60	20.53	31.80
90	30.16	45.03
120	37.67	56.40
150	44.87	66.64
180	50.91	73.67
210	54.01	83.77
240	62.88	90.13
270	65.65	96.64
300	**71.56**	**99.89**

Table 5.10. Moxifloxacin drug release results in terms of correlation coefficient (R^2), slope and intercept of the different kinetic models.

Name of the kinetic model	R^2	Slope	Intercept
Zero order	0.967	19.79	10.61
First order	0.636	-0.506	2.458
Higuchi	**0.976**	0.02	0.243
Korsmeyer-Peppas	0.467	1.243	1.207
Hixson-Crowell	0.934	0.767	-0.282

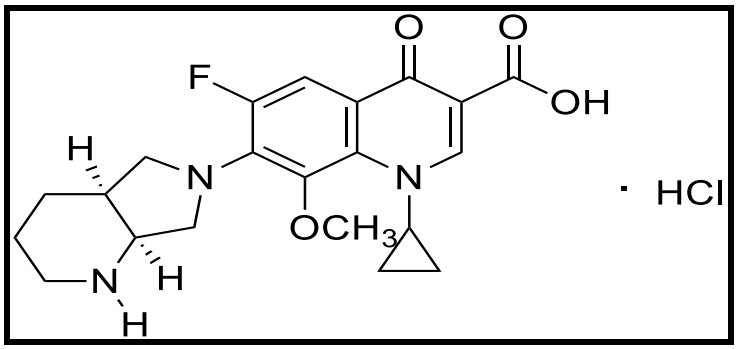

Figure 5.1. The molecular composition of the moxifloxacin hydrochloride.

Figure 5.2. Preparation stages of hydrogel (a) initial stage in solution, (b) gel shape, (c) dryness and (d) swelling.

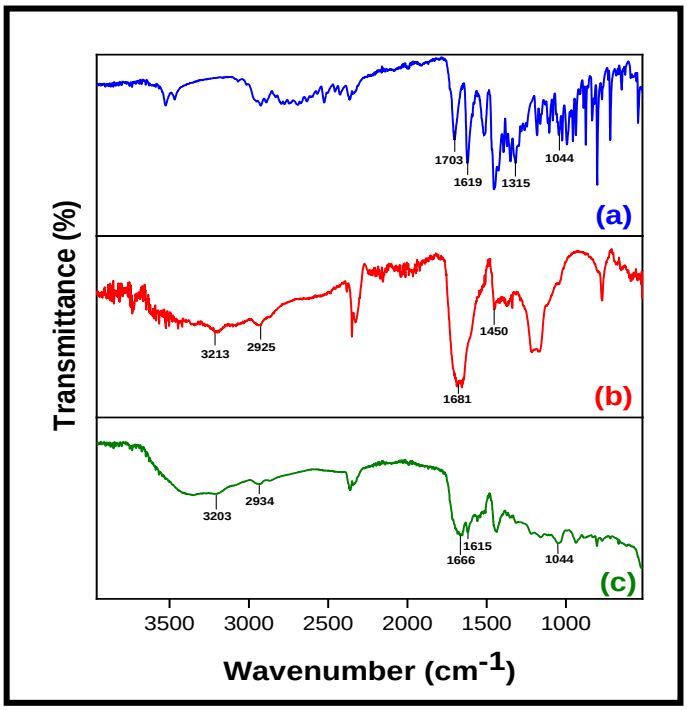

Figure 5.3. FTIR spectrum of (a) Moxifloxacin, (b) poly(acrylamide-co-acrylic acid) hydrogel and (c) Moxifloxacin loaded hydrogel.

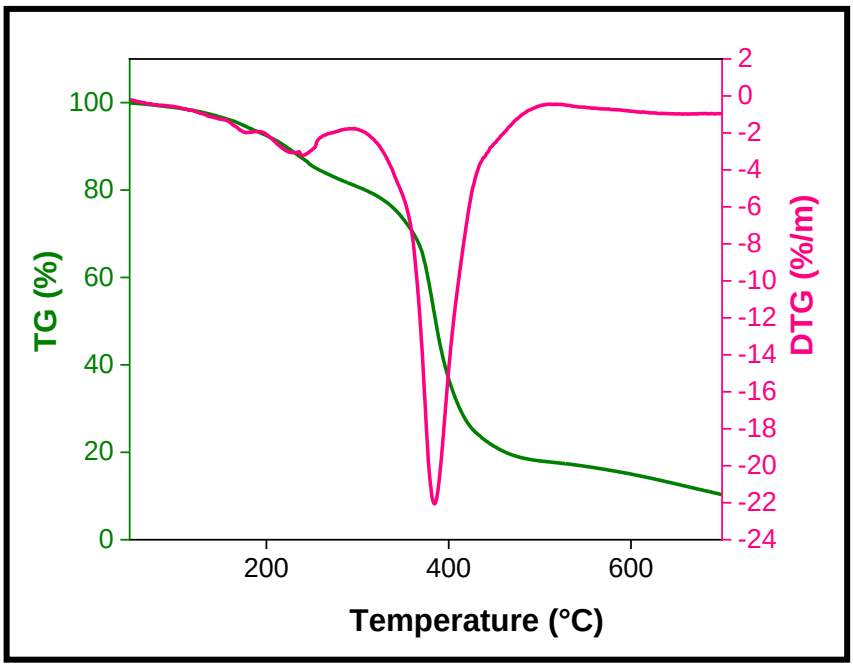

Figure 5.4. Poly(acrylamide-co-acrylic acid) hydrogel TGA graph.

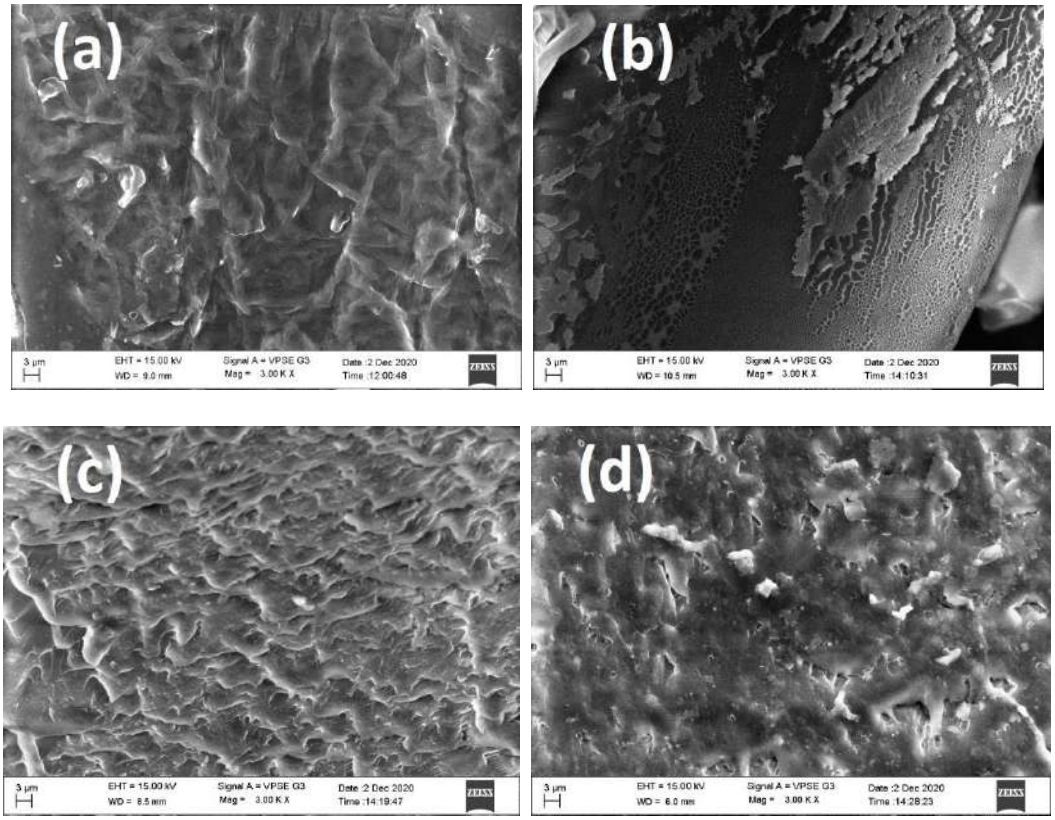

Figure 5.5. SEM images of the dried poly(AAM-co-AAC) hydrogels (a) AAMCH1, (b) AAMCH2, (c) AAMCH3 and (d) AAMCH4.

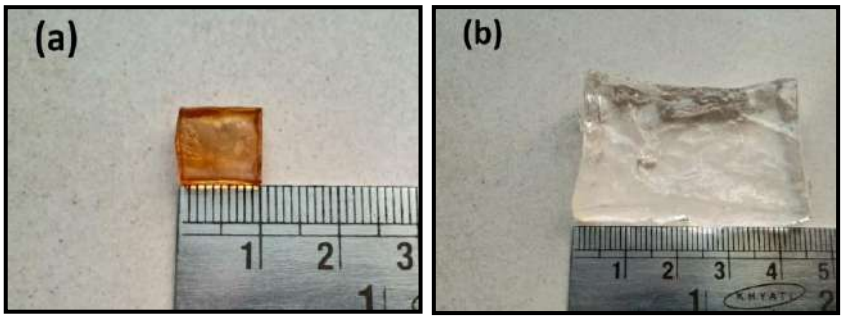

Figure 5.6. Images of (a) dried and (b) swollen poly(AAM-co-AAC) hydrogel in water on a digital camera.

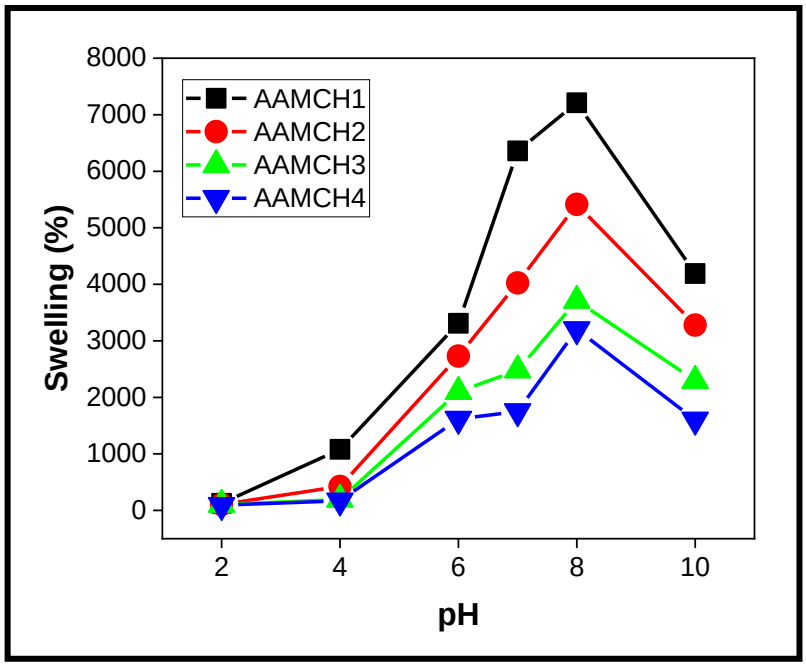

Figure 5.7. Poly(AAM-co-AAC) hydrogel swelling (%) of different formulations.

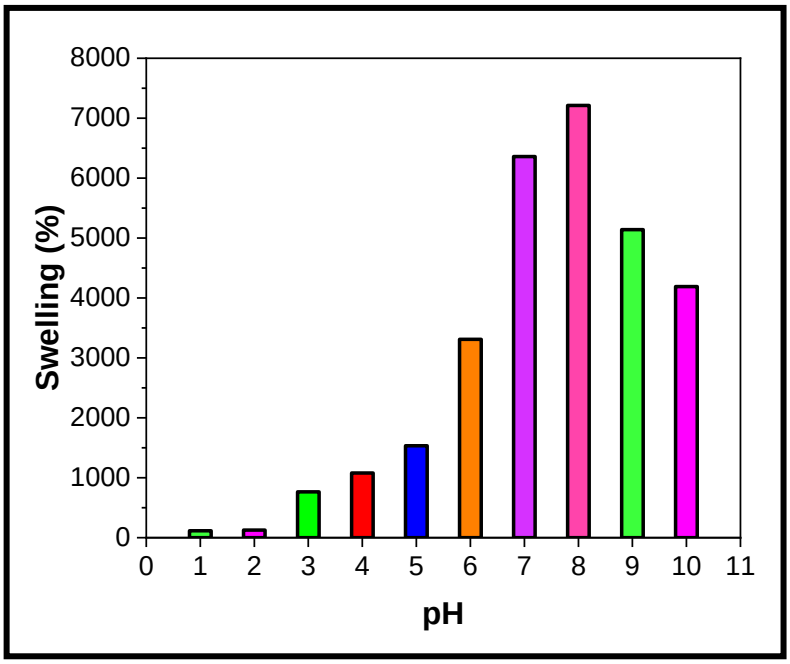

Figure 5.8. Poly(AAM-co-AAC) hydrogel swelling (%) at pH 1 to 10.

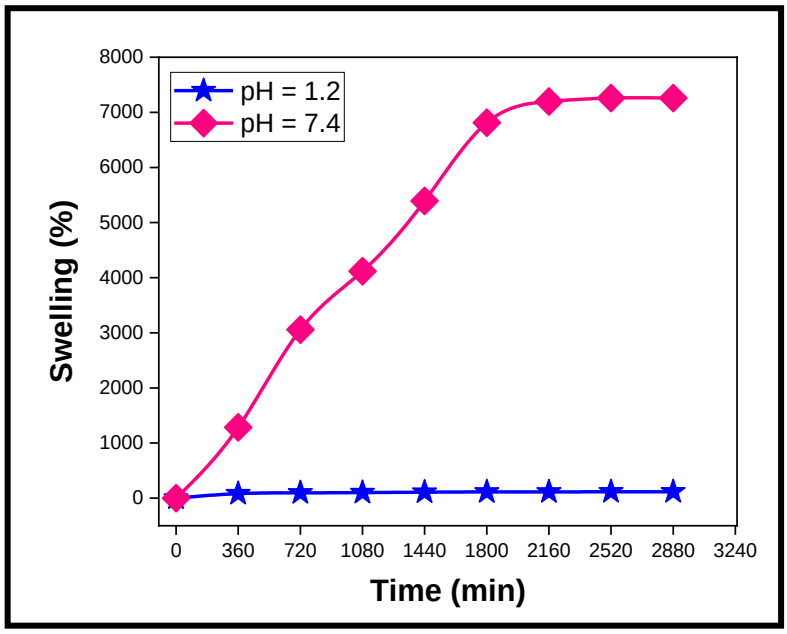

Figure 5.9. Poly(AAM-co-AAC) hydrogel swelling (%) at pH 1.2 and pH 7.4.

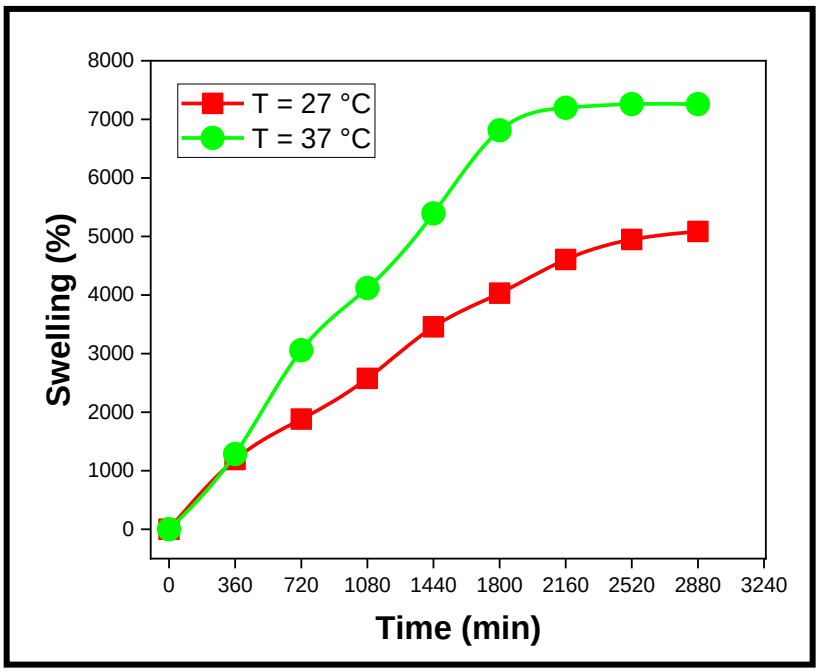

Figure 5.10. Poly(AAM-co-AAC) hydrogel swelling (%) at temperatures of 27°C and 37°C in pH 7.4.

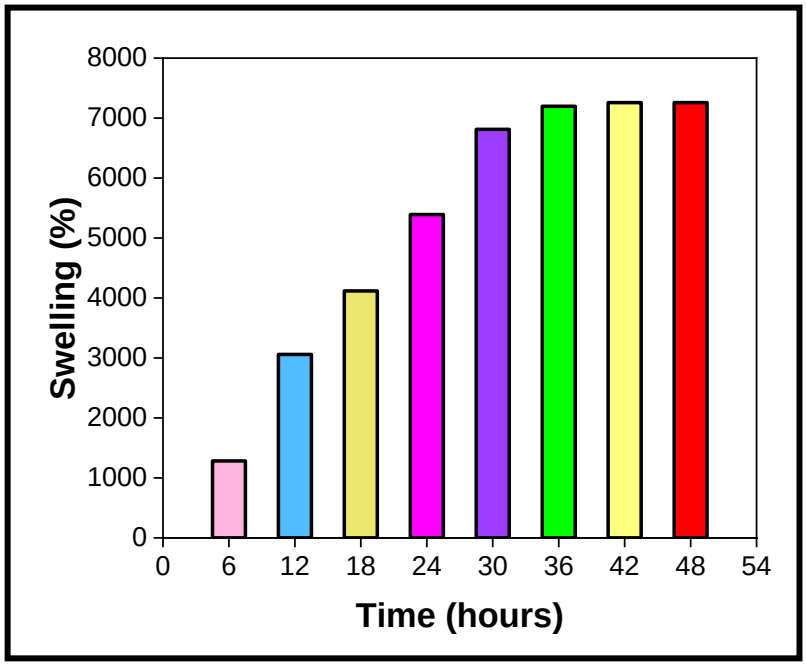

Figure 5.11. Changes in the poly(AAM-co-AAC) hydrogel swelling (%) over time in pH 7.4.

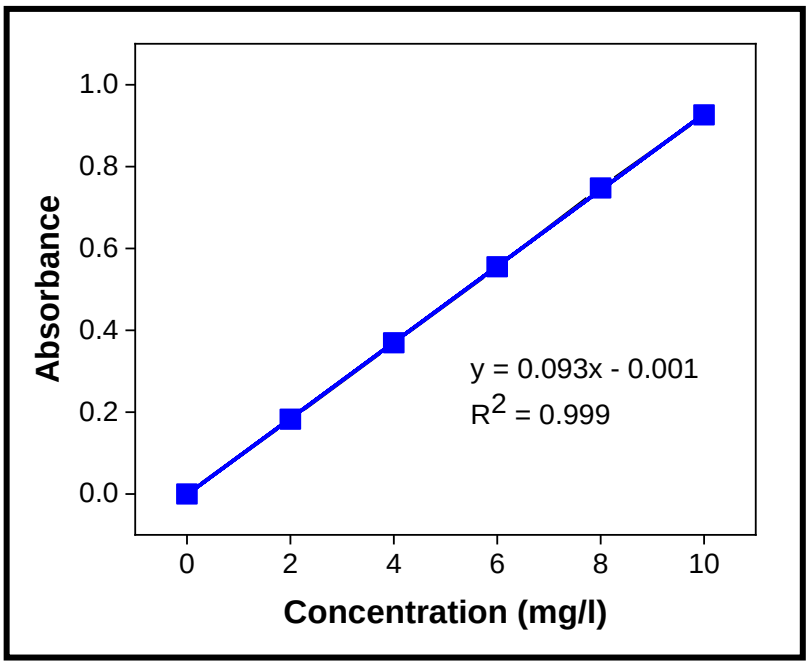

Figure 5.12. Moxifloxacin calibration curve (Absorbance v/s Concentration).

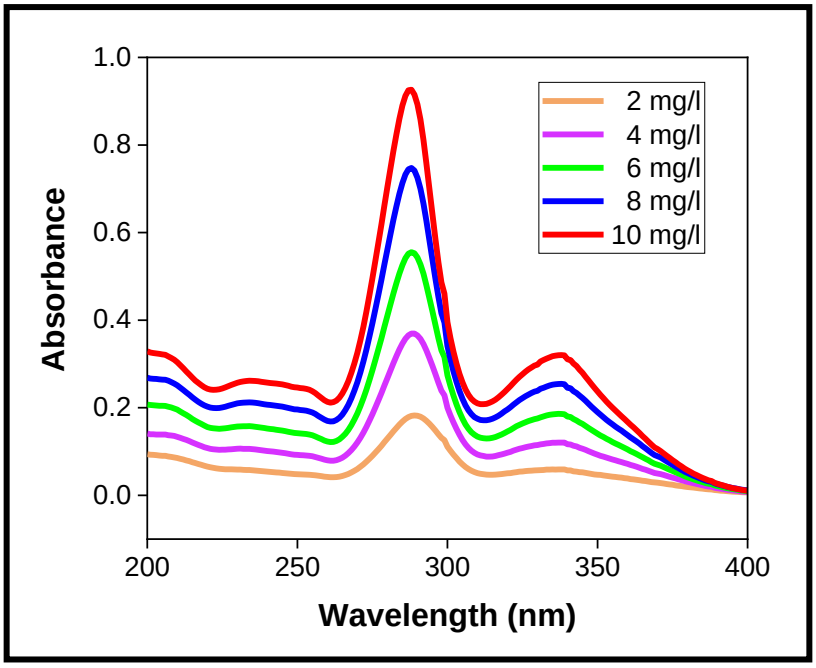

Figure 5.13. Moxifloxacin calibration curve spectral graph.

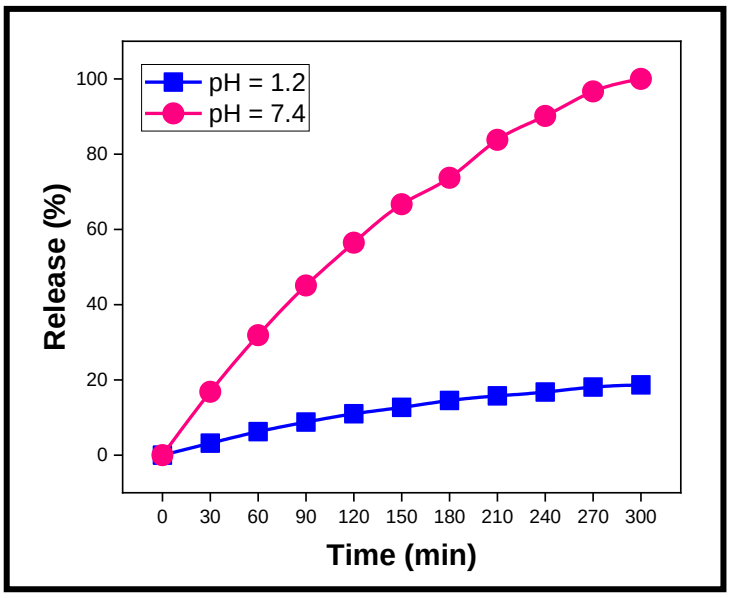

Figure 5.14. Release of moxifloxacin drug from poly(AAM-co-AAC) hydrogel at pH 1.2 and pH 7.4 over time.

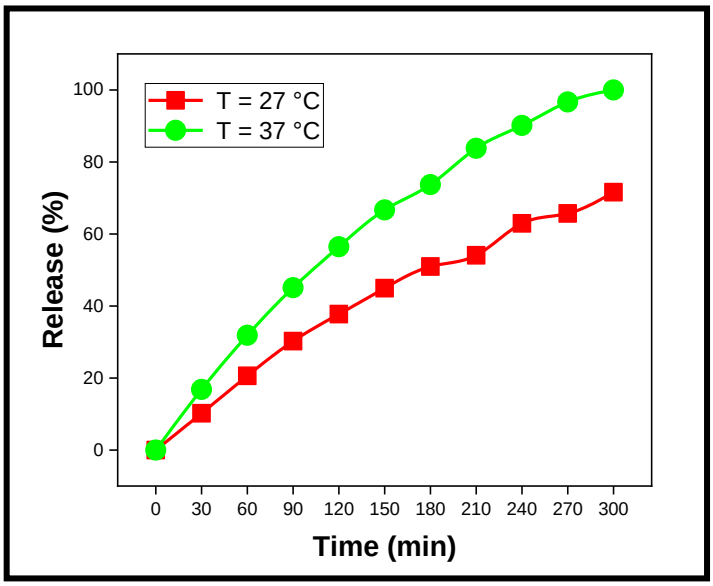

Figure 5.15. Moxifloxacin drug released at 27°C and 37°C temperatures from poly(AAM-co-AAC) hydrogel with time.

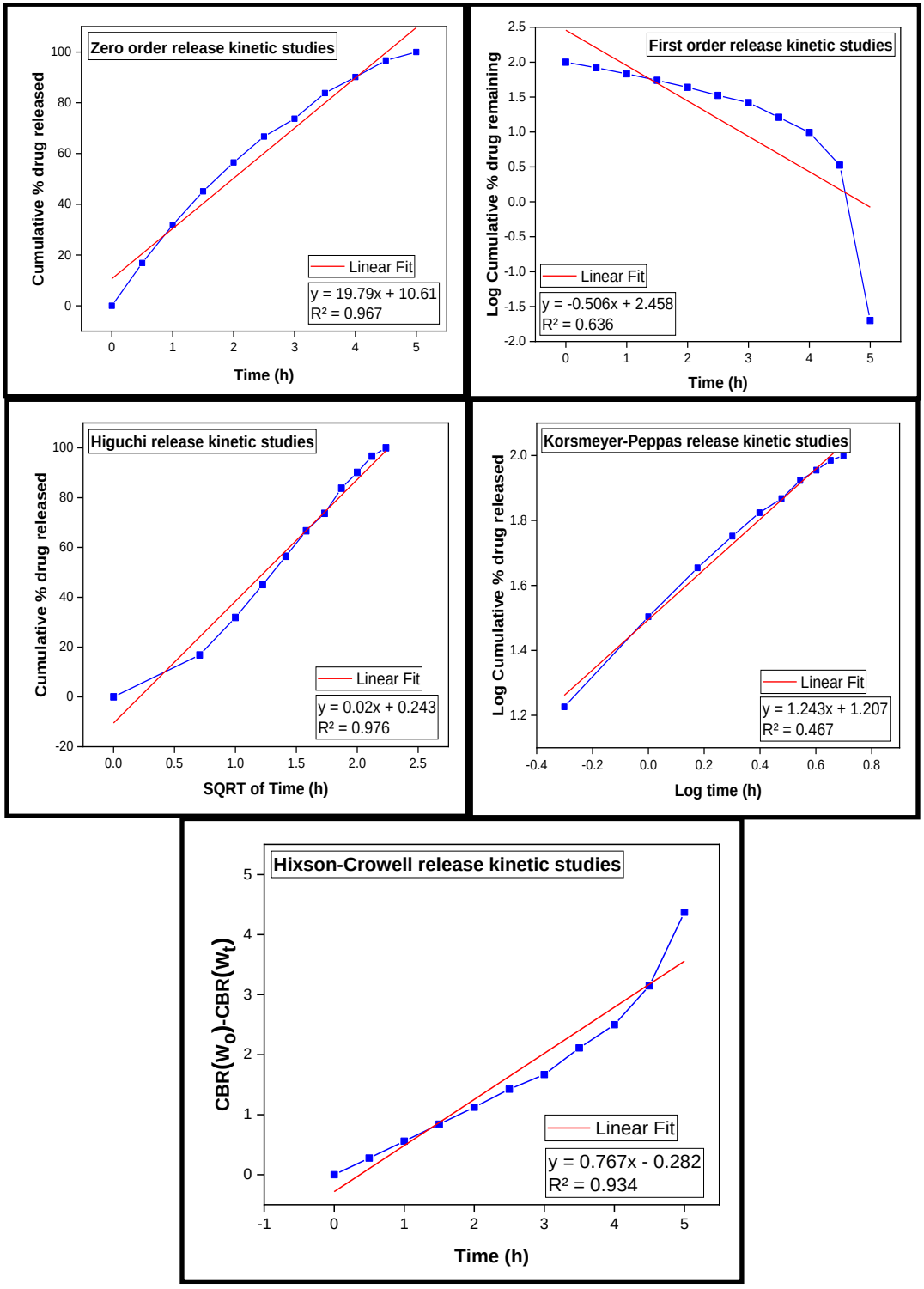

Figure 5.16. Graphical representation of kinetic model drug release from poly(AAM-co-AAC) hydrogel.

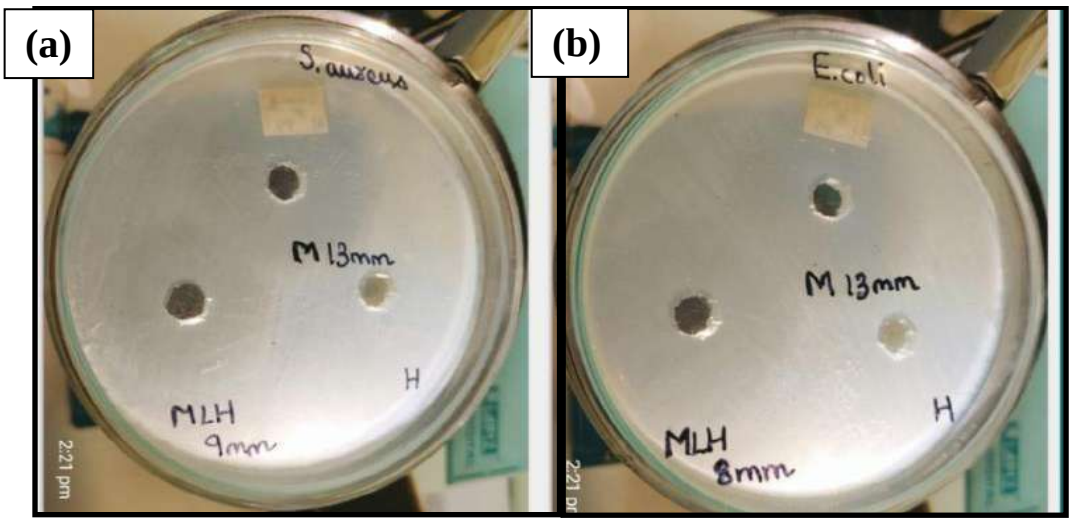

Figure 5.17. Antibacterial activity of moxifloxacin drug-loaded hydrogel on **(a)** *S.aureus* (Gram-positive bacteria) and **(b)** *E.Coli* (Gram-negative bacteria).

5.5. References

[1] Peppas N. A., Khare A. R.; Preparation, structure and diffusional behavior of hydrogels in controlled release. *Advanced Drug Delivery Reviews*, 1993, 11, 1–35.

[2] Peppas N. A., Langer R.; New challenges in biomaterials. *Science*, 1994, 263, 1715-1720.

[3] Ratner B. D., Hoffman A. S.; Hydrogels for Medical and Related Applications. *American Chemical Society*, 1976, 31, 1-36.

[4] Varaprasad K., Raghavendra G. M., Jayaramudu T., Yallapu M. M., Sadiku R.; A mini review on hydrogels classification and recent developments in miscellaneous applications. *Materials Science* and *Engineering*: *C*, 2017, 79, 958-971.

[5] Moghimi S. M., Hunter.; Poloxamers and poloxamines in nanoparticle engineering and experimental medicine. *Trends in Biotechnology*, 2000, 18, 412–420.

[6] Peppas N. A.; Hydrogels and drug delivery. *Current Opinion in Colloid & Interface Science*, 1997, 2, 531-537.

[7] Shah N., Patel K. R.; Formulation and Development of Hydrogel for Poly Acrylamide-Co-acrylic acid. *Journal of Pharmaceutical Science and Bioscientific Research*, 2014, 4, 114-120.

[8] Vinu R., Madras G.; Photocatalytic Degradation of Poly(Acrylamide-co-acrylic Acid). *The Journal of Physical Chemistry B*, 2008, 112, 8928–8935.

[9] Charoo N. A., Abdallah D. B., Parveen T., Abrahamsson B., Cristofoletti R., Groot D. W., Langguth P., Parr A., Polli J. E., Mehta M., Shah V. P., Tajiri T., Dressman J.; Biowaiver Monograph for Immediate-Release Solid Oral Dosage Forms: Moxifloxacin hydrochloride. *Journal of Pharmaceutical Sciences*, 2020, 109, 2654-2675.

[10] Biedenbach D. J., Jones R. N.; The comparative antimicrobial activity of Levofloxacin tested against 350 clinical isolates of Streptococci. *Diagnostic Microbiology and Infectious Disease*, 1996, 25, 47-51.

[11] Dalhoff A., Petersen U., Endermann R.; *in-vitro* activity of Bay 12-8039, a new 8-methoxyquinolone. *Chemotherapy*, 1996, 42, 410-425.

[12] Davis R., Bryson H. M.; Levofloxacin: a review of its antibacterial activity, pharmacokinetics and therapeutic efficacy. *Drugs*, 1994, 47, 677-700.

[13] Imming P., Sinning C., Meyer A.; Drugs, their targets and the nature and number of drug targets. *Nature Reviews Drug Discovery*, 2006, 5, 821-834.

[14] Reece R. J., Maxwell A.; DNA gyrase: structure and function. *Critical Reviews Biochemistry and Molecular Biology*, 1991, 26, 335-375.

[15] Pestova E., Millichap J. J., Noskin G. A., Peterson L. R.; Intracellular targets of moxifloxacin: a comparison with other fluoroquinolones. *Journal of Antimicrobial Chemotherapy*, 2000, 45, 583-590.

[16] Baishya H., Gouda R., Qing Z.; Application of Mathematical Models in Drug Release Kinetics of Carbidopa and Levodopa ER Tablets. *Journal of Developing Drugs*, 2017, 06, 1-8.

[17] Peppas N. A., Bures P., Leobandung W., Ichikawa H.; Hydrogels in pharmaceutical formulations. *European Journal of Pharmaceutics and Biopharmaceutics*, 2000, 50, 27–46.

[18] Mahdavinia G., Pourjavadi A., Hosseinzadeh H., Zohuriaan M.; Modified chitosan 4. Superabsorbent hydrogels from poly (acrylic acid-co-acrylamide) grafted chitosan with salt-and pH-responsiveness properties. *European Polymer Journal*, 2004, 40, 1399-1407.

[19] Madhusudana T., Mamatha G. P., Demappa T., N. D. Satyanarayan.; Synthesis and Characterization of Poly(acrylamide) Hydrogels as pH and Salt Sensitive Material. *Asian Journal of Chemistry*, 2021, 33(5), 1019-1024.

[20] Isık B., Kıs M.; Preparation and determination of swelling behavior of poly(acrylamide-co-acrylic acid) hydrogels in water. *Applied Polymer Science*, 2004, 94, 1526–1531.

[21] Madhusudana T., Mamatha G. P., Demappa T., Satyanarayan N. D.; Controlled drug release of levofloxacin from poly (acrylamide) hydrogel. *International Journal of Research in Pharmaceutical Sciences*, 2021, 12(2), 1037-1043.

[22] Teo B. M., Prescott S. W., Ashokkumar M., Grieser F.; Ultrasound initiated miniemulsion polymerization of methacrylate monomers. *Ultrasonics Sonochemistry*, 2008, 15, 89–94.

[23] Pravin K. P., Rajesh K., Dipak K. M.; Design and evaluation of moxifloxacin hydrochloride ocular inserts. *Acta Pharmaceutica*, 2012, 62, 93–104.

[24] Tomar R. S., Gupta I., Singhal R., Nagpal A. K.; Synthesis of Poly (Acrylamide-co-Acrylic Acid) based Superabsorbent Hydrogels: Study of Network Parameters and Swelling Behaviour. *Polymer-Plastics Technology and Engineering*, 2007, 46, 481-488.

[25] Ebrahimi R., Salavaty M.; Controlled drug delivery of ciprofloxacin from ultrasonic hydrogel. *e-Polymers*, 2018, 18, 187-195.

[26] Aouada F. A., Chiou B. S., Orts W. J., Mattoso L. H.; Physicochemical and morphological properties of poly (acrylamide) and methylcellulose hydrogels: effects of monomer, crosslinker and polysaccharide compositions. *Polymer Engineering* & *Science*, 2009, 49, 2467-2474.

[27] Chen J., Liu M., Liu H., Ma L.; Synthesis, swelling and drug release behavior of poly (N, N-diethylacrylamide-co-N-hydroxymethyl acrylamide) hydrogel. *Materials Science and Engineering: C*, 2009, 29, 2116-2123.

[28] Pourjavadi A., Mahdavinia G. R.; Superabsorbency, pH-Sensitivity and Swelling Kinetics of Partially Hydrolyzed Chitosan-g-poly(Acrylamide) Hydrogels. *Turkish Journal of Chemistry*, 2006, 30, 595-608.

[29] Wu J., Lin J., Li G., Wei C.; Influence of the COOH and COONa groups and crosslink density of poly (acrylic acid)/montmorillonite superabsorbent composite on water absorbency. *Polymer International*, 2001, 50, 1050-1053.

[30] Drago L., De Vecchi E., Nicola L., Tocalli L., Gismondo M. R.; Effect of Moxifloxacin on Bacterial Pathogenicity Factors in Comparison with Amoxicillin, Clarithromycin and Ceftriaxone. *Journal of Chemotherapy*, 2004, 16(1), 30–37.

Chapter – 6

Synthesis and characterization of poly(acrylic acid) hydrogel for doxycycline drug release study

Chapter – 6

Synthesis and characterization of poly(acrylic acid) hydrogel for doxycycline drug release study

This chapter discusses the synthesis and characterization of poly(acrylic acid) hydrogels for the controlled release of doxycycline.

Abstract

In modern pharmaceutical drug delivery design, controlled drug release has become more appealing research work for obtaining a better drug delivery system with reliability, efficiency and safe drug release. In controlled drug delivery applications, different polymers are extremely useful. In the current study poly(acrylic acid) hydrogels were made using a redox polymerization process using methylenebisacrylamide as the crosslinker with potassium persulfate and sodium metabisulfite as free-radical initiators. Various analytical methods, such as TGA, SEM and FT-IR were used to identify the prepared hydrogels. The water intake behavior of the synthesized hydrogels was investigated under various experimental conditions at various pH, chemical composition and swelling bath temperature. The controlled drug release behavior of a doxycycline-loaded hydrogel was investigated under *in-vitro* conditions and the impact of various factors such as temperature, the chemical composition of the hydrogel and pH of the media. According to the drug release studies, drug release was found to be 39% at acidic pH 1.2 and 99% at alkaline pH 7.4 after 10 hours and followed the Higuchi model.

6.1. Introduction

Hydrogels are one of the most versatile and well-suited technologies for biomedical applications [1]. These are three-dimensional materials that have a strong tendency to incorporate bioactive molecules and water into their polymer network. The water absorption tendency of hydrogels is influenced by the presence of hydrophilic functional groups, crosslink density and the elasticity of the polymer network [2]. The amount of water in the products is generally more than the amount of polymer. Some gels referred to as "superabsorbent" materials, can absorb an extremely more amount of water. pH-sensitive drug delivery systems can be made using a variety of natural and synthetic polymers [3]. Polymer hydrogels have piqued interest as a pH-sensitive drug delivery system and have played an important role in drug delivery systems [4]. In addition, pH-sensitive polymer hydrogels also have mucoadhesive and bioadhesive properties, making them good drug carriers [5].

Continuous developments in materials science have helped medicine and biomedical fields by enabling the production of novel implantable materials through surgery and drug delivery it can be used to treat physiological disorders and other complex diseases [6]. Microbial infections caused by fungi and bacteria have shown a significant danger to patients undergoing surgical or other healthcare procedures such as wound healing and implantation despite the introduction of modern and novel materials [7]. The infection may either delay the wound's healing or result in implant failure. As a consequence, infection management at material-tissue interfaces necessitates the creation of new techniques such as increasing implant biocompatibility or delivering antibiotics to the infected site [8]. Antibiotic drug delivery at the diseased tissue, implanted organ or injection site is one of the most

effective ways to suppress infections. A suitable medication may be impregnated into the substance and administered in a desirable manner over a period of time [9].

Doxycycline is a broad-spectrum antibiotic that belongs to the tetracycline family **(Fig. 6.1).** The drug doxycycline was selected as the model drug to be loaded onto the hydrogels. Doxycycline is a synthetic oxytetracycline antibiotic that affects gram-positive bacteria, gram-negative bacteria and certain parasites. It is commonly used to treat a variety of bacterial infections including skin infections [10,11].

Doxycycline is classified as a Biopharmaceutical Classification System (BCS) class I drug due to its high permeability and high solubility. If a drug substance has an absorption rate of 85% in humans, it is characterized as "highly permeable". Doxycycline is chosen as a model drug because of its fast and complete absorption in humans with an absolute bioavailability of around 90% [12].

This study aimed to prepare poly(acrylic acid) hydrogels using acrylic acid as a monomer and a combination of the crosslinking agent with potassium persulphate and sodium metabisulfite as free-radical initiators. Acrylic acid encourages water to swell further and methylenebisacrylamide increases the mechanical strength of the hydrogel, these hydrogels have both high swelling potential and mechanical strength. The presence of amide and acidic groups in the polymer induces pH sensitivity. The drug release study was carried out using doxycycline hydrochloride as a model drug.

6.2. Materials and Methods

6.2.1. Materials

Acrylic acid (AAC), potassium persulphate (PPS), *N*, *N*′-methylene-bis-acrylamide (MBA), Potassium dihydrogen orthophosphate and sodium hydroxide were received from SDFCL, Mumbai, India. Hydrochloric acid and disodium

hydrogen phosphate anhydrous were from Merck, Mumbai, India. Sodium metabisulfite (SMBS) was received from Avra Synthesis Pvt Ltd, Hyderabad, India. Doxycycline hydrochloride was obtained as a gift sample from Micro labs limited, Bangalore, India.

6.2.2. Poly(AAC) hydrogel synthesis

The poly(AAC) hydrogel was prepared by redox polymerization in a glass vial with PPS and SMBS as free radical initiators which were dissolved in distilled water to produce free radicals. Then add the AAC monomer and the crosslinker MBA and mix for 10 minutes at room temperature. The mixture was then put in a water bath (80°C) to form a gel. After gel formation, the gel was washed with distilled water to extract any unreacted constituents and then dried in a hot air oven at 50°C for 24 hours.

6.2.3. FT-IR analysis

The Shimadzu ATR spectrometer was used to measure the FTIR absorption spectra of synthesized poly(AAC) hydrogels, doxycycline hydrochloride and doxycycline-loaded hydrogels in the range of 400–4000 cm^{-1}.

6.2.4. Thermogravimetric analysis (TGA) study

The thermal stability of poly(AAC) hydrogel was determined using a Hitachi STA7300 thermogravimetric analyzer. TGA was carried out on samples in a nitrogen atmosphere with a heating rate of 20°C per minute.

6.2.5. Scanning electron microscope (SEM) Study

Under a scanning electron microscope (SEM), the surface morphology of different poly(AAC) hydrogels was studied using SEM Zeiss, LS15. The hydrogel

samples were deposited on a brass holder and sputtered with a thin coat of gold under a vacuum before microscope analysis.

6.2.6. Swelling or absorption study

Dried poly(AAC) hydrogels were immersed in various temperature and pH solutions at various time intervals. Dilute NaOH and HCl solutions are used to prepare pH solutions. Before immersing the dried hydrogel in the solution take the initial weight of the dried hydrogel. After swelling, before being weighed again, the hydrogel samples were gently squeezed with filter papers to remove any leftover water that had clung to the hydrogel surfaces. The following Equation was used to measure the absorption capacity.

$$\textbf{Swelling (or)Absorption } (\%) = \frac{\mathbf{W_y - W_x}}{\mathbf{W_x}} \textbf{ x 100} \qquad \ldots\ldots\ldots\ldots (\mathbf{6.1})$$

Where, $\mathbf{W_x}$ and $\mathbf{W_y}$ are the dry and wet hydrogel masses respectively.

6.2.7. Construction of Doxycycline calibration curve

The stock solution of 1000 mg/l of Doxycycline drug solution was prepared using phosphate buffer pH 7.4 as a solvent, then 4, 8, 12, 16 and 20 mg/l solutions were prepared by dilution of the stock solution. Using a UV-9000A spectrophotometer (Shanghai Metash), scan the solutions between 200 to 400 nm and the absorption maximum was recorded to construct the calibration curve.

6.2.8. Doxycycline drug loading and drug release studies

An equilibrium swelling method was used to load the doxycycline drug into the poly(AAC) hydrogel. The dried pre-weighed 0.1g hydrogel was allowed to absorb the drug solution with a known concentration (1 mg/ml) in water. The drug-loaded hydrogel was removed, then washed with ethanol to avoid burst release and

dried at room temperature. The loaded hydrogel weight was recorded and the drug loading was calculated by using Equation (6.2). At 37°C, the drug-loaded hydrogels *in-vitro* release efficiency was measured in acidic buffer pH 1.2 and phosphate buffer pH 7.4 using the paddle method in the dissolution test apparatus (LabIndia, DS-8000, India). The release solution was removed at regular intervals (30 minutes) and the solutions were scanned between 200 to 400 nm with enough dilution, the maximum absorbance at λ_{max} 270 nm was reported using a UV-Visible spectrophotometer. The release percentage was calculated and the statistical kinetic models of drug release were measured using the Zero-order, First-order, Korsmeyer-Peppas, Higuchi and Hixson-Crowell models [13, 14].

$$\textbf{Drug solution absorption}\ (\%) = \frac{\mathbf{W_2 - W_1}}{\mathbf{W_1}}\ \mathbf{x\ 100} \qquad \ldots\ldots\ldots\ldots\ldots\ (\mathbf{6.2})$$

Where, $\mathbf{W_1}$ denotes the initial weight of the hydrogel and $\mathbf{W_2}$ indicates the weight of the drug-loaded hydrogel.

6.2.9. Antibacterial study

The synthesized hydrogel and doxycycline drug-loaded hydrogel was used for the *in-vitro* antibacterial test by using the agar diffusion method. For this purpose 30 µg/ml of doxycycline drug, doxycycline drug-loaded hydrogel and synthesized hydrogel were prepared in distilled water and loaded on nutrient agar plates. After 24 hours of incubation at 37°C the inhibition zones were calculated.

6.3. Results and Discussion

Scheme III depicts the reaction mechanism of synthesized hydrogel, while **Table 6.1** lists the various hydrogel formulations (AACH1, AACH2, AACH3 and AACH4).

6.3.1. Poly(AAC) hydrogel preparation

Fig. 6.2 depicts the hydrogel preparation steps. It was initially in a liquid state (a), but after being placed in an 80°C water bath it will form a gel (b), the prepared hydrogel was then dried in a hot air oven at 50°C for 24 hours (c) and finally a swelling study was performed on the dried hydrogel to determine the swelling capacity of the synthesized hydrogel (d).

6.3.2. FT-IR analysis

The characteristic bands for functional groups of poly(AAC) hydrogel, doxycycline and drug-loaded hydrogel were identified based on FT-IR studies. **Fig. 6.3 (a-d)** shows a peak for poly(AAC) hydrogel at 1701 cm^{-1}, which is due to the presence of C=O stretching vibration. The wideband at 3044 cm^{-1} is caused by –OH group stretching vibrations, while the peak at 2932 cm^{-1} is caused by C-H stretch vibrations of the polymer backbone. **Fig. 6.3 (e)** indicates a doxycycline peak at 3325 cm^{-1} for the –OH group, 1668 cm^{-1} for the C=O group and 1611 cm^{-1} for the NH_2 group. **Fig. 6.3 (f)** depicts a peak for drug-loaded hydrogels at 3325 cm^{-1} for the –OH group and 1615 cm^{-1} for the NH_2 group. The peak at 1701 cm^{-1} is due to the presence of C=O stretching vibration. The stretching vibration of –OH groups induces the wide band at 3044 cm^{-1}. The peak at 2928 cm^{-1} is due to the C-H stretching of the polymer backbone [15-16].

6.3.3. TGA analysis of poly(AAC) hydrogel

The thermal stability of the synthesized hydrogel was investigated by TGA and the findings are shown in **Fig. 6.4.** The primary weight loss was observed due to the presence of moisture in the hydrogel. The poly(acrylic acid) hydrogel degraded at 177°C with a mass loss of 0.147 mg/min, 275°C with a mass loss of 0.886 mg/min

for the dehydration of adjacent carboxylic groups to form anhydrides, 372°C with a mass loss of 0.346 mg/min for the breaking of crosslinking chain, 433°C with a mass loss of 0.274 mg/min and 498°C with a mass loss of 0.501 mg/min are showed.

6.3.4. SEM Study of poly(AAC) hydrogel

Fig. 6.5 illustrates the morphology of hydrogels with varying degrees of cross-linking. SEM was used to examine the synthesized hydrogel micrographs. The surface is smooth in SEM images and as the crosslinker concentration increases, the surface becomes harder **Fig. 6.5 (a to d).**

6.3.5. Swelling study of poly(AAC) hydrogel in water and pH solutions

The swelling study of poly(AAC) hydrogel was performed in water. The dried hydrogel of 1cm in length was soaked in 100 ml of water for 24 hours, the result showed that the size of the hydrogel was increased to 4.0cm and their corresponding images are showed in **Fig. 6.6.** The poly(AAC) hydrogels were found to be sensitive to the pH and temperature of the solution hence we performed swelling studies. The swelling efficiency of the prepared hydrogels AACH1, AACH2, AACH3 and AACH4 were studied in the pH range 1 to 10. The maximum swelling of 4038.79% was observed for AACH1 compare to the swelling % of other hydrogel, hence for further swelling and drug release studies AACH1 is taken as standard. The results are tabulated in the **Table 6.2** and their corresponding graphical representation is showed in **Fig. 6.7.** Anionic hydrogel swelling capacity was reduced when counterions (Na^+) are added to the swelling medium [17]. At pH 7, the maximum swelling was achieved. The repulsion of anionic groups is decreased in acidic media due to carboxylate groups being protonated, resulting in a lower swelling rate. The carboxyl groups of AAC (pKa = 4.2) converted into COONa

groups at higher pH solutions due to the presence of excess Na^+ in the pH solution this will shield the carboxylate anions and prevents active anion-anion repulsion, from this the swelling (%) decreases at pH 8, 9 and 10 than at pH 7. The results are tabulated in the **Table 6.3** and their corresponding graphical representation is showed in **Fig. 6.8.** The swellig study of the AACH1 hydrogel are carried out in the solution of pH 1.2 and 7.4. the result showed that the maximum swelling % 4151.89 in pH 7.4 and the minimum swelling % 321.47 in pH 1.2. The results are tabulated in the **Table 6.4** and their corresponding graphical representation is showed in **Fig. 6.9.** The hydrogel swelled up to 4151.89% at pH 7.4 due to anion-anion (COO^-) repulsive electrostatic forces but shrink at pH 1.2 (321.47%) due to carboxylate protonation. The results of the swelling (%) in pH 7.4 are tabulated in the **Table 6.6** and their corresponding graphical representation is showed in **Fig. 6.11**. The hydrogel's sharp swelling (%) activity makes them good material for controlled drug delivery [18].

6.3.6. Construction of calibration curve

Doxycycline solutions of 4, 8, 12, 16 and 20 mg/l are scanned between 200 nm to 400 nm to determine the maximum absorption by using UV-Visible spectrophotometer. The maximum absorption was found to be at λ_{max} 270 nm. The results are tabulated in the **Table 6.7** and their corresponding graphical representation is showed in **Fig. 6.12 and 6.13.** The coefficient of correlation (R^2) is 0.999 according to the calibration curve.

6.3.7. Doxycycline drug release study from poly(AAC) hydrogel

6.3.7.1. Doxycycline drug release study in pH 1.2 and 7.4

Poly(AAC) hydrogel is a pH-sensitive hydrogel. The swelling study conducted in pH 1.2 and 7.4 similar to the gastrointestinal fluid-like solution of the

human body. The result showed that the maximum swelling % 4151.89 in pH 7.4 and the minimum swelling % 321.47 in pH 1.2. The results are tabulated in the **Table 6.4** and their corresponding graphical representation is showed in **Fig. 6.9.** The drug release study conducted under the same condition of pH 1.2 and 7.4. About 99.65% of Doxycycline drug was released in the solution of pH 7.4 and only 39.37% of drug was released in the solution of pH 1.2 due to the maximum swelling capacity at pH 7.4. The results are tabulated in the **Table 6.8** and their corresponding graphical representation is showed in **Fig. 6.14.**

6.3.7.2. Doxycycline drug release study at different temperature

The effect of temperature on Doxycycline drug release was studied at temperatures of 27^{o}C and 37^{o}C respectively. Poly(AAC) hydrogel is a temperature-sensitive. The swelling (%) at 27°C is 3645.04% and 4151.89% at 37°C. The results are tabulated in the **Table 6.5** and their corresponding graphical representation is showed in **Fig. 6.10.** The Doxycycline drug release results showed that maximum amount of drug release observed at 37°C temperature **(Fig. 6.15)**. About 66.88% of drug has released at 27°C and at 37°C 99.65% of drug has been released. This indicates that as the temperature increases, the drug release also increased. The results are tabulated in the **Table 6.9** and their corresponding graphical representation is showed in **Fig. 6.15.**

6.3.8. Kinetic model drug release study

Different mathematical models were used to predict the best drug release method for synthesized poly(AAC) hydrogel and the results of the correlation coefficient (R^2) are shown in **Table 6.10** and their corresponding graphical representation is showed in **Fig. 6.16.** The maximum degree of the coefficient of

correlation aids in the prediction of a mathematical model that matches the release kinetics. The highest correlation coefficient (R^2) is 0.997 suggesting that hydrogel matches the Higuchi model of drug release.

6.3.9. Antibacterial activities

The doxycycline drug-loaded hydrogel was investigated for *in-vitro* antibacterial effect. **Fig. 6.17** illustrated that doxycycline (D) pure drug and doxycycline drug-loaded hydrogel (DLH) had an antibacterial effect on *S. aureus* and *E. coli* bacteria and no effect at unloaded hydrogel (H) after 24 hours incubation at 37°C. After measuring the inhibition zone the doxycycline pure drug exhibited 7 mm and 5 mm for the doxycycline drug-loaded hydrogels against *S. aureus* **(Fig. 6.17a)** and 13 mm and 9 mm against *E. coli*, respectively **(Fig. 6.17b)**. As the result showed, doxycycline pure drug and doxycycline drug-loaded hydrogel shows antibacterial activity because of the bioactivity of the drug but the unloaded hydrogel will not show a zone of inhibition compared to pure drug and drug-loaded hydrogel. This effect could be due to the presence of doxycycline in drug-loaded hydrogel [19].

6.4. Conclusion

Poly(AAC) hydrogels were prepared by using AAC and MBA with PPS and SMBS as free-radical initiators. Swelling and drug release tests were carried out at various temperatures and pH levels. The pH sensitivity of the superabsorbent hydrogels was found to be high with many swelling changes observed across a broad pH range. The main driving force behind such sudden swelling changes may be ionic repulsion between charged groups integrated into the gel matrix as a result of external pH modulation. Our findings suggested that redox polymerized cross-linked hydrogels could be used as a drug carrier for localized and regulated drug delivery. Owing to increased electrostatic repulsion between negatively charged polymer chains, the release value of doxycycline drug from hydrogels was higher at pH 7.4 than at pH 1.2. Overall the hydrogels described in this study could be used to boost the bioavailability of drugs with controlled drug release in a variety of pharmaceutical applications. This hydrogel follows the Higuchi model kinetic release and drug-loaded hydrogel shows good antibacterial activity and hence can be used in biomedical applications.

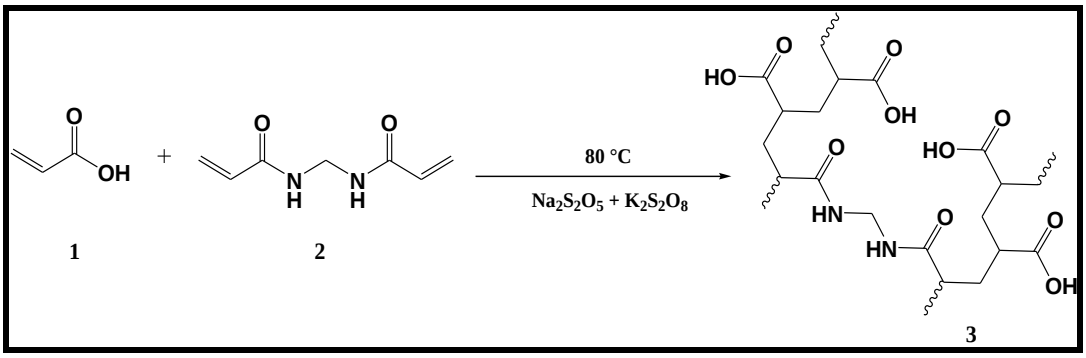

Scheme III. Synthesis of poly(AAC) hydrogel. (1) AAC, (2) MBA and (3) poly(AAC) hydrogel.

Table 6.1. Poly(AAC) hydrogel synthesis formulations.

Formulation code	Water (ml)	Monomer AAC (ml)	Initiator		MBA (mg)
			SMBS (mg)	PPS (mg)	
AACH1	10	0.6	32	45	21
AACH2	10	0.6	32	45	26
AACH3	10	0.6	32	45	31
AACH4	10	0.6	32	45	36

Table 6.2. Statistical data of Swelling (%) of different formulation poly(AAC) hydrogels.

pH	AACH1 Swelling (%)	AACH2 Swelling (%)	AACH3 Swelling (%)	AACH4 Swelling (%)
2	395.77	216.83	103.97	47.25
4	1002.24	812.38	594.32	471.42
6	2736.20	2048.78	1588.57	1353.65
7	4038.79	3438.65	2928.03	2252.04
8	3649.53	3105.78	2320.39	1816.58
10	**3109.09**	2517.05	2131.50	1688.16

Table 6.3. Statistical data of swelling (%) of poly(AAC) hydrogels at pH 1 to 10.

pH	**1**	**2**	**3**	**4**	**5**
Swelling (%)	294.25	395.77	753.91	1002.24	1613.54
pH	**6**	**7**	**8**	**9**	**10**
Swelling (%)	2736.20	**4038.79**	3649.53	3460.55	3109.09

Table 6.4. Statistical data of the swelling (%) of the poly(AAC) hydrogel at pH 1.2 and 7.4

Time (min)	pH 1.2 Swelling (%)	pH 7.4 Swelling (%)
0	0.00	0.00
360	222.69	801.16
720	247.23	1509.03
1080	264.41	2092.71
1440	277.91	2944.89
1800	287.73	3617.49
2160	304.29	4072.59
2520	320.85	4150.43
2880	**321.47**	**4151.89**

Table 6.5. Statistical data of the poly(AAC) hydrogel swelling (%) in a pH 7.4 at 27°C and 37°C.

Time (min)	27°C Swelling (%)	37°C Swelling (%)
0	0.00	0.00
360	359.15	801.16
720	804.50	1509.03
1080	1448.64	2092.71
1440	2172.07	2944.89
1800	2754.95	3617.49
2160	3365.16	4072.59
2520	3545.04	4150.43
2880	**3645.04**	**4151.89**

Table 6.6. Statistical data of the poly(AAC) hydrogel swelling (%) changes in pH 7.4 over time.

Time (hours)	pH 7.4 Swelling (%)
0	0.00
6	801.16
12	1509.03
18	2092.71
24	2944.89
30	3617.49
36	4072.59
42	4150.43
48	4151.89

Table 6.7. Statistical data of the calibration curve for doxycycline (Absorbance v/s Concentration).

Concentration (mg/l)	Absorbance
0	0.00000
4	0.12681
8	0.25752
12	0.38575
16	0.51847
20	0.65968

Table 6.8. Statistical data of the doxycycline drug release (%) over time in pH 1.2 and 7.4 from poly(AAC) hydrogel.

Time (min)	pH 1.2 Drug release (%)	pH 7.4 Drug release (%)
0	0.00	0.00
30	5.56	13.20
60	9.00	21.62
90	12.71	29.77
120	15.75	36.59
150	17.89	44.02
180	20.51	47.73
210	22.12	55.85
240	24.26	61.26
270	26.52	65.34
300	28.60	68.11
330	28.96	71.17
360	32.12	76.06
390	35.00	78.68
420	35.48	83.41
450	35.62	87.74
480	36.71	90.25
510	37.88	92.14
540	37.94	94.92
570	39.12	97.54
600	**39.37**	**99.65**

Table 6.9. Statistical data of the doxycycline drug release (%) over time at 27°C and 37°C in pH 7.4 from poly(AAC) hydrogel.

Time (min)	27°C Drug release (%)	37°C Drug release (%)
0	0.00	0.00
30	12.62	13.20
60	20.16	21.62
90	24.85	29.77
120	31.13	36.59
150	35.32	44.02
180	39.99	47.73
210	43.66	55.85
240	47.86	61.26
270	50.74	65.34
300	52.47	68.11
330	54.33	71.17
360	56.84	76.06
390	59.75	78.68
420	60.85	83.41
450	62.74	87.74
480	62.98	90.25
510	65.42	92.14
540	66.65	94.92
570	66.88	97.54
600	**66.88**	**99.65**

Table 6.10. Doxycycline drug release results in terms of correlation coefficient (R^2), slope and intercept of various kinetic models.

Name of the kinetic model	R^2	Slope	Intercept
Zero order	0.964	8.746	19.83
First order	0.804	-0.178	2.248
Higuchi	**0.997**	0.027	0.377
Korsmeyer-Peppas	0.994	0.672	1.353
Hixson-Crowell	0.963	0.338	-0.311

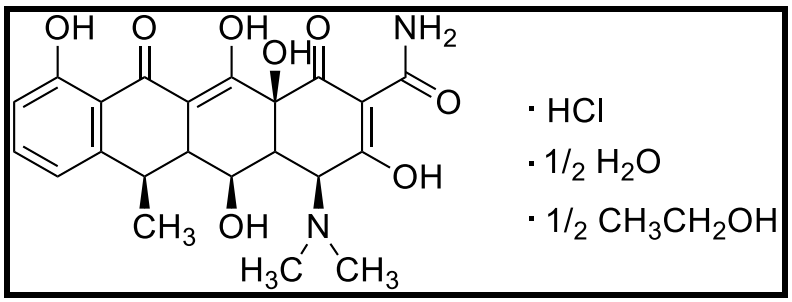

Figure 6.1. The chemical structure of doxycycline hydrochloride.

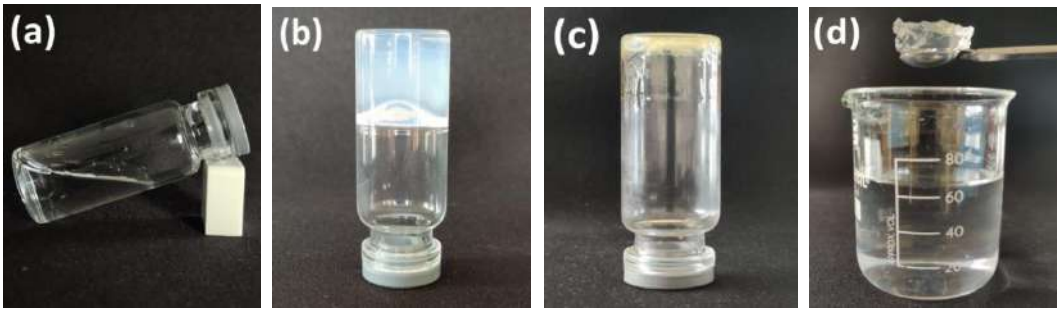

Figure 6.2. Poly(AAC) hydrogel preparation stages (a) in the liquid state, (b) after gel formation, (c) in a dried state and (d) in the swelling state.

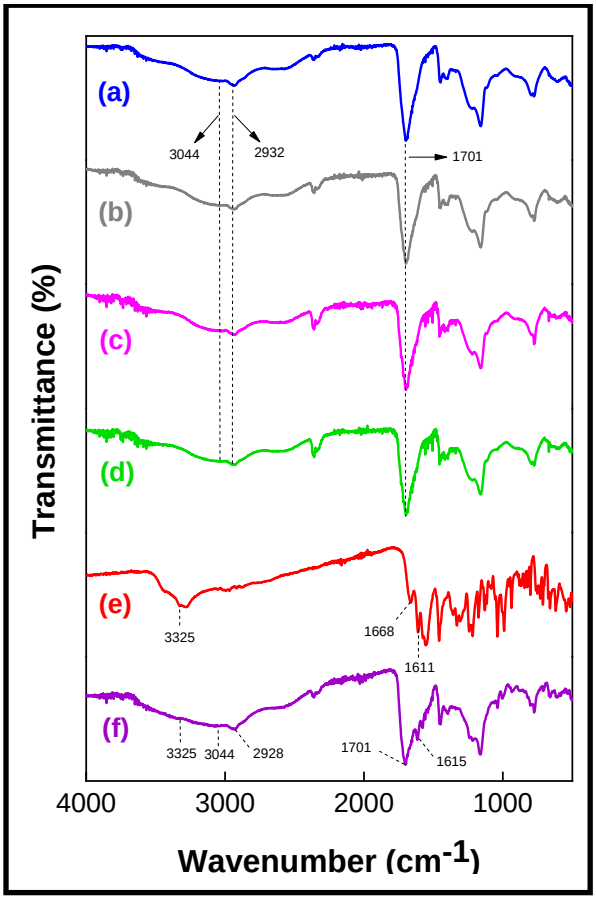

Figure 6.3. FTIR spectra of poly(AAC) hydrogels (a) AACH1, (b) AACH2, (c) AACH3, (d) AACH4, (e) Doxycycline and (f) Doxycycline-loaded hydrogels.

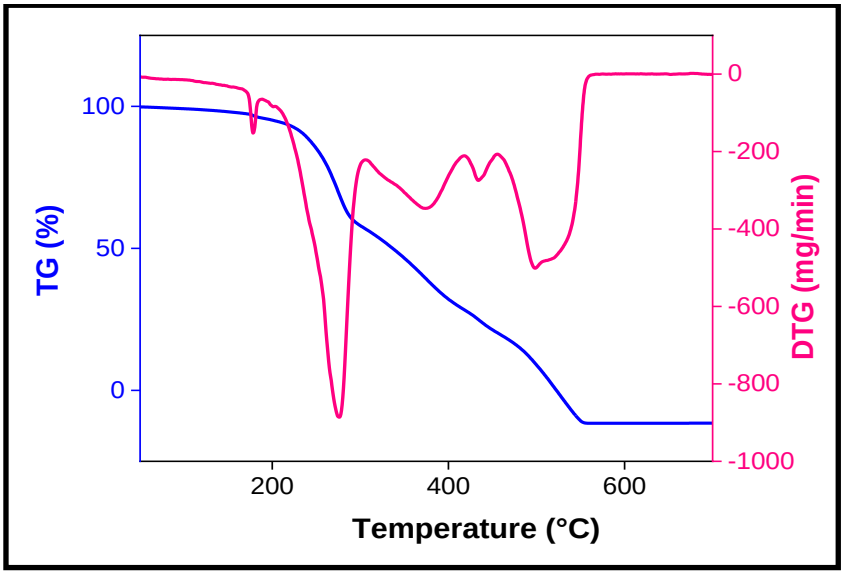

Figure 6.4. TGA graph of poly(AAC) hydrogel.

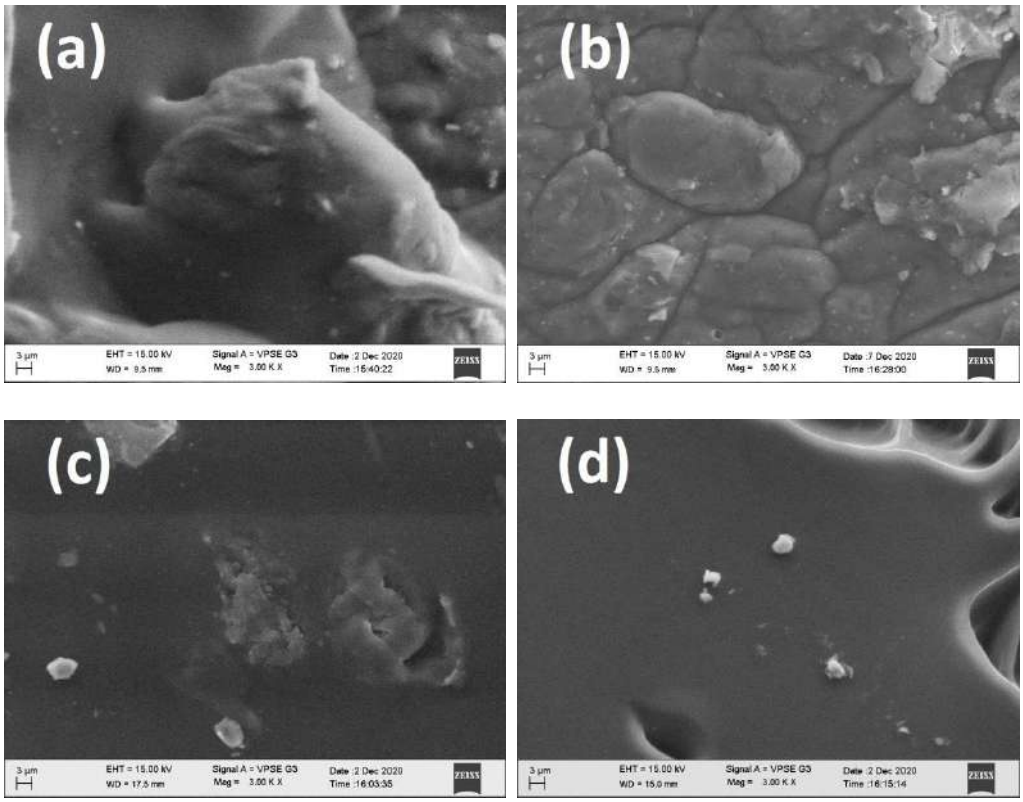

Figure 6.5. SEM images of (a) AACH1, (b) AACH2, (c) AACH3 and (d) AACH4 dried poly(AAC) hydrogels.

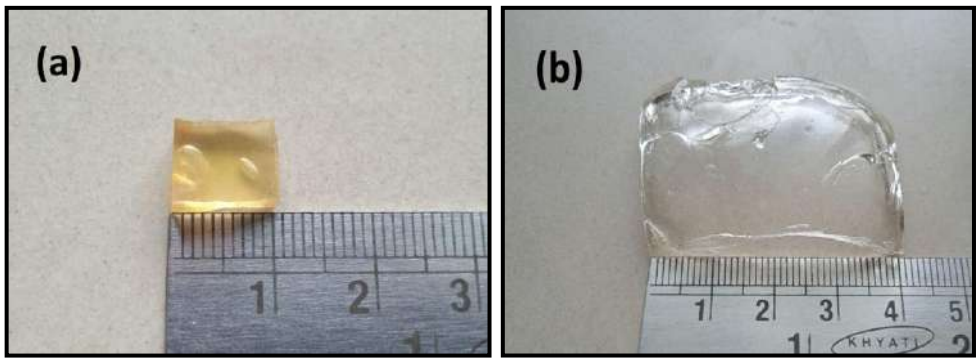

Figure 6.6. Digital camera photographs of (a) dried and (b) swollen poly(AAC) hydrogel.

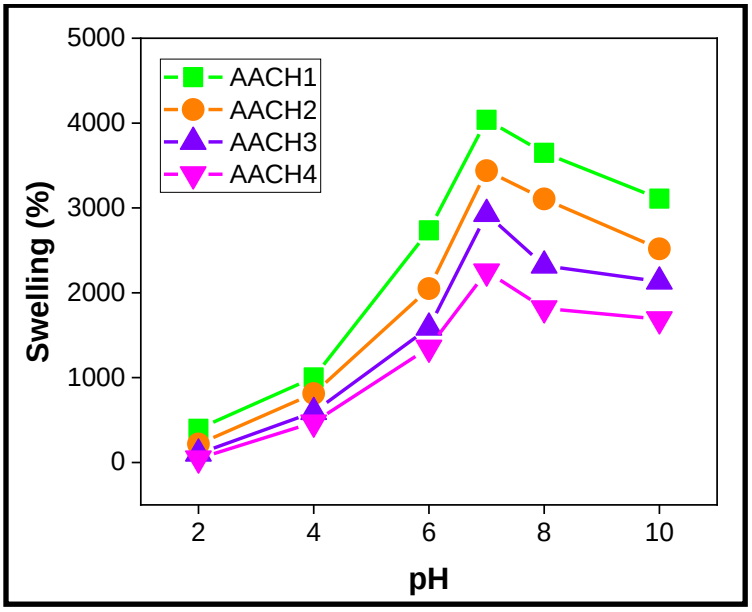

Figure 6.7. Swelling (%) of different formulation of poly(AAC) hydrogels.

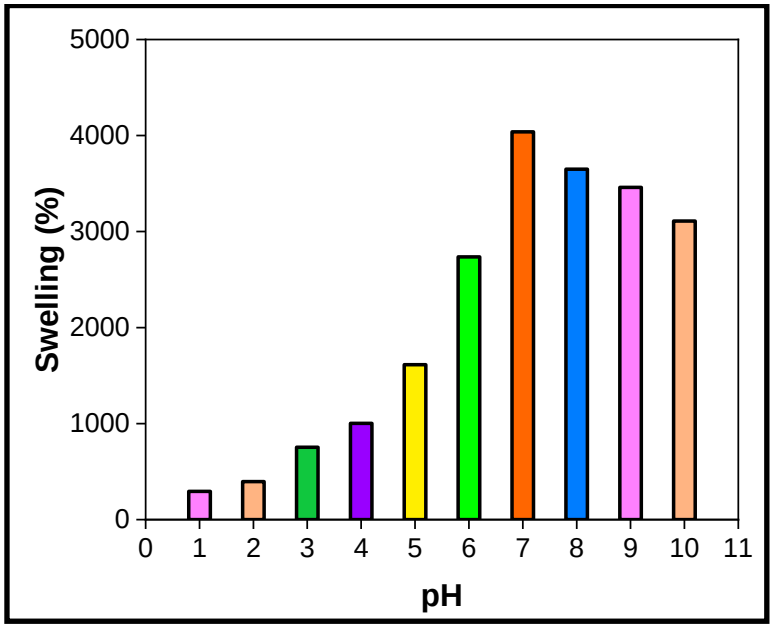

Figure 6.8. The swelling (%) of poly(AAC) hydrogel at pH range 1 to 10.

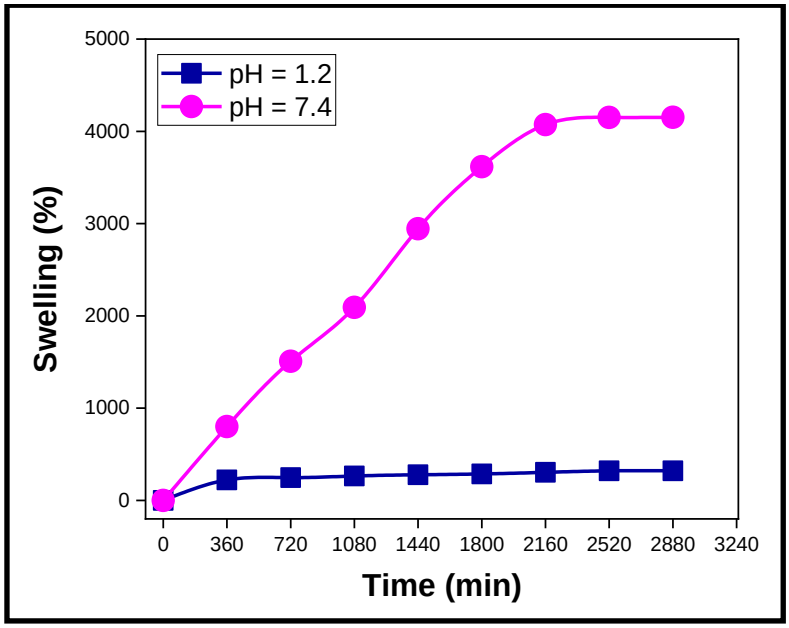

Figure 6.9. The swelling (%) of poly(AAC) hydrogel at pH 1.2 and pH 7.4.

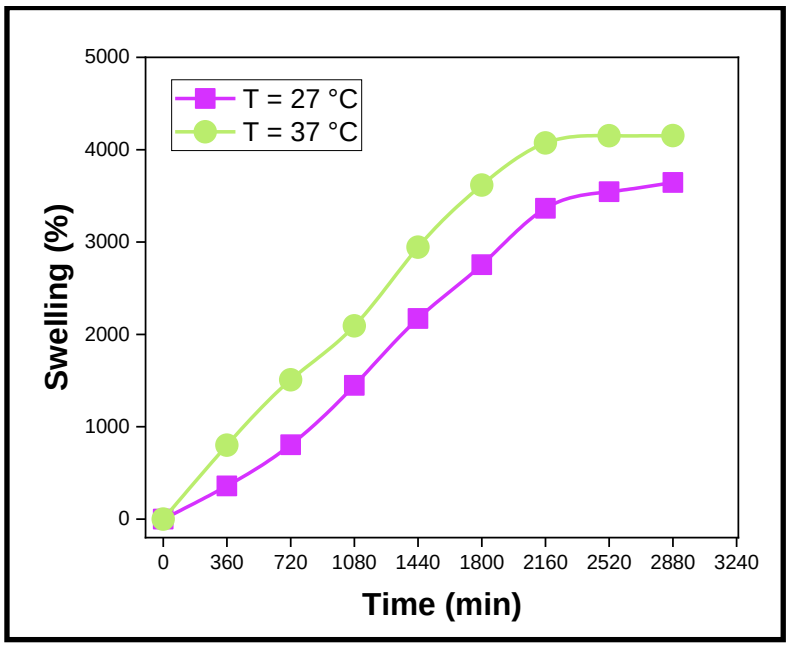

Figure 6.10. The swelling (%) of poly(AAC) hydrogel at temperatures 27°C and 37°C in pH 7.4.

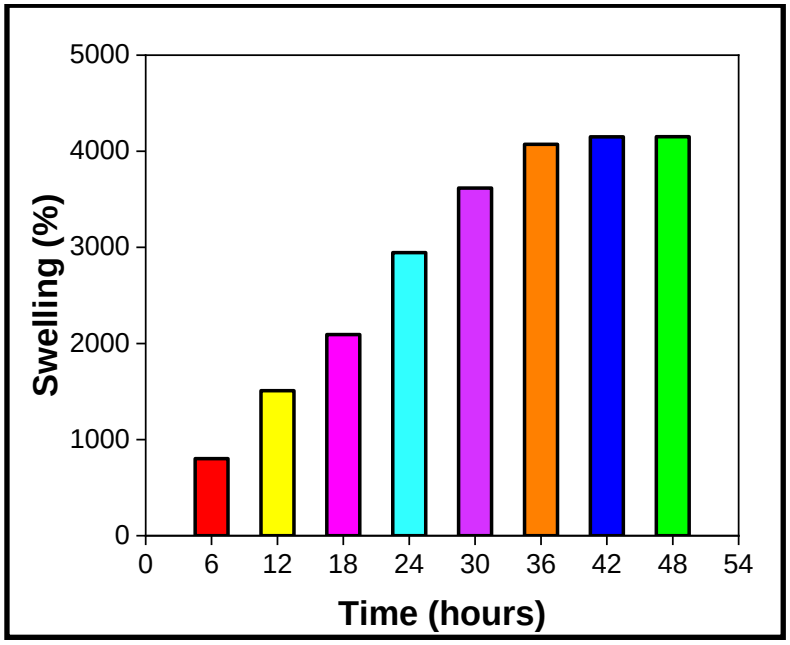

Figure 6.11. Changes in the poly(AAC) hydrogel swelling (%) over time in pH 7.4.

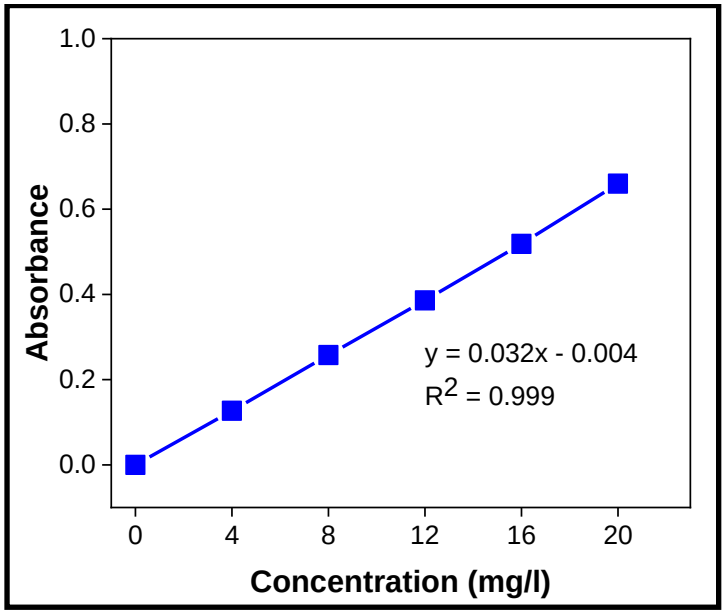

Figure 6.12. The calibration curve for doxycycline (Absorbance v/s Concentration).

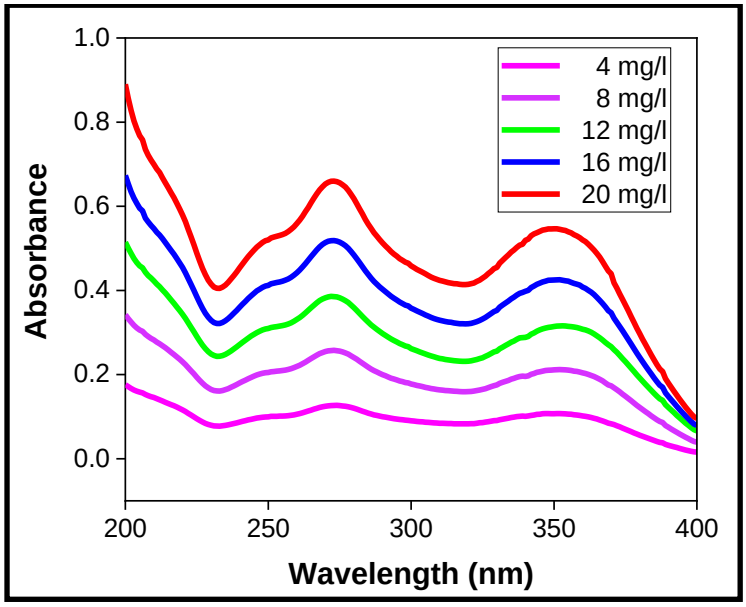

Figure 6.13. Doxycycline calibration curve spectral graph.

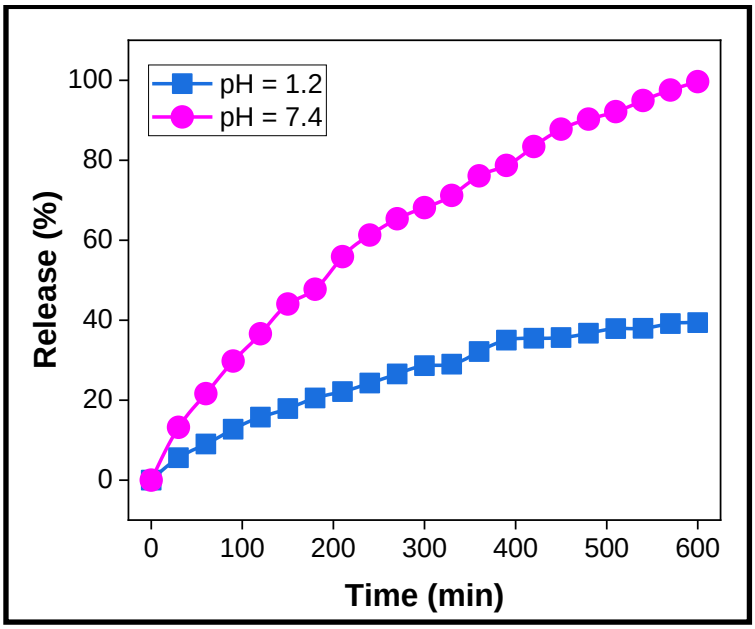

Figure 6.14. Doxycycline drug release (%) over time in pH 1.2 and 7.4 from poly(AAM-co-AAC) hydrogel.

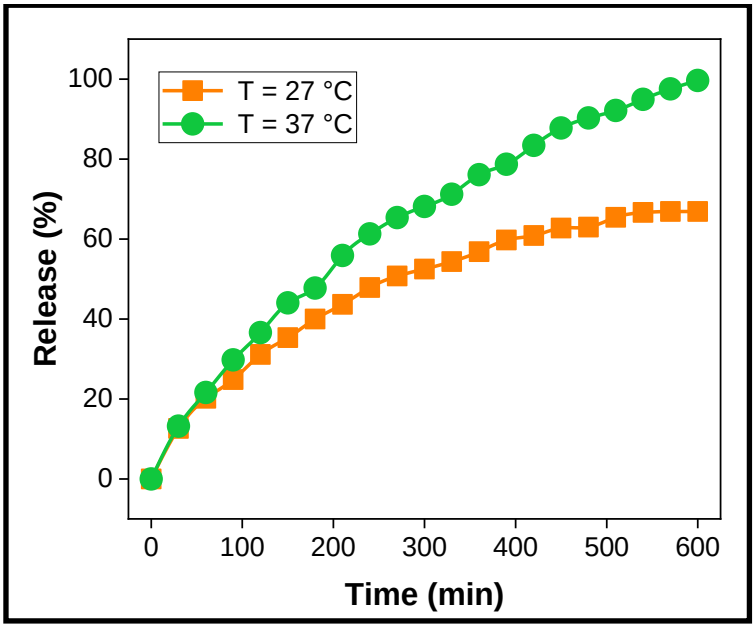

Figure 6.15. The release of Doxycycline drug with time from poly(AAC) hydrogel at temperature 27°C and 37°C.

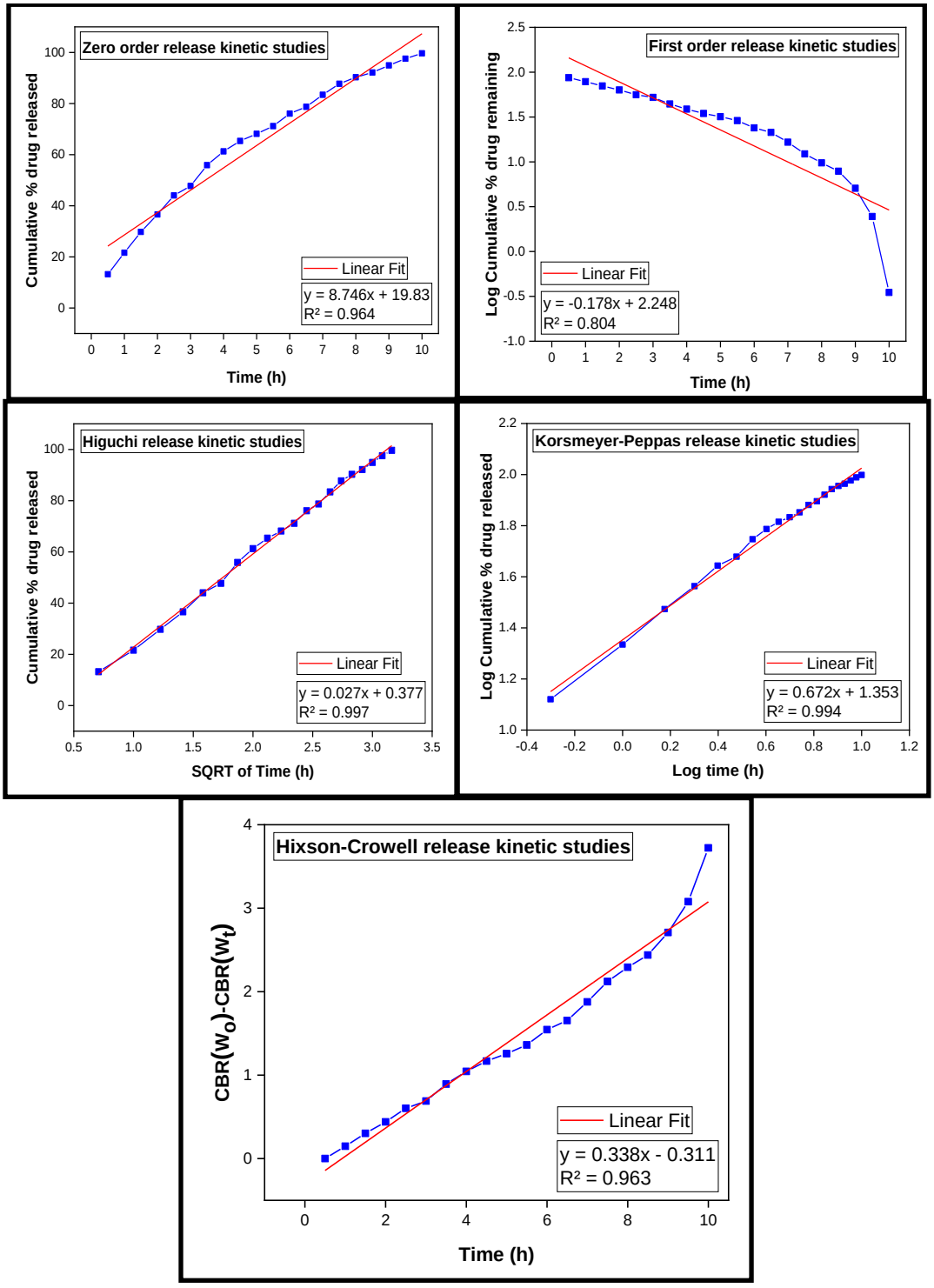

Figure 6.16. Graphical representation of kinetic model drug release from poly(AAC) hydrogel.

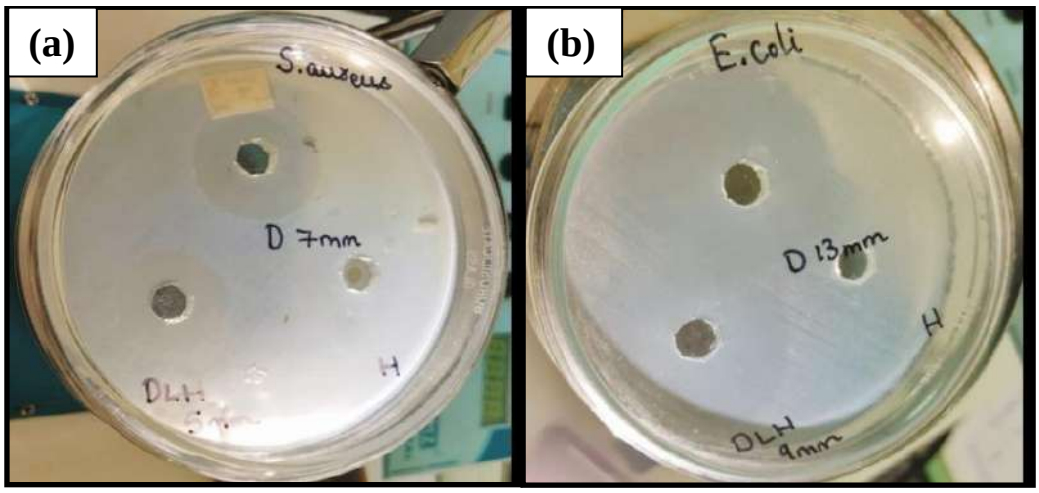

Figure 6.17. Antibacterial activity of doxycycline drug-loaded hydrogel on **(a)** *S.aureus* (Gram-positive bacteria) and **(b)** *E.Coli* (Gram-negative bacteria).

6.5. References

[1] Eid M., Hegazy S. A.; Radiation synthesis of stimuli-responsive hydrogels for biological applications. *Journal* of *Radiation Research and Applied Sciences,* 2009, 2, 717–736.

[2] Nguyen M. K., Alsberg E.; Bioactive factor delivery strategies from engineered polymer hydrogels for therapeutic medicine. *Progress in Polymer Science,* 2014, 39, 1234–1265.

[3] Mansuri S., Kesharwani P., Jain K.; Mucoadhesion: a promising approach in drug delivery system. *Reactive & Functional Polymers,* 2016, 100, 151-172.

[4] Li Y., Tan Y., Xu K.; A biodegradable starch hydrogel synthesized via thiol-ene click chemistry. *Polymer Degradation* and Stability, 2016, 137, 75-82.

[5] Gao X., He C., Xiao C.; Biodegradable pH-responsive polyacrylic acid derivative hydrogels with tunable swelling behavior for oral delivery of insulin. *Polymer*, 2013, 54, 1786-1793.

[6] Bajpai A. K., Shukla S. K., Bhanu S.; Responsive polymers in controlled drug delivery. *Progress in Polymer Science,* 2008, 33, 1088–1118.

[7] Viega A. S., Schneider J. P.; Antimicrobial hydrogels for treatment of infection. *Biopolymers,* 2013, 100, 637–644.

[8] Slaughter B. V., Khurshid S. S., Fisher O. Z.; Hydrogels in regenerative medicine. *Advanced Materials*, 2009, 21, 3307–3329.

[9] Siafaka P. I., Zisi A. P., Exindari M. K.; Porous dressings of modified chitosan with poly (2-hydroxyethyl acrylate) for topical wound delivery of levofloxacin. *Carbohydrate Polymers*, 2016, 143, 90–99.

[10] Anumolu S. S., DeSantis A. S., Menjoge A. R.; Doxycycline loaded poly(ethylene glycol) hydrogels for healing vesicantinduced ocular wounds. *Journal of Biomaterials,* 2010, 31, 964–974.

[11] He Z. X., Wang Z. H., Zhang H. H.; Optimization of a doxycycline hydroxypropyl-β-cyclodextrin inclusion complex based on computational modeling. *Acta Pharmaceutica Sinica B* , 2013, 3, 130–139.

[12] Jantratid E., Strauch S., Becker C.; Biowaiver monographs for immediate release solid oral dosage forms: Doxycycline hyclate, *Journal of Pharmaceutical Sciences,* 2010, 99(4), 1639–1653.

[13] Baishya H., Gouda R., Qing Z.; Application of Mathematical Models in Drug Release Kinetics of Carbidopa and Levodopa ER Tablets, *Journal of Developing Drugs*, 2017, 06, 1-8.

[14] Sagar K., Dattatray A., Dhananjay L.; Formulation and evaluation of colon targeted matrix tablet of azathioprine. 2019, 9, 3157-168.

[15] Junejo Y., Safdar M.; Highly effective heterogeneous doxycycline stabilized silver nanocatalyst for the degradation of ibuprofen and paracetamol drugs. *Arabian Journal of Chemistry*, 2019, 12, 2823-2832.

[16] Lim L., Rosli N., Ahmad I.; Synthesis and Swelling Behavior of pH-Sensitive Semi-IPN Superabsorbent Hydrogels Based on Poly(acrylic acid) Reinforced with Cellulose Nanocrystals. *Nanomaterials*, 2017, 7, 399.

[17] Mohammad S.; Synthesis of starch-*g*-poly(acrylic acid-*co*-2-hydroxy ethyl methacrylate) as a potential pH-sensitive hydrogel-based drug delivery system. *Turkish Journal of Chemistry*, 2011, 35, 723–733.

[18] Wu J., Lin J., Li G.; Influence of the COOH and COONa groups and crosslink density of poly (acrylic acid)/montmorillonite superabsorbent composite on water absorbency. *Polymer International*, 2001, 50, 1050-1053.

[19] Cunha B. A., Sibley C. M., Ristuccia A. M. Doxycycline. *Therapeutic Drug Monitoring*, 1982, 4(2), 115.

Chapter – 7

Conclusion

Chapter – 7

Conclusion

This chapter discus with the conclusion of the whole research thesis.

7.1. Conclusion of the thesis

The thesis has projected on the synthesis of polymer-based Smart Hydrogels for drug delivery applications. The poly(acrylamide), poly (acrylamide-co-acrylic acid) and poly(acrylic acid) hydrogels are synthesized by using *N*, *N*′-methylene-bis-acrylamide as a crosslinker and used to study the controlled release of Levofloxacin, Moxifloxacin and Doxycycline drugs respectively.

The topics of the thesis focus on current ways for creating controlled-release drug delivery systems using polymers and the hydrogel formulations that produced longer-lasting effects. The findings of this research are likely to have a bigger impact on the pharmaceutical industry. However, in order to produce appropriate formulations and maintain their stability, the controlled-release formulations developed in this work will be further detailed in the future. Formulations must also be tested in animal models for intoxication, effectiveness and feasibility before being used in humans.